Regulation of innate immune signalling by hypoxia



Biao Ma

Balliol College

University of Oxford

A thesis submitted for the degree of

Doctor of Philosophy

Michaelmas 2021

Acknowledgements

I would very much like to thank my supervisor Professor Mads Gyrd-Hansen. I still remember that day when we had a brainstorm together in the office that you accidentally mentioned different immune response in villus-crypt axis of intestine and I said there is an oxygen gradient in there. Unexpected, but that's how we initiate this amazing project. I used to be very independent on ideas and I am still is, but you make me realised that communication is really not a bad thing, especially in research. I am very grateful that you completely support my research by giving me enough time and space and also by providing guidance in my research, thus making me have extremely mentally-relaxed and also productive four years that I can enjoy doing my research, just like playing a puzzle game. I am also glad having you to share the happiness with when I have new discoveries.

I would like to thank Dr. Jelena Mirkovic for her role as my second supervisor as well as Dr. Skirmantas Kriaucionis for their support and advice with this work. I would also like to show my gratitude to all the staff from the Ludwig institute for their support and help during the past four years.

My Viva examiners Dr. Jan Rehwinkel and Dr. Mathew Coleman have kindly helped with the revision of this thesis and provided great suggestions for better interpretation of the data and for expanding the scope of this thesis.

This thesis cannot be done without the help and support from the whole lab members, past and present (Derek, Mattia, Lisa, Corrine, Gianluca, Jenny, Ruoshi, Xuan and Yusuf).

It is all because of you so that we can have such a collaborative and fun working atmosphere. I am very grateful to be a member of this big family.

I would like to thank, Jingyi, Jiayuan, Mingda, Pablo, Vinny, Xiaotian, Xiaoyue, Zhu and all my friends here in Oxford for making me feel not alone during the early time when I just arrived Oxford and making Oxford like home later. The adventures we shared together across land and sea in UK and Europe are unforgettable memories in my life.

Thanks to my parents for your understanding and firmly support. You make me have the courage to pursuit my dreams.

Thanks to University of Oxford. Every time when I pass through the alleys that those great minds like Edmond Halley or Robert Hooke had walked through, making me feel I am walking through the history of science and being part of it.

Finally, I would like to thank Cancer Research UK, Clarendon Fund, Jason Hu Scholarship, Phizackerley Senior Scholarship and Balliol College for providing financial support for my study and research in Oxford.

Abstract

Innate immunity is the first line of defence against invading pathogens and is also required for the initiation of adaptive immunity. Innate immune responses and inflammation are stimulated by pattern recognition receptors and cytokine receptors. A well-functioning immune defence is crucial for clearance of invading pathogens, but the knowledge of how the immune system is influenced by microenvironmental cues such as hypoxia is still limited. Hypoxia is a common feature in inflammatory sites as well as in solid tumours. In this thesis, I describe a mechanism that hypoxia suppresses immune signalling by receptors such as TNFR1, NOD2, IL-1R and IFN-γR2 that are encoded by uORF-containing mRNAs. This finding unveils an immunological mechanism for desensitisation by hypoxia.

The mechanism may be applicable to different physiological or pathophysiological processes, such as autoimmune diseases and cancer. In this thesis, I describe how this mechanism affects tumour immune evasion. Specifically, hypoxic-inhibition of TNF and IFN-γ signalling results in suppression of MHC-I expression levels on the cell surface, which are essential for activation of CD8 T cell dependent anti-tumour immunity. Genetic deletion of uORFs in *TNFRSF1A* and *IFNGR2* counteracts hypoxic inhibition of the expression of MHC-I induced by TNF and IFN-γ in Yumm1.7 mouse melanoma cells, leading to enhanced CD8 T cell-dependent anti-tumour immunity in this syngeneic mouse model. Consistently, higher TNF and IFN-γ signatures predict better clinical outcomes and tumour hypoxia negatively correlates with T cells infiltration and disease specific survival rates in melanoma patients. These data indicate that targeting uORFs counteracts hypoxia-mediated immune suppression in cancer.

The finding of oxygen level regulating immune signalling activity may contribute to our understanding of inflammation regulation and development of therapeutics against cancer.

Contents

1 Introduction 1

1.1 The innate immune system and receptor signalling 2
1.1.1 Pattern recognition receptors (PRRs) 2
1.1.2 NOD2 receptor signalling 4
1.1.3 Cytokine receptor signalling pathways 6
1.1.4 IL-1R receptor signalling pathway 8
1.1.5 TNF receptor signalling pathway 9
1.1.6 Interferons (IFNs) and IFN-γ signalling pathway 12
1.1.7 Mechanisms underlying IFN-γ anti-tumour effects 15
1.1.8 Immune regulation by microenvironment 18

1.2 Oxygen sensing and hypoxia response 19
1.2.1 Oxygen sensing is evolutionarily conserved 19
1.2.2 Hypoxia inducible factors in regulation of hypoxia signalling 20
1.2.3 HIF prolyl hydroxylases regulate the stability and activity of HIFs 21
1.2.4 Tumour hypoxia 24
1.2.5 Hypoxia in regulation of inflammation 25

1.3 Regulations of protein translation in eukaryotic cells 27
1.3.1 Current model of translation initiation 28
1.3.2 Regulation of initiation factors 30
1.3.3 Upstream open reading frames (uORFs) 32
1.3.4 Hypoxia regulates protein translation 33

1.4 Aims and objectives of the study 36
2 Materials 37

2.1 Chemicals and reagents 38

2.2 Cell lines, organoids and mouse strain 40

2.3 Antibodies 41

2.4 Oligos 43

2.5 DNA constructs 46
3 Methods 48

3.1 Mice 49

3.2 Cell culture, plasmids and transfection 49

3.3 Generation of cell lines by CRISPR/Cas9-mediated gene editing 49

3.4 Lentiviral cloning, production and infection 50

3.5 Immunoblotting 50

3.6 Immunofluorescence 51

3.7 RNA isolation, cellular fractionation and quantitative real-time PCR 51

3.8 Click chemistry labelling 51

3.9 Cell viability assay 52

3.10 Purification of endogenous ubiquitin conjugates 53

3.11 Allograft tumour model 53

3.12 Flow cytometry analysis 54

3.13 3'mRNA Sequencing (services provided by Oxford Genomic Centre) 54

3.14 Bioinformatics analysis 55

3.15 Quantification and statistical analysis 56

4 Mechanism of hypoxia-induced repression of immune receptor signalling 58

4.1 Hypoxia inhibits TNF-, IL-1β- and L18-MDP-mediated signalling 59

4.2 Hypoxia downregulates TNF receptor 1 (TNFR1) 63

4.3 Hypoxia inhibits TNF-induced cell death 68

4.4 Hypoxia-induced TNFR1 reduction is regulated at translational level 70

4.5 uORF2 of *TNFRSF1A* inhibits TNFR1 translation under hypoxia 76

4.6 Deleting uORF2 of *TNFRSF1A* increases TNFR1 translation and amplifies TNF sensitivity 81

4.7 Downregulation of eIF4G1 mirrors hypoxia and partially reduces TNFR1 and TNF signalling 86

4.8 uORFs regulate the expression of multiple immune receptors under hypoxia 92

5 Translated uORFs promote tumour immune evasion 97

5.1 TNF and IFN-γ synergistically induce MHC-I expression 98

5.2 Hypoxia inhibits MHC-I expression induced by TNF and IFN-γ 103

5.3 Deleting uORFs of *TNFRSF1A* and *IFNGR2* sustains TNF- and IFN-γ-induced MHC-I expression under hypoxia 104

5.4 Deleting uORFs of *TNFRSF1A* and *IFNGR2* upregulates anti-tumour signatures 109

5.5 Deleting uORFs in *TNFRSF1A* and *IFNGR2* enhances immune control of melanoma tumour growth 111

5.6 Melanoma patients with higher TNF and IFN-γ signatures have better clinical outcomes 115

6 Discussion 120

6.1 Regulation of immune receptor signalling 121

6.2 Regulation of translation via uORFs during hypoxia 121

6.3 Hypoxia in regulation of inflammation 123

6.4 Hypoxia inhibits a potential feedforward loop in T cell activation 125

6.5 Study limitations 128

6.6 Conclusion 129

7 Appendices 130

7.1 Supplementary figures 131

References 135

1

Introduction

1.1 The innate immune system and receptor signalling

The immune system contains two parts, the innate immune system and the adaptive immune system. Comparing with the adaptive immune system, the innate immune system responds quickly, but lacks specificity and only has limited power to eliminate pathogens. However, the activation of the innate immune system is essential for the initiation of adaptive immunity, which is required to generate specific and long-lasting immunity against pathogens. Thus, the innate immune response is the first line of defence against invading microorganisms, including viruses, bacteria, fungi and parasites and it also plays important roles in other pathological conditions such as autoimmunity and cancer [1].

1.1.1 Pattern recognition receptors (PRRs)

During infection, the body needs to react to the potentially harmful pathogen. This process is achieved by a series of receptors localised on the cell surface and within the cytosol, namely pattern recognition receptors [2]. These receptors are present on various types of cells, predominantly expressed by immune cells, such as macrophages, dendritic cells and neutrophils, but they are also found in non-immune cells, such as intestinal epithelial cells and keratinocytes.

The cognate ligands for these receptors are known as pathogen or damage associated molecular patterns (PAMPs and DAMPs). PAMPs are usually found specifically in microorganisms such as viruses, bacteria, fungi and parasites, whereas DAMPs are cellular molecules released from damaged or dying cells, such as DNA and ATP, which can be sensed by PRRs as danger signals [3, 4]. Because of the specificity of these molecular patterns, the innate immune system can recognise them and initiate immune responses. For example, lipopolysaccharide (LPS), one of the most studied PAMPs, known as a specific molecule on the surface of Gram negative bacteria, can be recognised by the surface localised Toll-like receptor 4 (TLR4).

These receptors are an essential element of the innate immune system as they are the first

line of defence engaging the pathogens. Based on the recognition specificity for ligands, PRRs can be categorised into at least five families, including Toll-like receptors (TLRs), Nucleotide-binding oligomerisation domain-like receptors (NLRs), C-type lectin receptors (CLRs) and RIG-I like receptors (RLRs). Additionally, a group of DNA sensing receptors (DSRs) such as AIM2 and cGAS also play a pivotal role in activating host defence responses [5, 6]. These receptors recognise specific components from invading pathogens and also self-molecules, such as DNA.

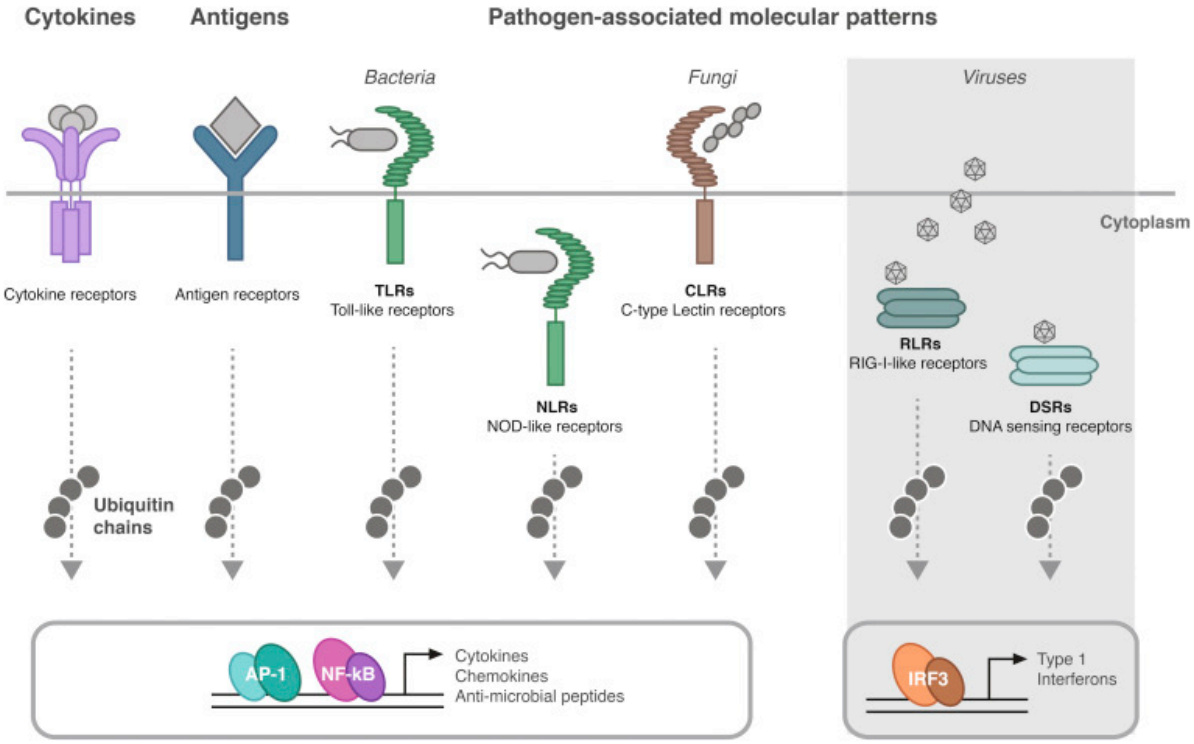


Figure 1.1 Pattern recognition receptor signalling (Mol Cell. 2017 Oct 19;68(2):265-280) Cytokine receptors, antigen receptors and pattern recognition receptors rely on the formation of ubiquitin chains to activate their downstream transcription factors, including AP-1, NF-κB and IRF3.

During infection, the activation of PRRs by their cognate ligands triggers ubiquitination and phosphorylation signalling cascades that dictate the expression of various cytokines and chemokines, typically by the transcription factor NF-κB and/or other transcription factors such as IRFs [7] (Figure 1.1). This may result in inflammation, which involves the recruitment of different types of circulating immune cells, including monocytes, neutrophils and lymphocytes to the infection site due to the release of cytokines and chemokines from non-immune or

immune cells. In addition, the innate immune response also facilitates the activation of antigen-specific adaptive immune responses mediated by B and T cells. Thereby, the pathogens can be eliminated by both innate and adaptive immunity, which ultimately resolve the infection and generate immunological memory.

1.1.2 NOD2 receptor signalling

The Nod-like receptor (NLR) family members NOD1 and NOD2, which are cytosolic PRRs, can recognise the components in the bacterial cell wall, known as peptidoglycan (PGN); thus they can sense invading intracellular bacteria [8]. Early work indicated that NOD1 and NOD2 respond to distinct PGN fragments and subsequent studies showed that γ-d-glutamyl-meso-diaminopimelic acid (iE-DAP), a motif present in many Gram negative bacteria and certain Gram positive bacteria, can activate NOD1 [8-11], whereas muramyl dipeptide (MDP), a PGN motif widely distributed in both Gram negative and Gram positive bacteria, can trigger NOD2 activation [8, 12-17].

Though the ligands for NOD1 and NOD2 are different, they are structurally similar as they both contain a Caspase recruitment domain (CARD) at their N-termini (except NOD2 has two CARDs), a central nucleotide-binding oligomerisation NACHT domain (named by proteins contain it including NAIP (NLP family apoptosis inhibitor protein), CIITA (class II, major histocompatibility complex, transactivator), HET-E (incompatibility locus protein from Podospora anserina) and TEP1 (telomerase-associated protein 1)), and multiple leucine-rich repeats (LRRs) at their C-termini. However, among NLRs, considerable attention has been given to NOD2 because mutations in the gene encoding it have been found associated with the inflammatory bowel disease, Crohn's disease, as well as Blau syndrome [8].

The binding between NOD2 and its cognate ligand MDP or L18-MDP results in a conformation change, thus allowing the recruitment of its adaptor protein RIPK2 through the interaction between CARDs on both NOD2 and RIPK2 (Figure 1.2). RIPK2 then recruits and

activates TAK1, which is essential for activation of the IKK complex and MAPK pathway [8, 18].

In addition, RIPK2 binds multiple ubiquitin ligases, including XIAP, cIAP1/2, ITCH, TRAF2/4/5, RNF34 and Pel3, which can regulate the ubiquitination on RIPK2, which affects its stability and activity [19-23]. For example, XIAP generates poly-ubiquitin chains on RIPK2 that recruit the Linear Ubiquitin chain Assembly Complex (LUBAC), consisting of SHARPIN, HOIP and HOIL [24]. The recruitment of LUBAC generates linear poly-ubiquitin chains on RIPK2, leading to the recruitment and activation of IKK and subsequently proteasomal degradation of IκBα and activation of NF-κB (Figure 1.2) [8, 18, 24].

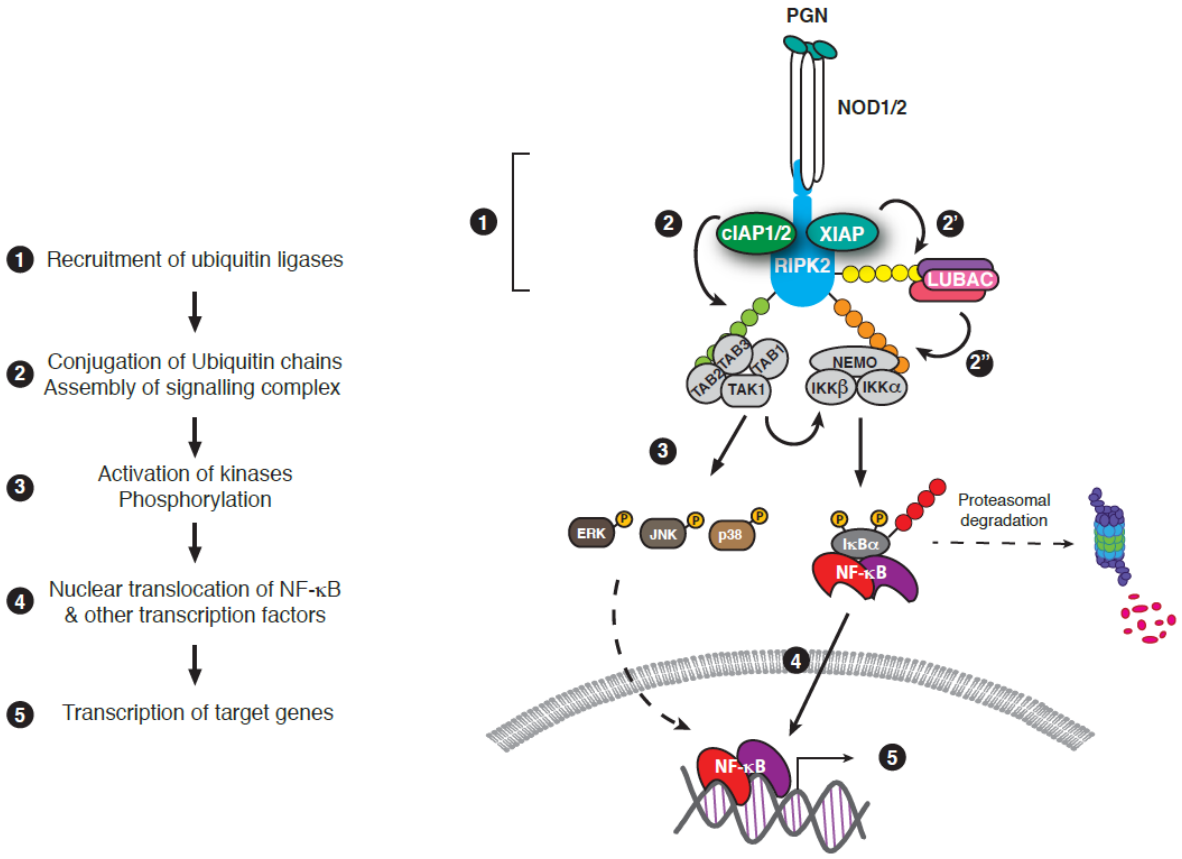


Figure 1.2 NOD2 receptor signalling. The activation of NOD2 signalling requires ubiquitination on the adapter protein RIPK2 for signalling transduction. The activated receptor recruits ubiquitin ligases cIAP1/2 and XIAP to promote K63 (green) and potentially other undefined type (yellow) of ubiquitin chains on RIPK2. The ubiquitinated RIPK2 recruit the LUBAC complex to generate linear ubiquitin chains (orange), which can further recruit the kinase IKK and facilitate the activation of TAK1. The kinase complexes further phosphorylate the downstream effectors, including ERK, JNK, p38 and IκBα. The phosphorylation on IκBα promotes its degradation and activation of NF-κB.

1.1.3 Cytokine receptor signalling pathways

Apart from the role of PPRs in recognising the PAMPs or DAMPs, cytokine receptor signalling plays regulatory functions during infection [1]. For instance, the activation of PPRs triggers the expression and release of cytokines, which can then activate their corresponding cytokine receptor signalling, such as amplifying the inflammatory signal, controlling adaptive immune responses and also modulating tissue barrier function [25-27].

Cytokines are small proteins and represent a large and diverse family. Almost all nucleated cells can express cytokines, but they are predominantly expressed by immune cells, such as macrophages and T cells [28]. The activation of a particular cytokine receptor signalling is initiated by the high affinity binding between the corresponding receptor on the cell surface and its cognate ligand, which can act in autocrine, paracrine or endocrine manners [29].

The activation of a subset of cytokine receptors triggers intracellular ubiquitination and phosphorylation cascades leading to the activation of downstream effectors, such as NF-κB [7], a process which is very similar to PRR activation. The biological effects caused by cytokines may result in differentiation, proliferation and activation of the target cells [30]. A cytokine can have different effects on different target cells, whereas multiple cytokines may also have a redundant effect on the same target cells. In addition, different cytokines may counteract each other's biological effects or have a synergistic effect. Thus, different cytokine receptor signalling can form a complex network, which makes it possible to have different biological effects through a single input.

Activation of cytokine receptor signalling needs to be tightly regulated to avoid overactivation. In healthy individuals, cytokine production is transient when stimulated by either a specific antigen or inflammatory stimuli [31]. Also, the half-life of cytokines and their respective receptors on the cell surface are also fine-tuned. Dysregulation of cytokine receptor signalling may result in diseases, such as autoimmune diseases and cancer.

Here I discuss three major cytokine receptor signalling pathways mediated by IL-1R, TNFR1 and IFN-γR1/2, as they play important roles in inflammatory responses and are closely related to auto-immune diseases and cancer [32, 33]. Adaptor proteins and core components within each signalling complex among these signalling pathways are varied. However, they share a similar mechanism of activation of their signalling and downstream effectors. For instance, similar to the NOD2 signalling pathway, the activation of both IL-1R and TNFR1 requires ubiquitination on their corresponding adaptor proteins, IRAK1 and RIPK1, respectively. The poly-ubiquitin chain on these proteins can further recruit IKK and subsequently promote the degradation of IκBα and the activation of transcription factor NF-κB (Figure 1.3) [7].

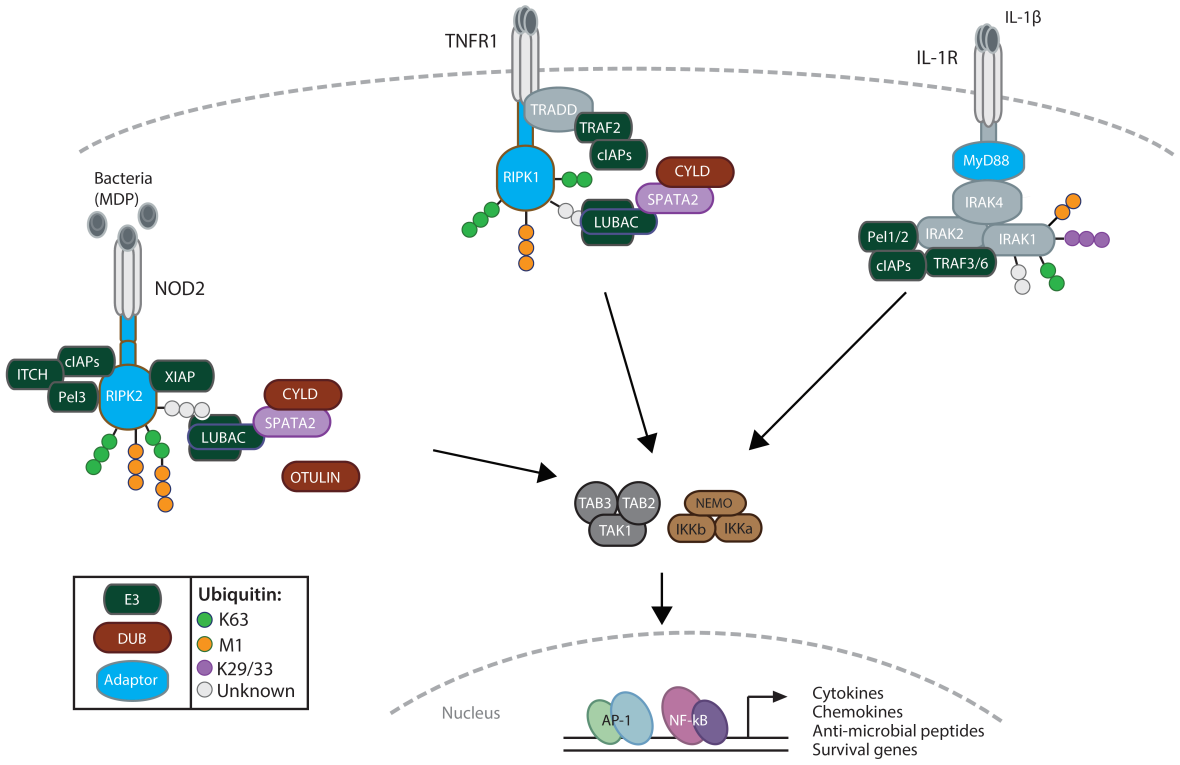


Figure 1.3 NOD2-, TNFR1- and IL-1R-mediated signalling. The activation of NOD2, TNFR1 and IL-1R shares similar mechanisms, as they all regulated by their corresponding ubiquitin ligases and deubiquitinating enzymes (DUBs). The ubiquitination and activation of their adaptor proteins facilitate the recruitment of the downstream kinases, such as TAK1 complex (consisting of TAB2, TAB3 and TAK1) and IKK complex (consisting of NEMO, IKKβ and IKKα), which subsequently phosphorylate and activate the downstream transcription factors, including AP-1 and NF-κB.

1.1.4 IL-1R receptor signalling pathway

During inflammation, cells release inflammatory cytokines, which can cause vascular changes and activation of leukocytes [34, 35]. Interleukin-1 (IL-1) is one the most studied cytokines that regulates the inflammatory response [36]. For example, IL-1 can promote the expression of cyclooxygenase, which can lead to the increase of prostaglandins, another pro-inflammatory mediator [37]. It can also regulate the expression of other chemokines, adhesion molecules, tissue degrading enzymes and acute-phase proteins, such as amyloid A [37].

The biological effect of IL-1 is mediated by type I IL-1 receptor (IL-1RI) [38, 39], which shares a sequence similarity in its cytosolic region with other members in interleukin-1 receptor/Toll-like receptor (IL-1R/TLR) superfamily, such as TLR4 and IL-18R [40, 41]. Therefore, although the ligands for these receptors are different, the mechanism of activation and the downstream effectors of these receptors are very similar. There are three cognate ligands for IL-1RI: IL-1α, IL-1β and IL-1RA [37]. Among which, only IL-1α and IL-1β can trigger IL-1R-mediated signalling, whereas IL-1RA functions as IL-1RI antagonist by competitive binding with IL-1RI and thus inhibits the interaction between IL-1α/ IL-1β and IL-1R [37, 42].

The activation of the IL-1R/TLR superfamily begins with formation of a complex containing the core adaptor protein MyD88, which recruits IRAK proteins to the complex [43, 44]. Similar to NOD2 activation, the activation of IL-1R also requires ubiquitination of its adapter protein MyD88 and IRAK1 [7, 37]. Transcription factor NF-κB and p38 MAPK are two key signalling molecules activated by IL-1 [45]. Both are also activated by the ligands of other members within IL-1R/TLR superfamily, such as IL-18 (by IL-18R) and LPS (by TLR4) (Figure 1.4).

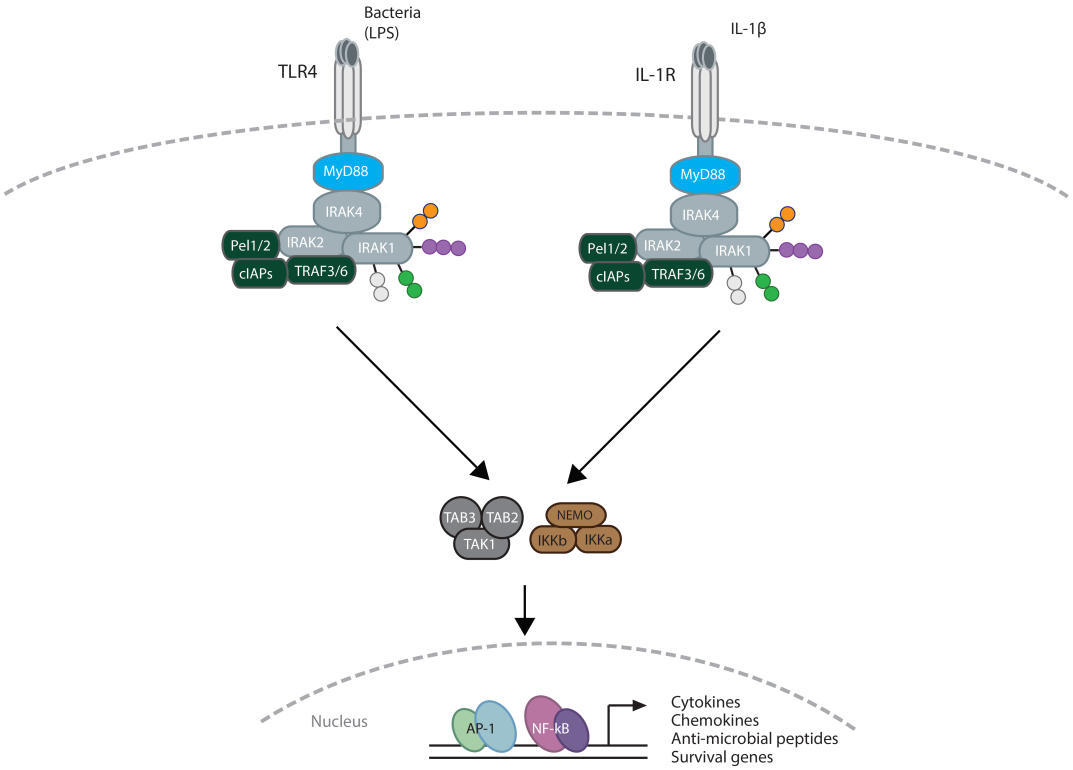


Figure 1.4 IL-1R/TLR -mediated signalling. The activation of TLR4 and IL-1R signalling shares a similar mechanism. The ubiquitination and activation of their adaptor proteins can facilitate the recruitment of the downstream kinase complexes including the TAK1 complex and IKK complex, which subsequently activate the downstream transcription factors AP-1 and NF-κB.

1.1.5 TNF receptor signalling pathway

TNF is a transmembrane protein on the cell surface and can be cleaved by tumour necrosis factor converting enzyme (TACE) to generate its soluble form [46, 47]. There are two types of TNF receptors, TNFR1 and TNFR2 [46, 48]. The binding affinities of TNFR1 with either membrane-bound TNF or soluble TNF are both very strong, whereas TNFR2 has much higher affinity with membrane-bound TNF [49]. Although both receptors have four homologous cysteine-rich domains (CRDs) in their extracellular region, their intracellular structures are different. Both TNFR1 and TNFR2 can interact with the TRAF family proteins and mediate the signalling. Compared with TNFR1, TNFR2 lacks an intercellular region called death domain (DD), which can mediate homo/hetero-typic interactions with other DD-containing proteins, such as RIPK1, FADD and TRADD [49, 50]. By interacting with DD-containing adaptor

proteins, TNFR1 can activate the transcription factor NF-κB and MAPK signalling as well as TNF-induced cell death, whereas TNFR2 cannot mediate TNF-induced cell death as it lacks DD [51, 52]. TNFR1 is ubiquitously expressed in most cell types whereas TNFR2 is specifically expressed in immune and endothelial tissues, hence TNFR1 plays a dominant role in mediating the biological effects of TNF [46].

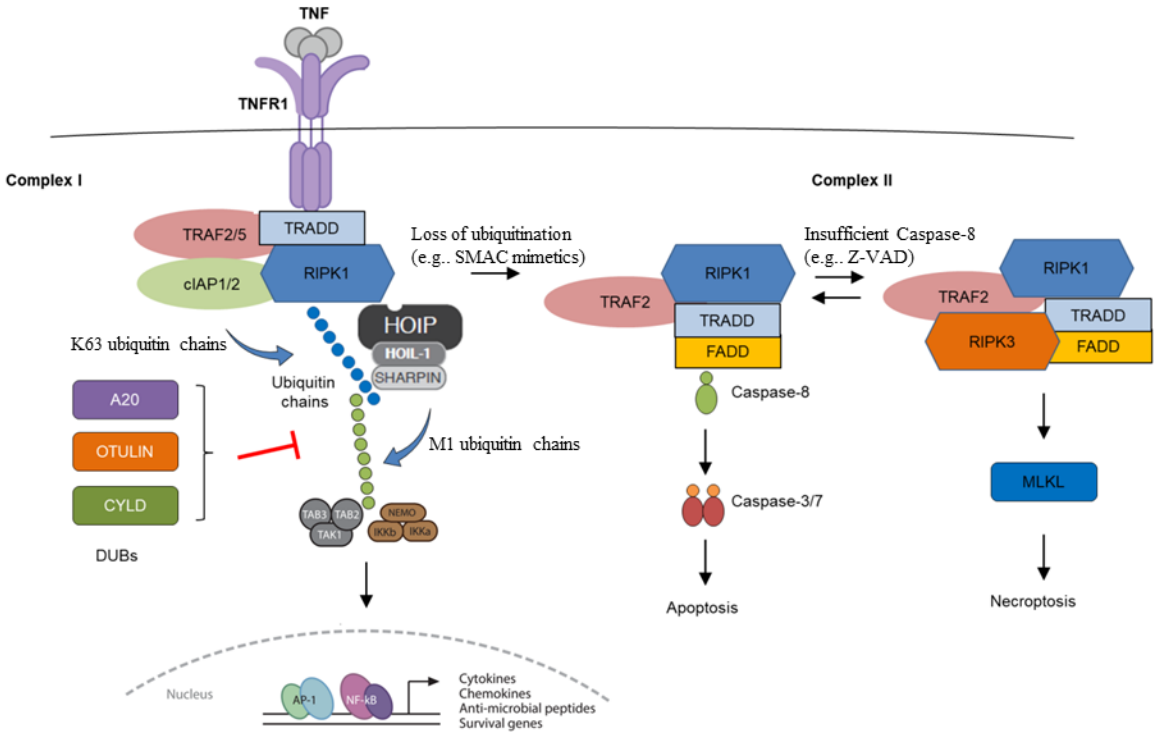


Figure 1.5 TNF signalling pathway. TNF regulates pro-inflammatory signalling and cell death via complex I and complex II, respectively. The activation of TNF receptor 1 (TNFR1) by soluble TNF triggers the oligomerisation of TNFR1 and the recruitment of its adaptor proteins including TRADD and RIPK1 to form pro-inflammatory complex I, which subsequently activates the downstream transcription factors including AP-1 and NF-κB. Complex I can also switch to pro-cell death complex II, which can promote apoptosis and necroptosis in a context dependent manner.

The TNFR1 signalling pathway is one of the most extensively studied cytokine receptor signalling pathways (Figure 1.5). Similar to NOD2 and IL1R signalling pathway, the activation of TNFR1 also involves poly ubiquitination and phosphorylation cascades [7]. Binding with TNF triggers the trimerisation of TNFR1 and promotes the assembly of TNFR1-associcated signalling complex (Complex I). Complex I consists of the adaptor proteins RIPK1 and TRADD, which are recruited to TNFR1 through their death domains [53]. Subsequently,

additional adaptor proteins including TRAF2 and TRAF5, are further recruited to complex I, allowing the engagement of the ubiquitin ligases c-IAP1 and c-IAP2, which promote the ubiquitination of various components within the complex [54, 55]. The poly ubiquitin chains provide a docking platform for recruiting additional proteins, such as the LUBAC complex [56]. LUBAC consists of 3 components, including SHARPIN, HOIL and HOIP. LUBAC promotes linear ubiquitination on several proteins within the TNFR1 complex, including TNFR1, RIPK1 and LUBAC itself [57, 58]. With the assistance of various types of ubiquitin chains, the signalling kinase complexes comprising of IKKα, IKKβ and NEMO, and TAK1 are recruited [56, 59]. The assembly of kinase complexes promotes the phosphorylation on NF-κB inhibitor IκBα and subsequently degradation, leading to the activation of NF-κB and MAPK signalling and subsequent gene expression [46].

In addition, these complexes are also negatively regulated by deubiquitinases (DUBs). For example, TNFAIP3 or A20, comprises DUB activity and it is also a NF-κB target gene, which can be induced by TNF, thus forming a feedback loop in regulating the activity of complex I [60]. Additional DUBs against K63 ubiquitin chains such as CYLD [61, 62], and those against linear ubiquitin chains such CYLD and OTULIN are also found dampening NF-κB activation [63-65]. Thus, fine-tuning the balance between ubiquitin ligases and DUBs in regulation of ubiquitin chains is essential for complex I-mediated signalling and subsequent gene expression.

RIPK1 not only can form pro-inflammatory signalling complex I, it also forms complex II, which promotes cell death via apoptosis or necroptosis (Figure 1.5) [46, 53, 66, 67]. Both apoptosis and necroptosis are forms of programmed cell death [68]. Apoptotic cell death is mediated by Caspase activation, whereas necroptotic cell death is induced by RIPK1-RIPK3-MLKL-mediated cell membrane permeabilisation. Necroptosis plays important roles during pathogen-mediated infections. For example, during viral affection, Caspase-dependent apoptosis can be inhibited by the viral Caspase inhibitors. Thereby, “cellular suicide” mediated by

Caspase-independent necroptosis can restrict virus replication and facilitate immune defence [69].

The formation of complex II is caused by the alterations of RIPK1 modification and other components within TNFR1 complex. The alterations of ubiquitin modifications play a critical role in regulating the assembly of RIPK1-dependent apoptotic complex II [53, 54, 70]. For instance, when ubiquitin ligases c-IAP1/2 are degraded by SMAC mimetics, unmodified RIPK1 dissociates from complex I and interacts with FADD through binding of their death domains. The association between RIPK1 and FADD further recruits pro-Caspase-8 to form complex II, which subsequently promotes apoptotic cell death. Similar to viral affection, this complex can switch from pro-apoptosis to pro-necroptosis if Caspase-8 is insufficient or inhibited [71-74]. For instance, when cells are treated with TNF and SMAC mimetics, the cells are going to apoptotic cell death. If the cells are additionally treated together with pan-Caspase inhibitor z-VAD-FMK (zVAD), instead of blocking apoptosis, it will trigger RIPK3-mediated formation of the necrosome (a protein complex consists of RIPK1, RIPK3 and MLKL) and subsequent phosphorylation and activation of MLKL by RIPK3, allowing MLKL to insert into and permeabilise cell membranes, thus resulting in necrotic cell death [69].

1.1.6 Interferons (IFNs) and IFN-γ signalling pathway

Interferons are found as group of cytokines that have anti-viral activity. The activation of interferon response relies on the binding of IFNs to a specific surface receptor, leading to the activation of a signal transduction cascade that ultimately regulates a broad range of interferon-regulated genes (IRGs). They can activate immune cells, such as natural killer (NK) cells and macrophages [75]. In addition, adaptive immune response can also be activated by interferons as IFN-induced antigen presentation can mobilise T cells. IRGs are now known involved not only in immune response, but also in regulation of many other biological processes, such as cell proliferation, metastasis and angiogenesis [76, 77].

There are three major types of interferons identified in humans, including type I IFN (IFN-α, IFN-β, IFN-ε, IFN-κ and IFN-ω), type II IFN (IFN-γ) and type III IFN (IFN-λ) [78]. All three types of interferon play important roles in many aspects of immunity, such as regulation of host-pathogen interactions, viral replication and cancer immunity [2, 78-80].

IFN-α and IFN-β are the best defined and the most broadly expressed type I IFN and they are best known for their activity of interfering with viral replication [81]. Almost all nucleated cells respond to type I IFN, whereas the type III IFN response is restricted to non-haematopoietic cells, owing to the restricted expression of the IFN-λR [82]. IFN-α and IFN-β also regulate the innate and adaptive immunity against other invading pathogens, including bacteria, parasites and fungi [83]. Additionally, type I IFN play important roles in multiple cancer therapeutic strategies [84-87], including radiotherapy, chemotherapy and immune therapy. Type I IFN can act directly on cancer cell to promote apoptosis [88] and they also trigger anti-cancer immune responses, both of which determine the efficacy of these therapeutic treatments.

IFN-γ is a homodimer comprised of two 17 kDa polypeptide subunits [89] and it is a single gene product from the type II IFN family. Type II IFN can potentiate type I IFN-mediated immune responses [90] and it also stimulates bacterial killing mediated by macrophages [91]. Notably, Type II IFN also plays a pivotal function in cancer immunity [92].

The secretion of IFN-γ is predominantly by activated lymphocytes, including CD4 T cells, CD8 T cells, γδ T cells and NK cells [93-96]. It can also be produced by NKT, B cells and antigen presenting cells, albeit to a lesser extent [97-100]. Apart from type I and type III IFN, which are induced by PAMPs and DAMPs, IFN-γ is predominantly induced by mitogens and cytokines, including IL-12, IL-15, IL-18 and type I IFN [101-105]. The pleiotropic functions of IFN-γ are achieved by cell-specific responsiveness and the expression of hundreds of IFN-γ-regulated genes, consisting of antigen presentation molecules, cell death regulators and

transcription factors [78].

The recognition of IFN-γ is mediated by the IFN-γ receptor, which is a hetero-tetramer consisting of two IFN-γR1 and two IFNγR2 chains. IFN-γR1 is responsible for direct binding with IFN-γ on the cell surface, while IFN-γR2 plays an essential regulatory function [106]. Although IFN-γR1 and IFN-γR2 work together, their expression pattern is different. IFN-γR1 is ubiquitously expressed in almost all cells with a moderate expression level, whereas IFN-γR2 expression is more dynamically regulated [78]. For example, *IFNGR2* mRNA level is downregulated in Th2 cells when stimulated with IFN-γ, whereas IFN-γR1 is not affected [107]. Hence, IFN-γR2 expression can be a regulatory component in IFN-γ signalling and modulate the subsequent activation of gene expression in immune response [106].

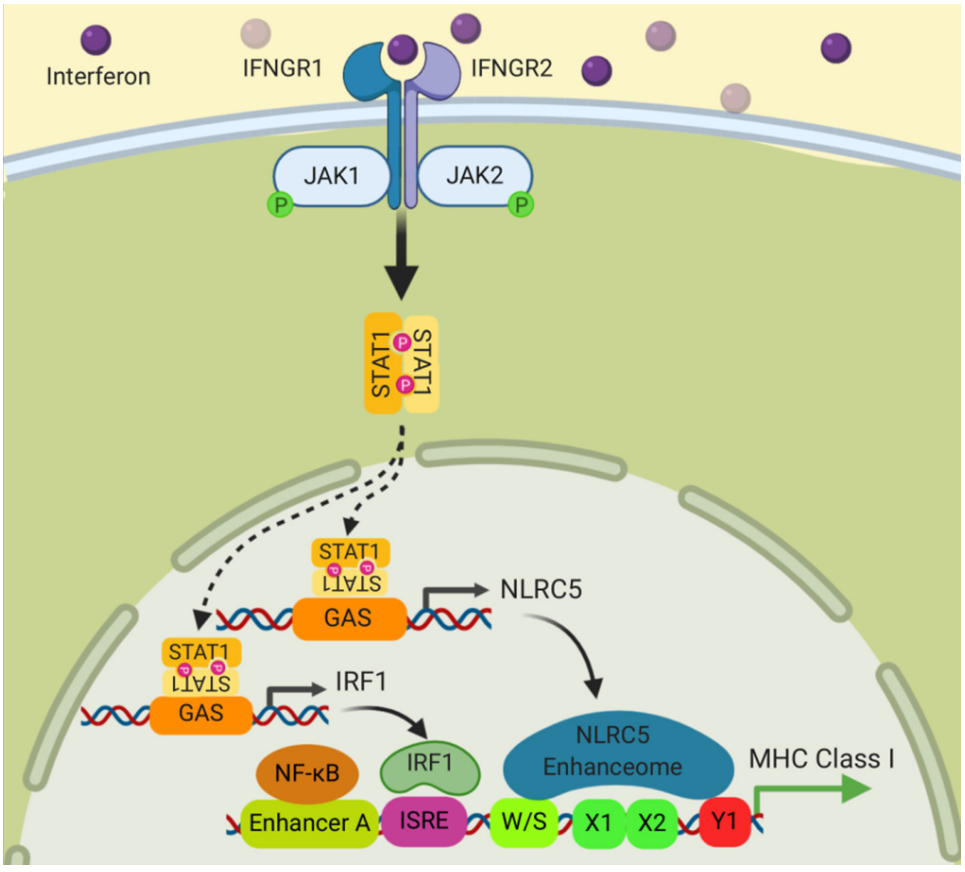


Figure 1.6 IFN-γ signalling pathway (Front Immunol. 2021; 12: 636568). The activation of IFN-γ signalling requires the phosphorylation of JAK1/2 and activation of STAT1. The phosphorylation of STAT1 triggers its homodimerisation and translocation to the nucleus, where STAT1 promotes the expression of IFN-γ-induced genes, including *NLRC5* and *IRF1*. These gene products function as transcription factors and they work together with NF-κB to promote the expression of genes in regulation of antigen presentation, such as MHC-I.

IFN-γ exerts its biological effects via activation of intracellular molecular signalling pathways, mainly through JAK-STAT signalling pathway, which modulates the transcriptional expression of hundreds IFN-γ induced genes (Figure 1.6) [108]. IFN-γR2 increases the binding affinity between IFN-γR1 and IFN-γ. Upon IFN-γ binding, IFNγ-R2 oligomerises through its intracellular domain and activates the downstream kinases JAK1 and JAK2 [109]. The activation of JAKs phosphorylate IFN-γR1 and thus create binding sites on the intercellular domains of IFN-γR1 for the transcription factor STAT1, which can be further phosphorylated and activated. Then the activated STAT1 translocates to the nucleus and promotes the expression of early response genes, such NLRC5 and IRF1 [78]. Both NLRC5 and IRF1 are transcription factors, which can cooperate with other transcription factors such as NF-κB, to regulate hundreds of secondary response genes, including chemoattractant gens *CXCL9*/*10*/*11* and components in antigen presentation, such as MHC-I [109].

1.1.7 Mechanisms underlying IFN-γ anti-tumour effects

The anti-tumour immunity induced by IFN-γ was initially noticed by increased tumorigenicity of cells with IFN-γR1 loss [110]. Later studies showed that tumour cells lacking IFN-γR1 grow as aggressively in immune-competent mice as in immune-deficient mice, whereas reintroducing IFN-γR1 expression in the *IFNGR1* deficient cells can increase the immunogenicity and promote T cell-dependent tumour rejection [108, 111].

IFN-γ exerts its anti-tumour properties mainly by two ways, immunity related and non-immunity related. The non-immunity related mechanisms include the direct effect on target cells and the influence on the supporting cells [108, 111]. IFN-γ directly regulates the expression of cyclin-dependent kinase inhibitor 1 (P21) through STAT1 activation in tumour cells, thus regulating the target cell proliferation [112, 113]. It also directly regulates the expression or secretion of Caspase-1/3/8, FAS and Fas ligand (FasL), regulating cell death of the target cells [114-117]. In addition, IFN-γ affects the cells within the tumour microenvironment. For

instance, IFN-γ impairs angiogenesis by inhibiting proliferation and promoting cell death of vascular endothelial cells, resulting in blood vessel destruction, an important mechanism that leads to tumour rejection [118-120]. This anti-angiogenesis property is not only restricted to IFN-γ, but also to the products of its target genes, such as CXCL9 and CXCL10 [78, 121, 122].

More importantly, the property of IFN-γ anti-tumour effect is more related to its function in promoting adaptive immunity (Figure 1.7) [78]. The target genes *CXCL9*, *CXCL10* and *CXCL11* of IFN-γ encode critical chemoattractant for infiltration of T cell, NK and NKT cell into the tumours [123, 124]. The migration of T cells to the tumour site is compromised in IFN-γ-deficient mice. In addition, IFN-γ can reverse the immunosuppressive functions of myeloid cells in tumours (Figure 1.7) [125, 126].

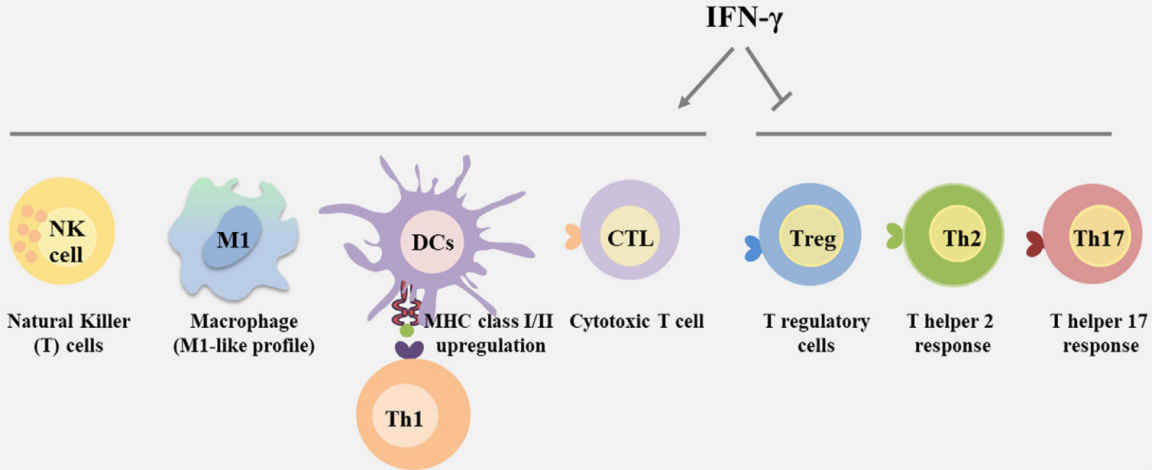


Figure 1.7 IFN-γ promotes anti-tumour immunity (Front Immunol. 2018 May 4;9:847). IFN-γ has multiple functions in regulating different types of immune cells. IFN-γ can activate NK cells, promote the polarisation of M1 macrophages, facilitate the antigen presentation process mediated by dendritic cells (DCs) and potentiate the cytotoxicity of T cells, whereas the functions of immune suppressive T cells are inhibited by IFN-γ.

Another important aspect regulated by IFN-γ is the Major Histocompatibility Class I (MHC-I) [127], which bind peptides and present this antigenic information on the cell surface, allowing CD8 T cells to recognise those cells that express non-self or abnormal peptides arising from mutations as is the case for cancer cells. IFN-γ plays an essential role in regulation of the expression of genes involved in antigen presentation mediated by MHC-I (Figure 1.8),

including MHC-I heavy chain, B2M, TAP, Tapasin and ERAP1. Most of these components have transcription binding sites for IRF1 and NLRC5 in the promoter regions [78, 108, 111], which are the downstream effector of IFN-γ signalling (Figure 1.6). This allows coordinated regulation of the expression of these genes by IFN-γ. Notably, antigen presentation by MHC-I is prerequisite for CD8 T cell-dependent immunity [128]. Considering CD8 T cell plays a major role in tumour immune surveillance, regulation of antigen presentation by MHC-I is hence closely related to tumour immune evasion.

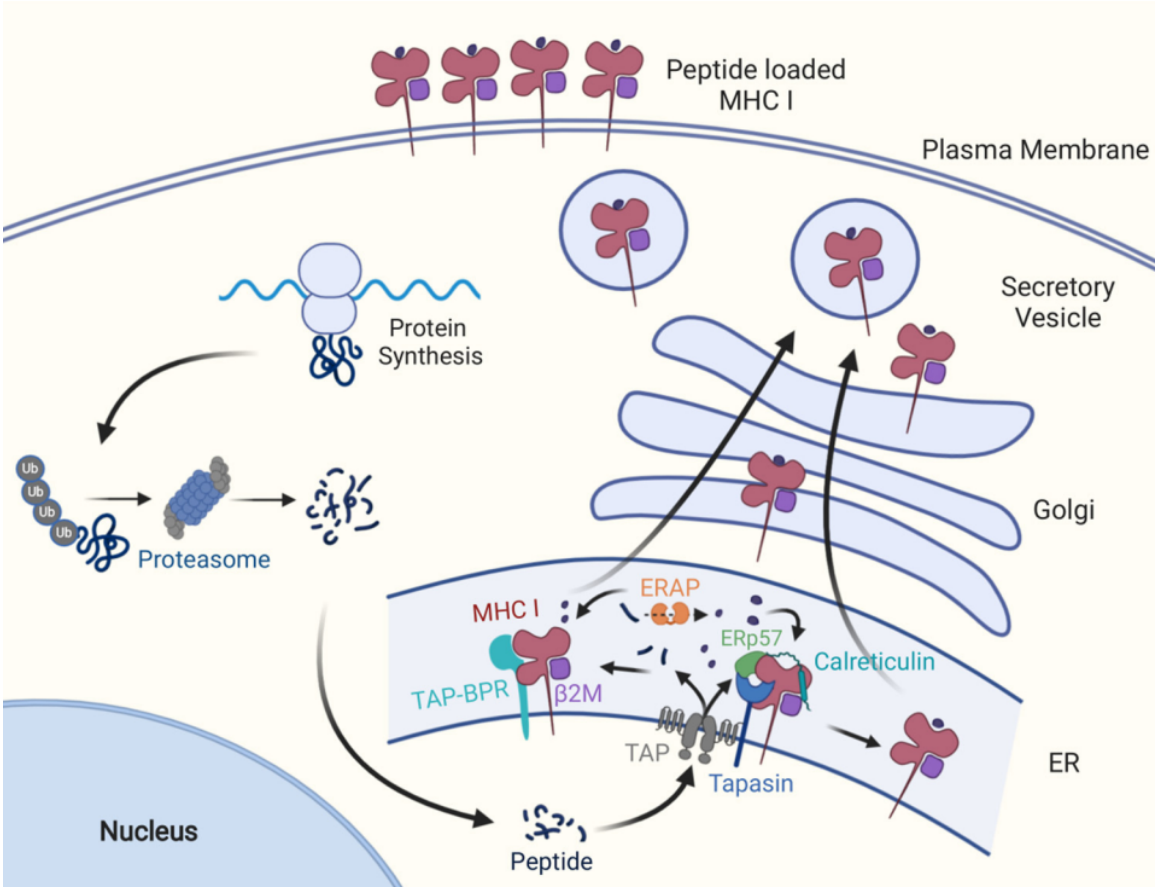


Figure 1.8 IFN-γ signalling induces antigen presentation (Front Immunol. 2021; 12: 636568) Peptides derived from proteasome degradation were loaded onto MHC-I in the ER lumen mediated by multiple antigen presentation factors including TAP-BPR, ERAP, TAPs and β2M. The peptide-loaded MHC-I molecules were then translocated and presented on the cell surface.

Deficiency or downregulation of MHC-I has been described in 40–90% of human tumours, which often correlates with worse prognosis [129]. Regarding the importance of IFN-γ signalling in cancer, IFN-γ-associated gene signatures positively correlate with cancer immune

phenotypes. Moreover, higher IFN-γ gene signatures function as a marker for predicting the efficiency of chemotherapy, radiotherapy and also for immunotherapy [130]. However, the molecular mechanisms leading to downregulation of IFN-γ signalling and MHC-I deficiency or downregulation in human cancers have remained ill defined.

1.1.8 Immune regulation by microenvironment

Cells are sensitive to their surrounding microenvironmental cues, such as extracellular matrix, mechanical force, pH and oxygen levels. These microenvironmental cues can modulate immune cell behaviour in inflamed tissues and also in tumours [131]. The extracellular matrix has been shown to regulate adaptive tumour responses by modulating T cell migration, activation and proliferation [132, 133]. The infiltration of monocytes into inflamed tissues is also regulated by the interaction between extracellular matrix and secreted proteases [134]. Additionally, the pH of the extracellular milieu has a direct impact on a broad range of immunological functions, including regulation of lymphocyte cytotoxicity, lymphocyte proliferation, chemotaxis of neutrophils and the activation of complement pathway [135-138].

The oxygen level plays an important part in the microenvironment. Low oxygen availability is a feature of most solid tumours, in part, because of the increased oxygen consumption due to the rapid growth of tumour cells. Some important immunotherapy targets are regulated by hypoxia, including CD137, OX40, FOXP3 and PD-L1 [139-142]. Hypoxia also has been shown to promote tumour progression through promoting the polarisation of immunosuppressive tumour-associated macrophages [143]. However, detailed molecular mechanisms of how hypoxia regulates immune signalling are still poorly understood. A better understanding of the interplay between oxygen sensing and immune signalling is warranted to improve the therapeutic avenues against cancer.

1.2 Oxygen sensing and hypoxia response

Oxygen plays a central role in the maintenance of life, at least for aerobic organisms, where oxygen is primarily involved in mitochondrial respiration and also protein maturation, such as di-sulphide bond formation [144]. To maintain oxygen homeostasis, higher eukaryotic cells have evolved oxygen sensing mechanisms and hypoxia responses [145]. These mechanisms are extremely conserved between species, indicating their important roles during development and under physiological or pathological conditions [145].

1.2.1 Oxygen sensing is evolutionarily conserved

2.5 billion years ago, oxygen started to accumulate in the atmosphere, leading to the evolution of a highly efficient ATP generating system, namely oxidative phosphorylation [146]. This system allows cells to extract more energy by breaking down the carbon-carbon covalent bond of organic compounds, whereas the energy derived from fermentation is insufficient for the cells to achieve more biological activities [147]. The diffusion of oxygen by passive movement of oxygen molecules is sufficient for some simple multicellular organisms, such as *c. elegans*. However, this may restrict the development of higher multicellular organism, as more complicated biological activities require more energy as well as oxygen. Hence, this led to the evolution of more complicated respiratory systems, which co-evolve with other systems including circulatory systems, digestive systems and nervous systems [147]. Cellular oxygen sensing systems are also evolved and kept until today. This explains why some oxygen sensors and effectors, such as prolyl hydroxylase domain (PHD) enzymes and hypoxia inducible factors (HIFs), are highly conserved among species, from worms, fruit flies to humans [148-150].

1.2.2 Hypoxia inducible factors in regulation of hypoxia signalling

One of the best described mechanisms of how cells respond to hypoxia is through hypoxia inducible factors (HIFs), a family of transcription factors mediating the cellular responses to low oxygen tension [147, 151]. The reason why it was named as hypoxia inducible factor is because it is stabilised under hypoxia. HIF family contains 6 members, including HIF1α, HIF1β, HIF2α, HIF2β, HIF3α and HIF3β [152]. They form heterodimers consisting of an oxygen sensitive HIFα protein subunit and a constitutively expressed HIFβ protein subunit [147, 153]. HIF1 and HIF2 are transcription factors mediating the cellular response to hypoxia, whereas HIF3α lacks of the transactivation domain found in HIF1α and HIF2α, thereby HIF3 is believed playing an inhibitory role during hypoxia response mediated by HIF1 and HIF2 [154-156]. Both HIF1α and HIF2α are important regulators during hypoxia as their broad impact on the transcriptome, including hundreds of hypoxia-induced genes [151]. These genes are mainly involved in metabolism, such as genes in glucose catabolism and mitochondrial genes involved in oxidative phosphorylation. Upregulation of these genes during hypoxia affects multiple biological functions, such as anaerobic metabolism, vasodilation and erythropoiesis [157-160], which ultimately facilitate cellular adaptions to low oxygen conditions and promote cell survival [151].

Comparing with the ubiquitous expression of HIF1α in nearly all cell types, the expression of HIF2α is restricted to specific cell types, such as endothelial cells, glial cells, cardiomyocytes, pancreatic interstitial cells, kidney fibroblasts and hepatocytes [161-164]. The heterodimeric transcription factor HIF2 shares certain overlapping target genes with HIF1, but HIF2 also has its unique targets including the genes in regulation of metabolism, such as the anti-oxidant enzyme SOD2 and HMOX1 [165, 166]. This specific activity of HIF2 is believed to be a critical driver for tumour progression in various types of cancer by downregulation of p53 activity and promoting MYC activity [167-169]. In addition, HIF2 was shown to be critical in driving hypoxic response under prolonged hypoxia, whereas HIF1 regulates the initial response

to hypoxia, thereby a switch from HIF1-dependent to HIF2-dependent hypoxia response is believed to facilitate a more aggressive tumour growth under prolonged hypoxic microenvironment [168].

Beyond the role of HIF2α as a component of transcription factor complex, it is also a component of a hypoxia-induced cap-dependent translation initiation complex, which comprises of RNA binding motif protein 4 (RMB4) and translation initiation factor eIF4E2. This hypoxia-induced form of the translation initiation complex suggests a close connection between oxygen sensing and protein translational regulation [170].

HIF3α competitively binds to HIFβ subunits, resulting in inhibition of HIF1 and HIF2 transcriptional activities, thereby it is believed having a dominant negative role in regulating the expression of HIF1 and HIF2 target genes [154]. However, recent studies showed that HIF3α also possesses transcriptional activity although it lacks of the transactivation domain found in HIF1α and HIF2α [171]. The functions of HIF3α remain to be fully revealed, however, it is an important hypoxia-induced factor for fine tuning cellular hypoxia response under physiological and pathological conditions [172, 173].

1.2.3 HIF prolyl hydroxylases regulate the stability and activity of HIFs

HIFα subunits are regulated by a similar mechanism under normoxic condition. Specifically, HIFα subunits are unstable under normoxic condition and constitutively being degraded, but rapidly stabilised under low oxygen condition (Figure 1.9) [151, 153]. The degradation of HIF1α is mediated through hydroxylation on prolines 402 and 564 of human HIF1α (Pro405 and Pro531 of HIF2α) by the PHD enzymes [148, 150, 174]. The hydroxylated HIF1α can be recognised by the ubiquitin ligase complex VHL, which subsequently promotes HIF1α poly-ubiquitination and degradation [175].

Three HIF prolyl hydroxylases (PHD1–3) and one asparaginyl hydroxylase, known as factor inhibiting HIF (FIH), have been identified [153]. These enzymes all belong to the non-

haem, Fe^{2+}-dependent, 2-oxoglutarate (2-OG)-dependent oxygenase superfamily (Figure 1.10). Oxygen is one of the substrates for hydroxylation on HIF1α by PHD enzymes, which have a low binding affinity with oxygen, conferring their sensitivity to oxygen levels [150, 176]. Iron binding by PHD, as well as other 2-oxoglutarate-dependent oxygenases is relatively unstable, resulting in these enzymes are readily inhibited by iron chelators, such as desferrioxamine (DFO), or by substitution with other divalent metal ions, including Co^{2+}, Cu^{2+}, Zn^{+} and Mn^{2+} [177, 178]. The presence of Fe^{2+} at the active site is required for binding with another substrate 2-OG, both of which are essential for catalysing the hydroxylation reaction [153]. Therefore, the analogues of 2-oxoglutarate, such as dimethyloxalylglycine (DMOG), are used as prolyl hydroxylase inhibitors [179, 180], which competitively bind to Fe^{2+} and inhibit the hydroxylation of HIFs, resulting in stabilisation of HIFs and enhanced its transactional activities even under normoxic conditions.

Apart from prolyl PHD enzymes, another member of dioxygenase family Factor Inhibiting HIF (FIH) is responsible for fine-tuning the transcriptional activity of HIFs. FIH hydroxylates asparaginyl residue 803 (N803) within the transactivation domain of HIF1α under normoxic condition to prevent the transcription co-activator p300 and CBP from binding to HIF1α, resulting in inhibited HIF1 transcriptional activity (Figure 1.9) [181].

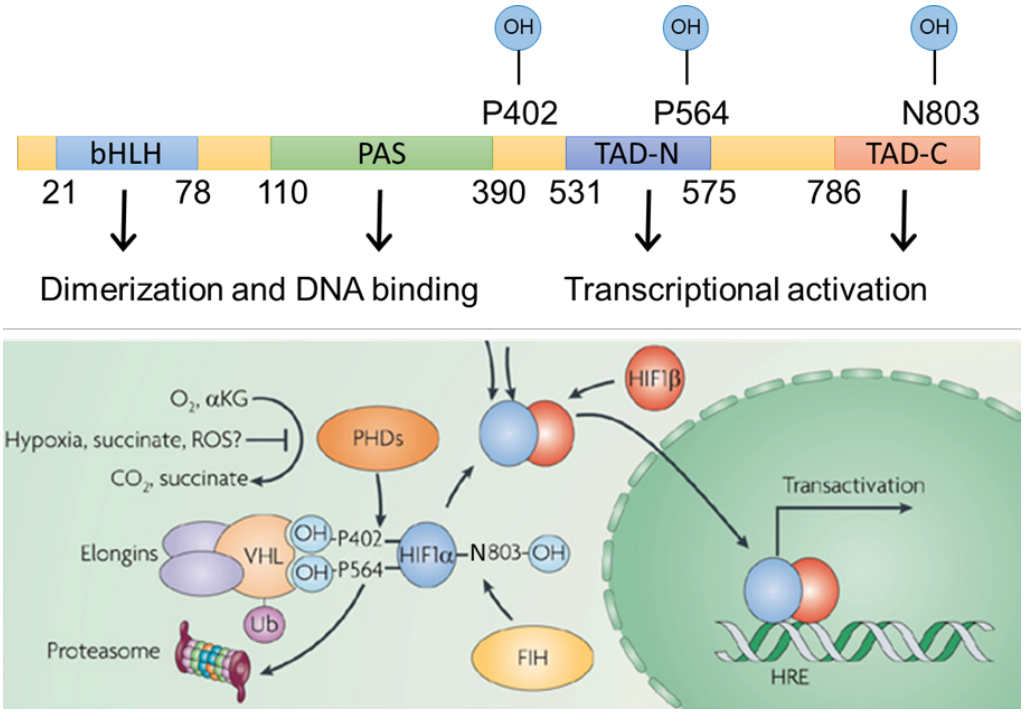


Figure 1.9 Hypoxia stabilises HIF1α (Nature Reviews Cancer 8, 705-713). HIF1α stability and transcriptional activity are regulated via hydroxylation. PHD enzymes hydroxylate HIF1α on P402 and P564 to regulate the binding between HIF1α and the ubiquitin ligase VHL. FIH hydroxylates HIF1α on N803 to regulate its transcriptional activity.

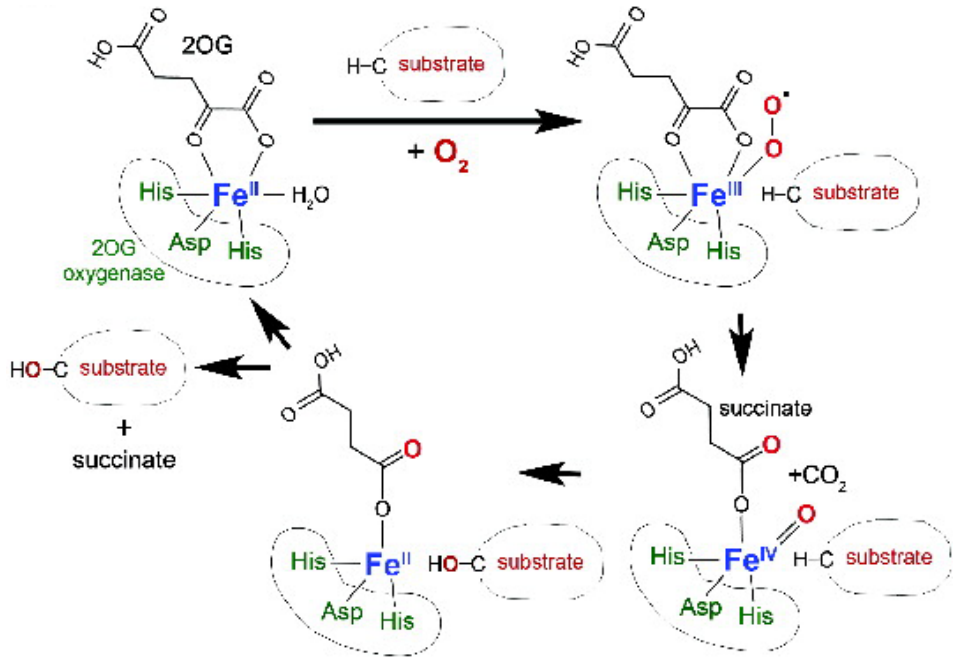


Figure 1.10 2-oxoglutarate (2-OG)-dependent oxygenase hydroxylates the substrates with molecular oxygen (Translation (Austin). 2015 Feb 3;3(1):e1009331). The His-Asp-His motif binds with Fe^{2+}, together with other cosubstrates including 2-OG and molecular oxygen (O_2) at the active site to promote the hydroxylation on the substrate. One oxygen atom from molecular oxygen is incorporated into the hydroxyl group in the substrate and another oxygen atom is incorporated into the by-product succinate.

1.2.4 Tumour hypoxia

Hypoxia is a common feature in most solid tumours [182]. According to different tissue origins of tumours, the severity of hypoxia varies. In solid tumours, oxygen demand is surpassed by its supply due to the rapid proliferation of tumour cells and blood vascular abnormalities. Oxygen levels in tumour tissues are reduced relative to the respective normal tissues, with an oxygen level between 0.8%-2.2% (Table 1.1) [182].

Table 1.1 Comparison of the oxygenation in organs and respective tumours

Tissue/organ	Median % O_2	Cancer	Median % O_2
Brain	4.6	Brain tumour	1.7
Breast	8.5	Breast cancer	1.5
Cervix	5.5	Cervical caner	1.2
Kidney cortex	9.5	Renal cancer	1.3
Liver	4.0-7.3	Liver cancer	0.8
Lung	5.6	Non-small-cell lung cancer	2.2
Pancreas	7.5	Pancreatic tumour	0.3
Rectal mucosa	3.9	Rectal carcinoma	1.8

Tumour hypoxia affects the clinical outcomes of cancer patients [147, 182]. The cellular hypoxia response facilitates tumour angiogenesis and promotes tumour metastasis [182, 183]. In addition, tumour hypoxia also promotes resistance to treatment such as chemotherapy and radiotherapy [184]. Hypoxia induces the expression of genes involved in cell cycle arrest, which slows down the cellular proliferation, thus protecting the quiescent tumour cells from incorporation of the drugs, such as Fluorouracil (5FU) into DNA [185, 186]. Also, hypoxia promotes drug efflux pump expression and inhibits cellular drug uptake [187]. Hypoxia was recently found to have connections with immune tolerance and immune escape [188], but the

underlying mechanisms are still largely undefined.

1.2.5 Hypoxia in regulation of inflammation

Hypoxia is a common feature during inflammation and HIFs has been investigated in the context of inflammation [189, 190]. There are several reasons for the occurrence of tissue hypoxia in inflammation. First, inflamed tissues have increased demand for oxygen as inflammation increases synthesis of cytokines and pro-inflammatory factors, which is an energy consuming process. Second, recruited immune cells at the inflamed site also increase oxygen consumption, which further lowers regional oxygen levels. Additionally, vascularisation during long term inflammation can disrupt blood oxygen supply, resulting in tissue hypoxia [190-192].

The role of HIFs during inflammation has been extensively studied and they appear to play different roles depending on the cell type [190, 193]. HIFs regulate cellular lifespan, apoptosis and antimicrobial peptide production in neutrophils [194, 195], whereas in macrophage, HIFs regulate polarisation, motility, bactericidal activity and tumour development [195, 196]. HIFs also modulate cell migration, differentiation, antigen presentation and cytokine production in dendritic cells [197, 198]. Additionally, HIFs not only regulate cell survival and differentiation in T cells, but also regulate antibody processing in B cells [189, 190, 193]. Although both HIF1 and HIF2 are activated by hypoxia, their role appears to be different. For example, in intestinal epithelial cells, HIF1 induces the expression of intestinal barrier protective genes and it also modulates ion transport and barrier function, which contribute to gut homeostasis [199-201], whereas HIF2 promotes inflammation [199, 202-204].

The links between hypoxia signalling and inflammation are bidirectional: The HIF-PHD pathway can be activated under normoxic conditions in response to inflammatory stimuli. For instance, LPS-induced upregulation of HIF1α regulates the production of inflammatory

cytokines in macrophages [205-207]. In addition, the activation of T cell receptor (TCR) signalling contributes to the accumulation of both HIF1α and HIF2α, which is important for the function and survival of T cells [208-211].

PHD enzymes not only play a role as an oxygen sensor by regulating HIFs stability, recent studies show that they may also regulate NF-κB activity directly, impacting on inflammation and cancer [212-214]. Similar to HIFs, NF-κB regulates the transcription of a diverse group of genes including cytokines, immune receptors and stress-response genes [215]. In some contexts, hypoxia signalling has been shown to regulate the activity of NF-κB in a HIF-dependent manner [216, 217]. HIF hydroxylases (PHD enzymes and FIH) have been found to interact with multiple components in the inflammatory signalling pathways and to regulate their activity, including cIAP1, RIPK1, RIPK4, IKKβ and IκBα [218-221]. Hypoxia and dimethyloxalylglycine (DMOG) have been shown to inhibit PHD-mediated hydroxylation of IKKβ and consequently activate its kinase activity, promoting the degradation of IκBα and subsequently activate NF-κB under hypoxia [190, 218, 222, 223]. Recently, PHD2 has been shown having anti-inflammatory function in a HIF2α dependent manner in a mouse model [204]. In addition, there are more than a dozen studies showing that hydroxylase inhibitors have anti-inflammatory effects in different inflammation models, as well as in clinical trials (Table 1.2) [189]. Although there is a wealth of data linking hypoxia to inflammation [213], the data is not conclusive as to whether hypoxia attenuates or stimulates inflammation and the molecular mechanisms underlying the regulation of hypoxia on inflammation also are not fully understood. Further studies are needed to understand how hypoxia affects inflammatory responses and the molecular mechanisms by which this occurs.

Table 1.2 Anti-inflammatory effects of pharmacological hydroxylase inhibition

Model	Hydroxylase inhibitor
DSS-induced colitis	DMOG
TNBS-induced colitis	FG4497
TNFΔARE ileitis	DMOG
Clostridium difficile toxin	DMOG
Intestinal ischaemia–reperfusion	DMOG
Indomethacin	DMOG
TNBS-induced colitis	AKB4924
Intestinal radiation injury	DMOG
TNBS-induced colitis	Rosmarinic acid
TNBS- and DSS-induced colitis	TRC160334
LPS-induced sepsis	DMOG
Ischaemic kidney injury	TRC160334
Renal transplant	FG4497
Pseudomonas aeruginosa infection	DMOG
Intestinal fibrosis	DMOG

DMOG, dimethyloxalylglycine; DSS, dextran sulfate sodium; LPS, lipopolysaccharide; TNBS, 2,4,6-trinitrobenzenesulfonic acid; TNFΔARE, targeted Disruption in the tumour necrosis factor (TNF) AU-rich element. [189]

1.3 Regulations of protein translation in eukaryotic cells

One of the mechanisms for cellular adaptation to hypoxia is through regulation of translation. Translation initiation is known to be the rate limiting step for the processes of translation of eukaryotic mRNAs, including initiation, elongation and termination [224, 225]. Comparing with elongation or termination, dynamic regulation at the initiation stage allows for a rapid, reversible and spatial control of gene expression [226].

1.3.1 Current model of translation initiation

Translation initiation on most eukaryotic mRNAs can be cap-dependent or cap-independent scanning of the mRNA by ribosomal 43S preinitiation complexes. The preinitiation complex scans the 5′ untranslated region (UTR) for the first start codon, a process mediated by multiple translation initiation factors [227]. Cap-dependent translation initiation requires the binding between initiation factors and the specially altered nucleotide m^7G (cap) on the 5' end of mRNAs. In addition to the role of cap in initiation, it also regulates mRNA nuclear export, stabilises mRNA from degradation by exonucleases, and promotes mRNA maturation [228-231]. Some mRNAs contain additional elements, such as internal ribosome entry site (IRES) and m6A modification, which mediate their direct bindings to the initiation factors and promote cap-independent translation [232, 233]. The activation of the 40S small subunit is induced by initiation factors eIF1 and eIF1A, together with the DEAD-box RNA helicase eIF4A, eIF4B and eIF4G (together called eIF4F). Initiation factor eIF2 forms a ternary complex with GTP and the initiator tRNA ($tRNA_i^{Met}$) and mediates the binding of $tRNA_i^{Met}$ to the ribosome in a GTP-dependent manner. The base pairing between codon and anticodon allows the displacement of eIF1 from the P-site and locks the 40S small subunit onto mRNA and initiates hydrolysis of eIF2-bound GTP by eIF5, which allows the dissociation of eIF2–GDP, eIF1 and eIF1A, and subsequently assembly with the 60S large subunit to form the 80S ribosome together with the initiator $tRNA_i^{Met}$ (Figure 1.11) [226]. With the help of the guanine nucleotide exchange factor (GEF) eIF2B, the GDP in eIF2 is exchanged for a GTP and the ternary complex reforms for a new round of translation initiation (Figure 1.12) [234].

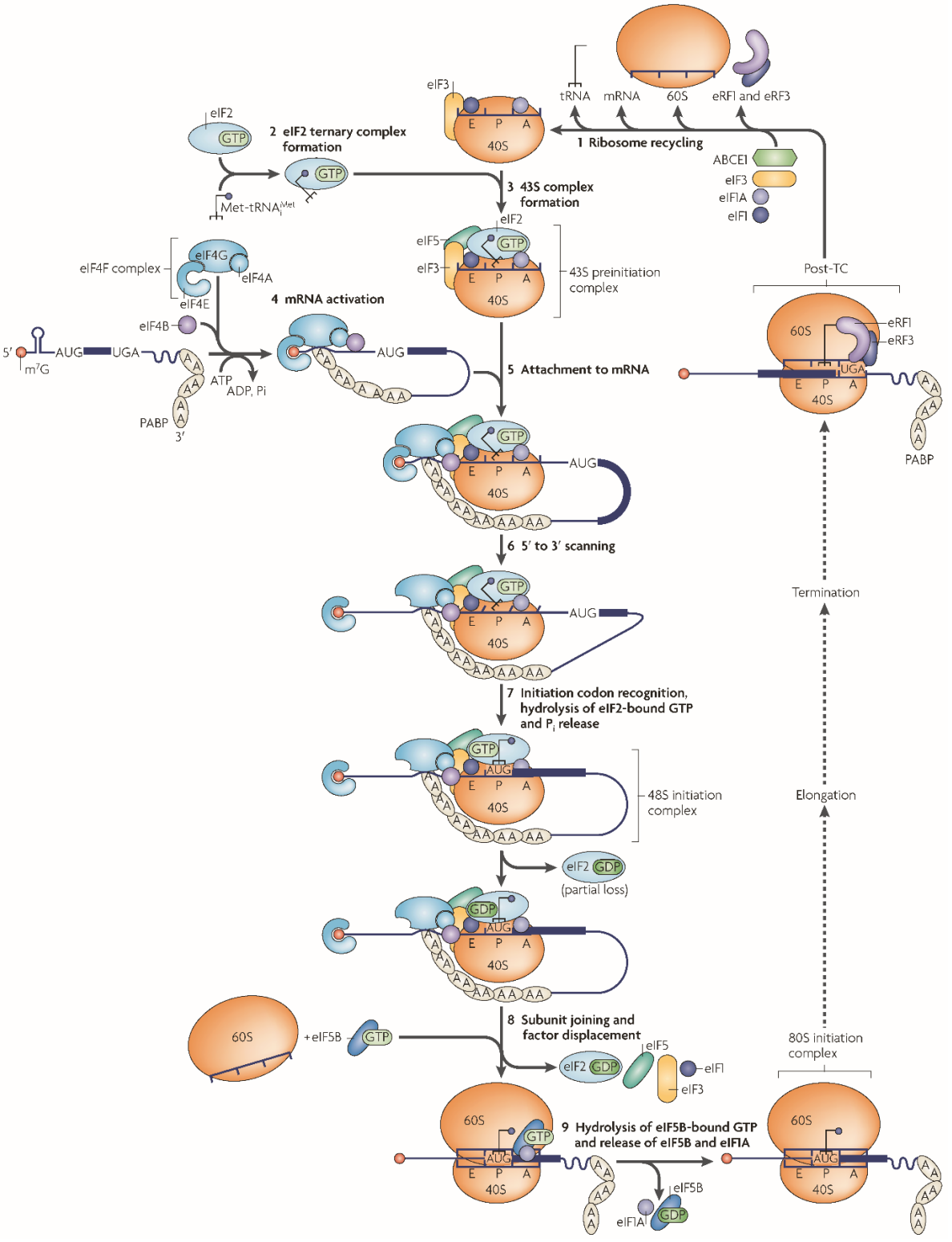


Figure 1.11 Translation initiation (Nat Rev Mol Cell Biol. 2010 Feb;11(2):113-27.). The current model of how protein translation is initiated. The mature mRNA is recognised by the cap binding protein complex eIF4F through eIF4E and activated by initiator $tRNA_i^{Met}$ to form 48S initiation complex with 43S preinitiation complex. Then other initiation factors including eIF3s and eIF5s join and facilitate the binding with 60S large ribosomal subunit to form an 80S initiation complex. Then the 80S complex initiates peptide elongation until the complex is disassembled once it scans a stop codon, a process which is regulated by termination factors. Ribosomes are ultimately released from the mRNA, split into subunits, and are free to bind new mRNAs.

1.3.2 Regulation of initiation factors

Phosphorylation of eukaryotic initiation factors is a mechanism in regulation of the activity of initiation factors. Arguably, the two best-characterised mechanisms in regulation of protein initiation are the phosphorylation of mammalian eIF2 (Figure 1.12) and phosphorylation of 4E binding proteins (Figure 1.13).

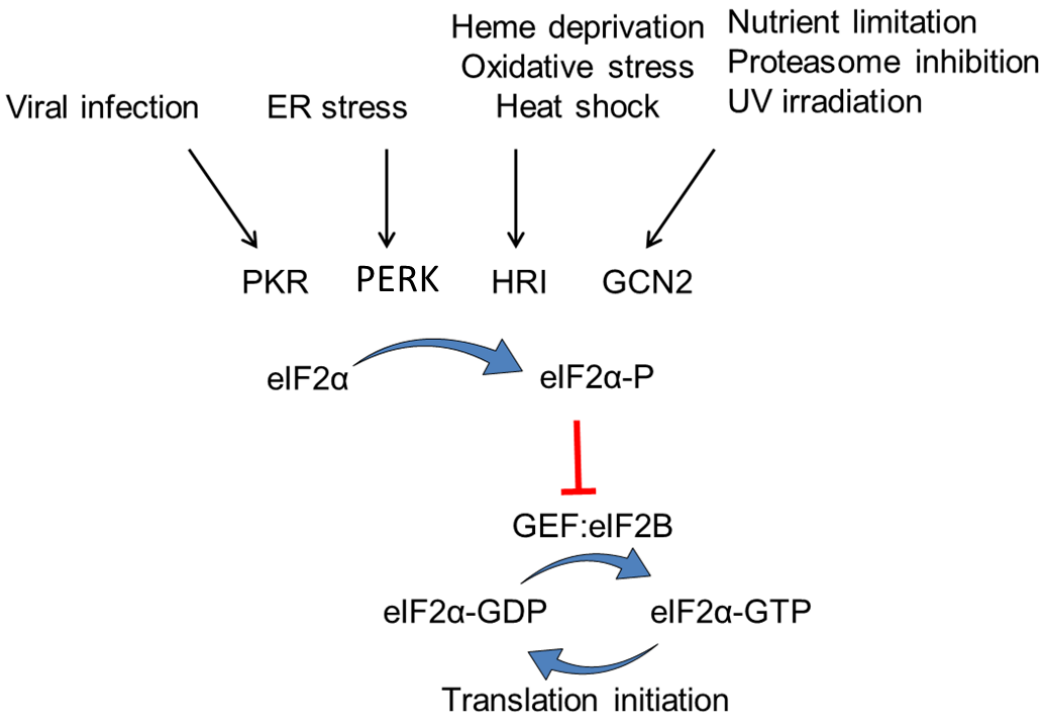


Figure 1.12 Regulation of initiation by eIF2α. Multiple stimuli promote the phosphorylation on eIF2α by various kinases and inhibit translation initiation by restricting the activity of eIF2α. Phosphorylated eIF2 forms eIF2-ternary complex (eIF2-TC) with eIF2B. Once GTP is hydrolysed, eIF2-GDP tightly binds with eIF2B and inhibits its guanine nucleotide-exchange factor (GEF) activity, thus reducing eIF2-TC levels and subsequently inhibiting translation initiation.

To date, eIF2 is known to be phosphorylated by four kinases, including HRI, PKR, PERK and GCN2, in response to different stresses [226, 235, 236]. Haem-regulated kinase (HRI) is significant only in erythroid cells. PKR can be activated by double-stranded RNAs and it plays a role in anti-viral response. PERK is a transmembrane endoplasmic reticulum kinase and can be activated by ER stress due to misfolded proteins in the ER lumen. GCN2 responds to amino acid deprivation. Phosphorylation of eIF2 can form initiation-competent eIF2-ternary complex

(eIF2-TC), however, once GTP is hydrolysed, eIF2-GDP tightly binds with eIF2B and inhibits its guanine nucleotide-exchange factor (GEF) activity, thus reducing eIF2-TC levels and subsequently inhibiting the formation of 80S ribosome. Hence, the general translation of mRNA is reduced.

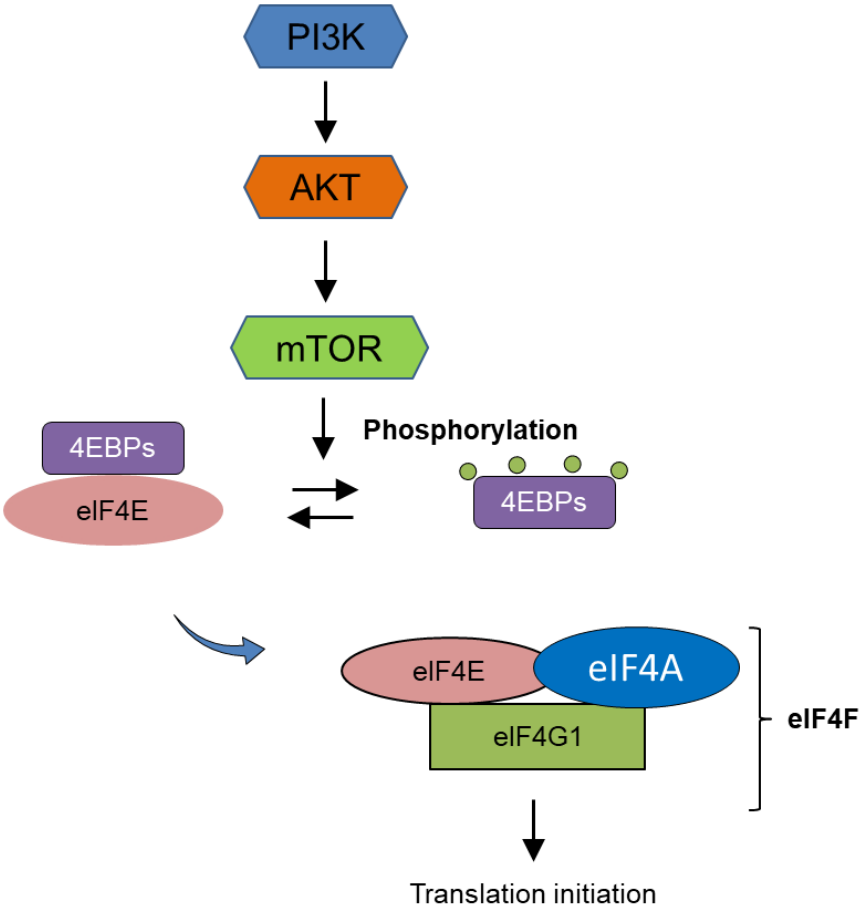


Figure 1.13 Regulation of initiation by mTOR. Phosphorylation of 4EBPs by mTOR kinase restricts its binding with eIF4E and promotes the formation of eIF4F complex. The eIF4F complex facilitates the formation of initiation complex and promotes protein translation.

Phosphorylation can also affect the binding between mRNA and the eIF4F complex [226, 237], which comprises of eIF4A, eIF4E and eIF4G via m^7G cap at the 5' end of mRNA. Phosphorylation on eIF4E-binding proteins (4EBPs) by mTOR, releases eIF4E from 4EBPs, allowing the formation of eIF4F complex, which is required for the initiation.

Phosphorylation on other initiation factors including eIF1, eIF2β, eIF2Bε, eIF3 subunits, eIF4G, eIF4B, eIF4H, eIF5, eIF5B and also on ribosome protein rpS6 has also been reported,

but the phosphorylation on these protein is only associated with the activation of translation [226]. How phosphorylation and other post-translational modification affect the initiation process are still unclear.

1.3.3 Upstream open reading frames (uORFs)

In over 40% of human genes, the first start codon is situated in a short upstream open reading frame within the 5'-untranslated region (UTR) and some genes even have multiple uORFs [238]. However, not every uORF is functional and can be translated, it depends on whether it has a protein translation initiation site, such as the Kozak sequence [239]. In order to start the translation of protein coding sequence (CDS) of uORF(s)-containing mRNA, 80S ribosomes need to finish a full cycle of the translation process of the uORF(s) [240]. Following termination of translation of the uORF, most of the subunits of ribosome are released from these mRNAs and recycled, while some small ribosomal subunits remain attached to the mRNAs and scan for the next start codon to initiate translation of the next open reading frame, a process called translation reinitiation (Figure 1.14) [225]. In general, the presence of uORF restricts the translation efficiency of the main CDS [238] and the sequence of uORF does not determine reinitiation efficiency, but there are some exceptions described in yeast [226].

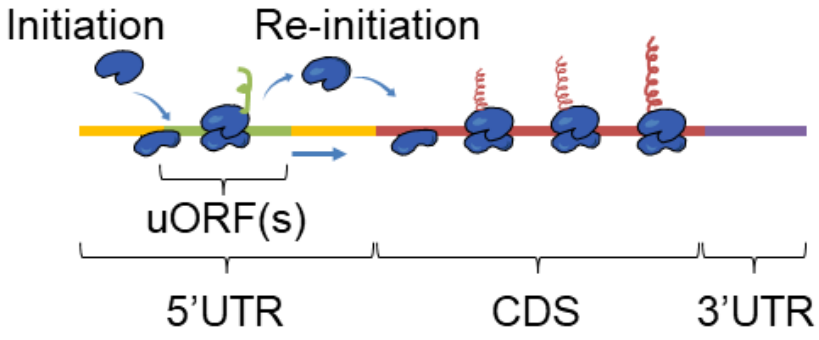


Figure 1.14 Protein translation reinitiation. Ribosome rescans mRNA after translation of the upstream open reading frame (uORF) and reinitiates the translation at the start codon of the CDS.

1.3.4 Hypoxia regulates protein translation

During hypoxia, global protein translation is restricted to conserve ATP consumption, whereas translation of factors, such as HIFs, that are essential for the hypoxia response is maintained. Hypoxia inhibits protein synthesis through multiple mechanisms, including activation of PERK, inhibition of mTOR kinase activity, alteration of ribosome protein modification and tRNA transcription, which are essential mechanisms for cell survival under low oxygen conditions [241-243].

Phosphorylation of eIF2α by PERK during hypoxia has been observed in multiple cell lines established from either normal or cancer cells (Figure 1.12) [244, 245]. The activated PERK phosphorylates and inactivates eIF2α during hypoxia, reducing general protein translation. However, specific gene expression during hypoxia is also regulated by this mechanism, such as activating transcription factor 4 (known as *ATF4*), an important transcription factor during stress conditions [246]. It contains two conserved uORFs at the 5'UTR. The second uORF overlaps with the CDS of *ATF4*. The current model is that during normoxia, the first uORF is translated, and then translation of the second uORF results in bypassing the CDS of *ATF4*, whose start codon is located within the second uORF. This leads to its translational repression. However, during hypoxia, the 40S ribosome bypasses the second uORF because of reduced availability of eIF2 ternary complex (eIF2-TC), resulting in the ribosome bypasses the start codon of the second uORF but continue scanning. Therefore, ATF4 is translated (Figure 1.15) [235, 247, 248]. However, recent studies showed that the translation of the second uORF is not inhibited under stress conditions, a result which is contradictory to the current model [249-251]. In addition, m^6A methylation on the 5'UTR of *ATF4* is shown to be required for regulation of ATF4 expression [235].

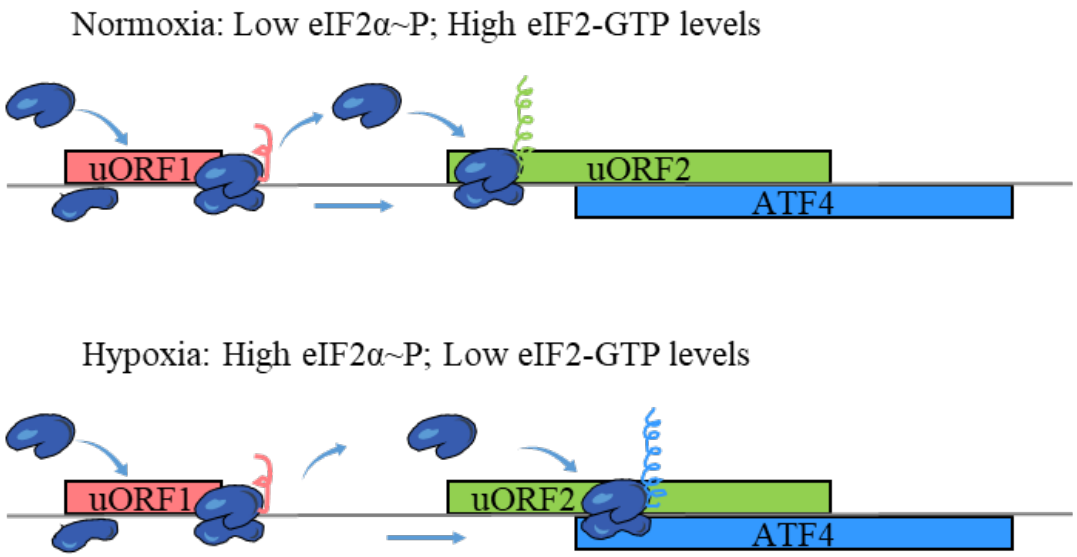


Figure 1.15 Current model of uORF-mediated ATF4 expression under hypoxia. Two uORFs (red and green boxes) in the ATF4 mRNA are preferentially translated. During normal conditions, the phosphorylated eIF2α (eIF2~P) is low and eIF2-GTP levels are high, after translation of the uORF1, the scanning ribosome readily acquires the eIF2-TC and reinitiates translation at the uORF2, which bypasses the start codon of ATF4 CDS (blue box). During hypoxia, the phosphorylated eIF2α (eIF2~P) is increased, which inhibits the formation of eIF2-TC, resulting in reduced translation efficiency of the uORF2. This allows the scanning ribosome to recognise the start codon of ATF4 and initiate its translation.

Hypoxia has been shown to activate the tuberous sclerosis protein 1 (TSC1)–TSC2 complex, which is a negative upstream regulator of the mTOR complex 1. Additionally, hypoxia regulates a group of mTOR interacting protein, including homolog enriched in brain (RHEB), promyelocytic leukaemia tumour suppressor (PML) and BCL2/adenovirus E1B 19 kDa protein-interacting protein 3 (BNIP3) to suppress mTOR kinase activity, resulting in reduced translation (Figure 1.13) [252-257].

Protein hydroxylation is a post-translational modification catalysed by 2-oxoglutarate-dependent dioxygenases, which requires molecular oxygen. Under hypoxia, protein hydroxylation can be inhibited. It is shown that the hydroxylation of eukaryotic release factor 1 (eRF1), small ribosomal subunit protein RPS23, large ribosomal subunit protein RPL8 and RPL16 are inhibited during hypoxia, which regulate different stages in protein translation, such elongation and termination [241, 242, 258]. Previous studies indicate that reduced hydroxylation

on eRF1 and RPS23 may affect the accuracy of stop codon recognition, resulting in stop codon readthrough, which may affect protein expression under hypoxia [242, 259] .

Additionally, translation not only requires translation factors, template mRNA, but also aminoacyl tRNAs. The availability tRNA also determines the translation efficiency. Hypoxia has been shown to regulate the modification, stability, transcription and codon preference of tRNAs [260-263]. Together, all these factors constitute a complicated network regulated by hypoxia that determines the translation efficiency of mRNAs.

1.4 Aims and objectives of the study

The research question of my DPhil project was to investigate if hypoxia would directly influence immune receptor signalling and, if so, to describe the molecular mechanism underlying this regulation.

In the intestine, immune responses are stimulated by invading pathogens and intrusive commensal microbes into the sterile body milieu, whereas immune tolerance is established towards the natural microbiome in the intestinal lumen [264]. Also, cells of the villi are situated in a hypoxic microenvironment and are considered immune tolerant, whereas cells within the crypts are situated in a normoxic microenvironment and more readily initiate immune responses [265, 266]. Similarly, in the context of solid tumours, hypoxia is common feature and it has been reported that hypoxia counteracts anti-tumour immunity [267].

Based on this, I hypothesised that immune signalling pathways may be directly regulated by hypoxia. My initial experiments indeed showed that subjecting cells (HCT-116 colorectal cancer cell line) to hypoxia (1% O_2) inhibited immune signalling mediated by several innate immune receptors; TNFR1, IL-1βR, NOD2.

Based on this observation, the objectives of my DPhil project were:

1) Determine how hypoxia affects signalling by innate immune receptors and identify the molecular mechanism of hypoxia-regulation of immune signalling. For this, I used a reductionist approach using established colorectal epithelial cell lines and human duodenum organoids.

2) Investigate the relevance of hypoxia *in vivo* for immune regulation. For this, I employed an allograft tumour model to address how tumour hypoxia affects tumour immune evasion.

2

Materials

2.1 Chemicals and reagents

Table 2.1 Reagents used in this study

Name	Source	Identifier
AbC™ Total Antibody Compensation Bead Kit	Life Technologies	A10513
ArC™ Amine Reactive Compensation Bead Kit (for use with LIVE/DEAD™ Fixable dead cell stain kits)	Life Technologies	A10628
Bovine serum albumin (BSA)	Sigma-Aldrich	A9418
CellTiter-Glo2.0	Promega	G9241
Chloroquine	Enzo Life Sciences	51005-CLQ
cOmplete™ Protease Inhibitor Cocktail	Roche	11836145001
cOmplete™ ULTRA Tablets, Mini, EDTA-free, EASYpack Protease Inhibitor Cocktail	Roche	5892791001
Compound A (CpA)	TetraLogic Pharmaceuticals	N/A
Cycloheximide	Sigma-Aldrich	C4859
DAPI (4',6-Diamidino-2-Phenylindole, Dihydrochloride)	Thermo Fisher Scientific	D1306
DMSO	Sigma-Aldrich	D2650
eBioscience™ Fixable Viability Dye eFluor™ 506	Thermo Fisher Scientific	65-0866-14
EZSolution™ Nec-1s	BioVision	2535
FBS (dialysed)	Life Technologies	A3382001
Fetal Bovine Serum, dialysed	Life Technologies	A3382001
Fixation buffer	BioLegend	420801
FuGENE 6 Transfection Reagent	Promega	E2692
GI254023X	Sigma-Aldrich	ML0789
GlutaMAX™ Supplement	Thermo Fisher Scientific	35050061
L18-MDP	InvivoGen	tlrl-lmdp
L-Azidohomoalaine (L-AHA)	Merck Life Science	900892
L-CYSTINE HYDROCHLORIDE SOLUTION	Merck Life Science	57579
Lipofectamine™ RNAiMAX Transfection Reagent	Thermo Fisher Scientific	13778150
L-Methionine (L-Met)	Sigma-Aldrich	M5308
MEM Non-Essential Amino Acids Solution (100X)	Thermo Fisher Scientific	11140050
MG132	Selleckchem	S2619
Monensin Solution (1,000X)	BioLegend	420701
paraformaldehyde	Sigma-Aldrich	16005
PD-10 Desalting Column	GE Healthcare	GE17-0851-01

Continuation of Table 2.1

Name	Source	Identifier
PEG4 carboxamide-Propargyl Biotin (Biotin Alkyne)	Merck Life Science	764213
penicillin and streptomycin	Thermo Fisher Scientific	15140122
Perm/Wash Buffer	BD Biosciences	554723
Pierce™ Streptavidin Magnetic Beads	Thermo Fisher Scientific	88817
Proteome Profiler Mouse Chemokine Array Kit	R&D systems	ARY020
Puromycin	InvivoGen	ant-pr-1
Recombinan human IL-1β	Thermo Fisher Scientific	PHC0811
Recombinan human TNF	PEPROTECH	300-01A
Recombinan mouse IFN-γ	Stemcell Technologies	78021.1
Recombinan mouse TNF	PEPROTECH	315-01A
Recombinant GST-1xUBA^{ubquitin}	Fiil et al, 2013	N/A
Renilla Luciferase Reporter Assay System	Promega	E2810
RevertAid reverse Transcriptase	Thermo Fisher Scientific	EP0441
RPMI-1640 Medium, Modified, with sodium bicarbonate, without methionine, cystine and L-glutamine(R7513)	Merck Life Science	R7513
Sodium ascorbate	Merck Life Science	A7631
SYBR™ Select Master Mix	Thermo Fisher Scientific	4472908
TAPI-2	Sigma-Aldrich	SML0420
Tris((1-hydroxy-propyl-1H-1,2,3-triazol-4-yl)methyl)amine (THPTA)	Merck Life Science	762342
z-VAD-FMK (zVAD)	InvivoGen	tlrl-vad
γ-Amino-octyl-GTP-Agarose	Jena Bioscience	AC-106S
γ-Aminophenyl-m^{7}GTP (C10-spacer)-Agarose	Jena Bioscience	AC-155S

2.2 Cell lines, organoids and mouse strain

Table 2.2 Cell lines and mouse strain

Name	Source	Identifier
HCT-116	ATCC	CCL-247
Caco-2	ATCC	HTB-37
SW48	ATCC	CCL-231
GP2d	ECACC	95090714
LS-174T	ATCC	CL-188
HT-29	ATCC	HTB-38
HEK293T	ATCC	CRL-3216
Yumm 1.7	ATCC	CRL-3362
EGFP-sgRNA control HCT116	This study	N/A
TNFRSF1Aknockout HCT116	This study	N/A
HIF1α knockdown HCT116 (clone 1)	This study	N/A
HIF1α knockdown HCT116 (clone 2)	This study	N/A
TNFRSF1A-uORF2 mutant HCT-116 (clone 1)	This study	N/A
TNFRSF1A-uORF2 mutant HCT-116 (clone 2)	This study	N/A
EGFP-sgRNA control Yumm 1.7	This study	N/A
TNFRSF1A-uORF2/IFNGR2-uORF double mutant Yumm 1.7	This study	N/A
EGFP-sgRNA control/B2M knockout Yumm 1.7	This study	N/A
TNFRSF1A-uORF2/IFNGR2-uORF double mutant/B2M knockout Yumm 1.7	This study	N/A
Duodenal organoids	This study	N/A
C57BL/6J mouse	Envigo	057

2.3 Antibodies

Table 2.3 Antibodies used for immunoblotting in this study

Name	Host	Dilution	Supplier	Catalog number	Monoclonal number
4E-BP1	Rabbit	1:1000	Cell Signaling	9644	53H11
Actin	Mouse	1:20000	Millipore	MAB1501	C4
AMPK	Rabbit	1:1000	Cell Signaling	2603	23A3
c-IAP1	Rat	1:4000	ENZO	ALX-803-335	1E1-1-10
c-IAP2	Rat	1:2000	ENZO	ALX-803-341	16E-6-3
CYLD	Rabbit	1:1000	Cell Signaling	8462	D1A10
EIF1/1B	Rabbit	1:1000	Cell Signaling	12496	D7G3L
EIF1A	Rabbit	1:10000	Abcam	ab177939	EPR12466(B)
EIF2D	Rabbit	1:1000	ATLAS ANTIBODIES	HPA028220	Polyclonal
EIF2α	Mouse	1:1000	Cell Signaling	2103	L57A5
EIF3A	Rabbit	1:1000	Cell Signaling	3411	D51F4
EIF3B	Mouse	1:1000	Santa Cruz	sc-137214	C-5
EIF3C	Mouse	1:1000	Santa Cruz	sc-74507	B-6
EIF4A1	Rabbit	1:1000	Cell Signaling	2490	Polyclonal
EIF4A2	Rabbit	1:10000	Abcam	ab31218	Polyclonal
EIF4E1	Rabbit	1:1000	Cell Signaling	2067	C46H6
EIF4E2	Rabbit	1:500	GeneTex	GTX103977	Polyclonal
EIF4G1	Rabbit	1:1000	Cell Signaling	8701	D6A6
EIF4G2	Rabbit	1:1000	Cell Signaling	5169	D88B6
EIF4G3	Rabbit	1:20000	GeneTex	GTX118109	Polyclonal
EIF5B	Rabbit	1:2000	Proteintech	13527-1-AP	Polyclonal
FLAG	Mouse	1:2000	SIGMA	F1804	M2
GFP	Rabbit	1:1000	Cell Signaling	2555	Polyclonal
HIF1α	Mouse	1:2000	BD Biosciences	610958	AB_398272, clone 54
HOIL	Mouse	1:1000	Santa Cruz	sc-365523	E-2
HOIP	Rabbit	1:1000	Aviva Systems Biology	ARP43241_P050	Polyclonal
IFN-γR1	Rabbit	1:1000	GeneTex	GTX54333	Polyclonal
IFN-γR2 (Human)	Rabbit	1:1000	Abcam	ab171081	EPR8813
IFN-γR2 (Mouse)	Rabbit	1:1000	GeneTex	GTX64548	Polyclonal
IκBα-alpha	Rabbit	1:1000	Cell Signaling	9242	Polyclonal
IRAK-1	Rabbit	1:1000	Santa Cruz	sc-7883	Polyclonal
OTULIN	Rabbit	1:1000	Cell Signaling	14127	Polyclonal
P70S6K	Rabbit	1:1000	Cell Signaling	9202	Polyclonal
PABP1	Rabbit	1:5000	Proteintech	10970-1-AP	Polyclonal
phospho-4E-BP1 (T37/46)	Rabbit	1:1000	Cell Signaling	2855	236B4
phospho-AMPK (T172)	Rabbit	1:1000	Cell Signaling	2535	40H9

Continuation of Table 2.3

Name	Host	Dilution	Supplier	Catalog number	Monoclonal number
phospho-EIF2α (S52)	Rabbit	1:1000	Cell Signaling	3597	119A11
phospho-P70S6K (T389)	Rabbit	1:1000	Cell Signaling	9234	108D2
phospho-RelA (S536)	Rabbit	1:1000	Cell Signaling	3031	Polyclonal
phospho-S6 (S235/236)	Rabbit	1:1000	Cell Signaling	4856	2F9
Puromycin	Mouse	1:12500	MERCK	MABE342	4G11
RelA	Rabbit	1:1000	Cell Signaling	8242	D14E12
RFP	Mouse	1:1000	Santa Cruz	sc-390909	E-8
RIPK1	Rabbit	1:1000	Cell Signaling	3493S	D94C12
RIPK2	Mouse	1:1000	Santa Cruz	sc-166765	A-10
S6	Rabbit	1:1000	Cell Signaling	2217	5G10
SHARPIN	Rabbit	1:2000	Proteintech	14626-1-AP	Polyclonal
TNFR1	Rabbit	1:1000	Cell Signaling	3736	C25C1
TNFR1	Mouse	1:1000	Santa Cruz	sc-7883	H-5
TNFR1 (rodent specific)	Rabbit	1:1000	Cell Signaling	3736	D3I7K
TRADD	Rabbit	1:1000	Santa Cruz	sc-7868	Polyclonal
TRAF2	Rabbit	1:1000	Santa Cruz	sc-876	Polyclonal
Streptavidin-HRP	N/A	1:5000	Cell Signaling	3999	N/A
anti-mouse-HRP	Goat	1:5000	Dako	P0447	Polyclonal
anti-rabbit-HRP	Goat	1:5000	Bio-Rad	1706515	Polyclonal
anti-rat-HRP	Goat	1:10000	ThermoFisher	31470	Polyclonal

Table 2.4 Antibodies used for flow cytometry and immunofluorescence in this study

Name	Host	Dilution	Supplier	Catalog number	Monoclonal number
anti-human TNFR1	Mouse	1:100	R&D Systems	MAB225	16803
PE anti-mouse H-2K^{b}	Mouse	1:100	BioLegend	116508	AF6-88.5
APC anti-mouse I-A/I-E	Rat	1:100	BioLegend	107614	M5/114.15.2
PE anti-mouse CD45	Rat	1:200	BioLegend	103106	30-F11
APC anti-mouse CD3	Rat	1:200	BioLegend	100236	17A2
Alexa Fluor 488 anti-mouse CD4	Rat	1:200	BioLegend	100425	GK1.5
PE-CY7 anti-mouse CD8a	Rat	1:200	BioLegend	100722	53-6.7
BV650 anti-mouse NK1.1	Mouse	1:100	BioLegend	108736	PK136
BV785 anti-mouse F4/80	Rat	1:200	BioLegend	123141	BM8
APC anti-human IL8	Mouse	1:100	BioLegend	511410	E8N1
RelA	Rabbit	1:400	Cell Signaling	8242	D14E12

Table 2.5 Antibodies used for neutralisation

Name	Host	Dilution	Supplier	Catalog number	Monoclone number	Function
TNF	mouse	1 μg mL^{-1}	R&D Systems	MAB210	1825	Neutralisation
CD16/32	Rat	1:100	BioLegend	156604	S17011E	FC blocking

2.4 Oligos

Table 2.6 Quantitative real-time PCR primer sequences

h*CXCL8* Forward: TCTGGCAACCCTAGTCTGCT
h*CXCL8* Reverse: AAACCAAGGCACAGTGGAAC
h*TNF* Forward: TGCTGCAGGACTTGAGAAGA
h*TNF* Reverse: GAGGAAGGCCTAAGGTCCAC
h*TNFAIP3* Forward: ATGCACCGATACACACTGGA
h*TNFAIP3* Reverse: GGATGATCTCCCGAAACTGA
h*TNFRSF1A* Forward: TCACCGCTTCAGAAAACCACC
h*TNFRSF1A* Reverse: GGTCCACTGTGCAAGAAGAGA
h*B2M* Forward: GAGGCTATCCAGCGTACTCCA
h*B2M* Reverse: CGGCAGGCATACTCATCTTTT
h*EIF1* Forward: GAAACGGCAGGAAGACCCTTA
h*EIF1* Reverse: CGGATGCTCAATTACAGTACCAT
h*EIF1B* Forward: AACTAAGGGTGACGACTTACTCC
h*EIF1B* Reverse: GTCTTTCTGCCGTTCCGTTG
h*EIF1A* Forward: AACAGACGCAGGGGTAAGAAT
h*EIF1A* Reverse: CCTGAGCATACTCCTGACCAT
h*EIF2D* Forward: GCCTTTCGGGTCAAGTCCAA
h*EIF2D* Reverse: CCTCCTTTCCAGGTACTAACTCA
h*EIF4A1* Forward: AAGGCGTCATCGAGAGTAACT
h*EIF4A1* Reverse: ATGTGGCCGTTTTCCCAGTC
h*EIF4A2* Forward: GAAGCCTTCCGCTATTCAGCA
h*EIF4A2* Reverse: CTTGGGTCTCCTTGAACTCAATC
h*EIF4A3* Forward: TGGCTCCCACAAGAGAGTTG
h*EIF4A3* Reverse: GCACTGGACATTCATGTAGTCA
h*EIF4E1* Forward: GAAACCACCCCTACTCCTAATCC
h*EIF4E1* Reverse: AGAGTGCCCATCTGTTCTGTA
h*EIF4E2* Forward: ACAACAAGTTCGACGCTTTGA
h*EIF4E2* Reverse: TCTCTTGCTACTGCTCTGATTCT
h*EIF4G1* Forward: CCCGAAAAGAACCACGCAAG
h*EIF4G1* Reverse: TTCCCCTCGATCCTTATCAGC
h*EIF4G2* Forward: AGGGCAAAACGCTCAGAAATG
h*EIF4G2* Reverse: TCCTGAAGATTGCATCATGTCG
h*EIF4G3* Forward: CCTAGAGCTACCATCCCGAAC
h*EIF4G3* Reverse: GGGCCACTATGACGGTACTG

Continuation of Table 2.6

h*EIF5B* Forward: AGGGCTTATGACAAAGCAAAACG
hEIF5B Reverse: CCCAAGTACGCAGATAATAGGGG
h*EIF3A* Forward: GCCGGAAAATGCCCTCAAAC
h*EIF3A* Reverse: TGGTTCGTGTATCTTTTGCCAT
h*EIF3B* Forward: GACCGCACTTCCATATTCTGG
h*EIF3B* Reverse: GCACATACGTCTCTGTCCATCT
h*EIF3C* Forward: TGAAGATTCGTGATGTCACCAAG
h*EIF3C* Reverse: AGATAGTCCTCTAGGTCAGCCA
h*EIF3D* Forward: CAGCGGAATCGAATGAGATTTGC
h*EIF3D* Reverse: GTTTGGCACTCTTAGGCAGGA
h*EIF3E* Forward: ACAGTGGTTGCACAACTGAAA
h*EIF3E* Reverse: CATCCCTGGTTGACTGCATTT
h*EIF3F* Forward: ACGGGCCATGACATCACAG
h*EIF3F* Reverse: AAGTGCTGACGTAGGCTTTGA
h*EIF3G* Forward: CGCTGCCCCTACAAGGATAC
h*EIF3G* Reverse: GCGGCACATACTTCCCTGTC
h*EIF3H* Forward: TCGGGAGATTCAGCCGTGA
h*EIF3H* Reverse: CTCCGCATCATTTCCATCTGATA
h*EIF3I* Forward: GGCCATGAGCGGTCCATTAC
h*EIF3I* Reverse: ACATTGACGATAGGGTCCTTGG
h*EIF3J* Forward: GTCAAGGATAACTGGGATGACG
h*EIF3J* Reverse: CGAGGTCTGACTCTTCCTGTAA
h*EIF3K* Forward: AAGTTGCTCAAGGGTATCGACA
h*EIF3K* Reverse: GGCCTGCGTCTCTACATAGC
h*EIF3L* Forward: GAACAGCAAACCTATCAGGTGA
h*EIF3L* Reverse: CTGGCCTGTAGCTCATACACT
h*EIF3M* Forward: TCAGAAGAGAACTCGGAAGGTG
h*EIF3M* Reverse: ACCACACTGTTCATCACACTTT
m*IFNGR2* Forward: TCCTCGCCAGACTCGTTTTC
m*IFNGR2* Reverse: ACGGCTCCCAAGTTAGAATCT
m*TNFRSF1A* Forward: GGGCACCTTTACGGCTTCC
m*TNFRSF1A* Reverse: TCTCCTTACAGGGGATTGTCAC
m*B2M* Forward: TTCTGGTGCTTGTCTCACTGA
m*B2M* Reverse: CAGTATGTTCGGCTTCCCATTC

Table 2.7 Oligonucleotides used in this study

Name	**Source**	**Identifier**
Anchored Oligo(dT)20	Sigma-Aldrich	N/A
Random primers	IDT	N/A
Alt-R® CRISPR-Cas9 tracrRNA, ATTO™ 550	IDT	1075927

Table 2.8 Sequences used for DNA editing and RNA knockdown

The siRNA sequences used for knockdown were as follows:		
Name	**Source**	**Identifier**
siRNA Universal Negative Control	Sigma-Aldrich	SIC001
si_h*EIF4G1* sense: CAGAUCAGUGGAAGCCUCU[dT][dT]	Sigma-Aldrich	SASI_Hs01_00222596
si_h*EIF4G1* anti-sense: AGAGGCUUCCACUGAUCUG[dT][dT]		
si_h*EIF1* sense: GGAAUAUGGAGAAGUAAUU[dT][dT]	Sigma-Aldrich	SASI_Hs01_00193439
si_h*EIF1* anti-sense: AAUUACUUCUCCAUAUUCC[dT][dT]		
The shRNA sequences used for knockdown were as follows:		
shRNA_#1_h*HIF1α* Forward: CCGG CCGCTGGAGACACAATCATAT CTCGAG ATATGATTGTGTCTCCAGCGG TTTTTG	IDT	N/A
shRNA_#1_h*HIF1α* Reverse: AATTCAAAAA CCGCTGGAGACACAATCATATCTCGAGATATGATTGTG TCTCCAGCGG	IDT	N/A
shRNA_#2_h*HIF1α* Forward: CCGGCCAGTTATGATTGTGAAGTTACTCGAGTAACTTC ACAATCATAACTGGTTTTTG	IDT	N/A
shRNA_#2_h*HIF1α* Reverse: AATTCAAAAA CCAGTTATGATTGTGAAGTTACTCGAGTAACTTCACAAT CATAACTGG	IDT	N/A
The sgRNA sequences used for knockout were as follows:		
EGFP-sgRNA- Forward: CACCGGAAGTTCGAGGGCGACACCC	IDT	N/A
EGFP-sgRNA- Reverse: AAACGGGTGTCGCCCTCGAACTTCC	IDT	N/A
h*TNFRSF1A*-sgRNA- Forward: CACCGAGAGGTGCACGGTCCCATTG	IDT	N/A
h*TNFRSF1A*-sgRNA- Reverse: AAACCAATGGGACCGTGCACCTCTC	IDT	N/A
The sgRNA sequences used for deletion of uORFs were as follows:		
h/m *TNFRSF1A* sgRNA Forward: CACCGTGGCCTCTCACTCCCCCATT	IDT	N/A
h/m *TNFRSF1A* sgRNA Reverse: AAACAATGGGGGAGTGAGAGGCCAC	IDT	N/A
m*IFNGR2* sgRNA Forward: CACCGGGCGGGCGCTCGGCTCGCCA	IDT	N/A
m*IFNGR2* sgRNA Reverse: AAACTGGCGAGCCGAGCGCCCGCCC	IDT	N/A
The crRNA sequences used for knockout were as follows:		
m*B2M*_#1_crRNA AGUAUACUCACGCCACCCACGUUUUAGAGCUAUGCU	IDT	N/A
m*B2M*_#2_crRNA AGUCGUCAGCAUGGCUCGCUGUUUUAGAGCUAUGCU	IDT	N/A

2.5 DNA constructs

Table 2.9 DNA constructs used in this study

Name	Source	Identifier
lentiCRISPR v2-sg_GFP	This study	N/A
lentiCRISPR v2-sg_hTNFRSF1A	This study	N/A
lentiCRISPR v2-sg_h/mTNFRSF1A(uORF2)	This study	N/A
hTNFRSF1A-5'UTR-pEGFP-N1	This study	N/A
hTNFRSF1A-5'UTR-uORF1-GFP	This study	N/A
hTNFRSF1A-5'UTR-uORF2-GFP	This study	N/A
mTNFRSF1A-5'UTR-pEGFP-N1	This study	N/A
mTNFRSF1A-5'UTR-uORF1-GFP	This study	N/A
mTNFRSF1A-5'UTR-uORF2-GFP	This study	N/A
RFP-pEGFP-N1	This study	N/A
RFP-hTNFRSF1A-5'UTR-pEGFP-N1	This study	N/A
RFP-hTNFRSF1A-5'UTR(-1_-55/-38A>T)-pEGFP-N1	This study	N/A
hTNFRSF1A-5'UTR-Flag-uORF2-pEGFP-N1	This study	N/A
hTNFRSF1A-5'UTR-Flag-uORF2-pEGFP-N1 (-20A>T)	This study	N/A
hTNFRSF1A-5'UTR-Flag-uORF2-pEGFP-N1 (-20A>T/-55A>T)	This study	N/A
hTNFRSF1A-5'UTR-Flag-uORF2-pEGFP-N1 (-21G>A)	This study	N/A
hTNFRSF1A-5'UTR-Flag-uORF2-pEGFP-N1 (-2OA>G/-21G>A)	This study	N/A
hTNFRSF1A-5'UTR-pEGFP-N1 (-31A>T)	This study	N/A
hTNFRSF1A-5'UTR-pEGFP-N1 (-30T>G)	This study	N/A
hTNFRSF1A-5'UTR-pEGFP-N1 (-29G>A)	This study	N/A
hTNFRSF1A-5'UTR-pEGFP-N1 (-20A>T)	This study	N/A
hTNFRSF1A-5'UTR-pEGFP-N1 (-21G>A)	This study	N/A
hTNFRSF1A-5'UTR-pEGFP-N1 (-20A>G/-21G>A)	This study	N/A
hTNFRSF1A-5'UTR-pEGFP-N1 (-26G>C/-27G>C/-28G>C)	This study	N/A
hTNFRSF1A-5'UTR-pEGFP-N1 (-25G>T)	This study	N/A
hTNFRSF1A-5'UTR-pEGFP-N1 (-34C>G/-35C>G/-36C>G)	This study	N/A
pcDNA3-RFP	This study	N/A
hIFNGR1-5'UTR-pEGFP-N1	This study	N/A
hIFNGR2-5'UTR-pEGFP-N1	This study	N/A
hIFNGR2-5'UTR (-89A>T)-pEGFP-N1	This study	N/A
hNOD2-5'UTR-pEGFP-N1	This study	N/A
hIL1R-5'UTR-pEGFP-N1	This study	N/A
hTLR4-5'UTR-pEGFP-N1	This study	N/A
hIFNAR1-5'UTR-pEGFP-N1	This study	N/A
hSTING-5'UTR-pEGFP-N1	This study	N/A
hRIG-I-5'UTR-pEGFP-N1	This study	N/A
hTLR4-5'UTR (-9G>A/-8A>G)-pEGFP-N1	This study	N/A
hIFNAR1-5'UTR (-65A>T/-32A>T)-pEGFP-N1	This study	N/A
hRIG-I-5'UTR (+TNFRSF1A uORF2)-pEGFP-N1	This study	N/A

Continuation of Table 2.9

Name	Source	Identifier
hEIF4G1-5'UTR-pEGFP-N1	This study	N/A
hEIF4G1-5'UTR (-156A>T)-pEGFP-N1	This study	N/A
hEIF4G1-5'UTR (-156A>T/-83A>T)-pEGFP-N1	This study	N/A
hEIF4G1-5'UTR (-156A>T/-83A>T/-17A>T)-pEGFP-N1	This study	N/A
hEIF4G1-5'UTR (-156A>T/-83A>T/-17A>T/-5A>T)-pEGFP-N1	This study	N/A

3

Methods

3.1 Mice

C57BL/6JOlaHsd Mice were purchased from Envigo and maintained in a specific pathogen-free facility. Animal experiments were performed in accordance with protocols approved by the Institutional Animal Care and Use Committee of Ludwig Institute of Cancer Research, Oxford.

3.2 Cell culture, plasmids and transfection

HCT-116, Caco-2, SW48, LS-174T, HT-29, HEK293T and Yumm 1.7 cell lines were from the American Type Culture Collection (ATCC) and GP2d cell line was from the European Collection of Authenticated Cell Cultures (ECACC). All cell lines were cultured under conditions specified by the supplier and were tested as free from mycoplasma contamination by using MycoAlert Mycoplasma Detection kit (Lonza). Hypoxic condition was achieved by a hypoxia working station maintaining the culture conditions at 1 % O_2, 5 % CO_2, and 94 % N_2. The constructs were listed in the Key Resources Table. Mutations were achieved by site-directed mutagenesis using the QuikChange Lightning Kit (Agilent Technologies). The constructs and mutagenesis were confirmed via Sanger Sequencing. Plasmids and siRNAs were transfected into cells with FuGENE 6 transfection reagent (Promega, E2692) and Lipofectamine RNAiMAX transfection reagent (Thermo Fisher Scientific, 13778150) according to the manufacturer's protocols.

3.3 Generation of cell lines by CRISPR/Cas9-mediated gene editing

For gene knockout, sgRNA against *TNFRSF1A* was cloned into pSpCas9(BB)-2A-GFP (PX458). HCT-116 cells were transiently transfected with the plasmids and GFP positive cells were single-cell sorted and deletion were confirmed by immunoblotting, functional assay and sequencing.

For uORF editing, sgRNAs against *GFP*, uORF2 of human or mouse *TNFRSF1A* (h/m_*TNFRSF1A*) and uORF of mouse *IFNGR2* (m_*IFNGR2*) were cloned into

lentiCRISPR v2 accordingly. U6 promoter and sgRNA against uORF of m*IFNGR2* were cloned into sg_m/h*TNFRSF1A*_lentiCRISPR v2 with *EcoRI*. The reconstructed lentiCRISPR v2 plasmids were used to produce lentivirus to generate cells stably expressing Cas9 with puromycin resistance gene, which were subjected to positive selection by 1 μg mL $^{-1}$ puromycin for one week and single-cell sorted. Gene editing was confirmed by immunoblotting, functional assay and sequencing.

For generating *B2M* knockout Yumm1.7 polyclonal cells, tracrRNA-ATTO-550 (Integrated DNA Technologies, 1075927) and crRNAs against *B2M* were annealed and transfected into Cas9 stably expressing sg*GFP*-control and *TNFRSF1A*/*IFNGR2* uORF double mutant Yumm1.7 cells by Lipofectamine RNAiMAX transfection reagent. ATTO-550 positive transfected cells were sorted, which then were treated with 1 ng mL $^{-1}$ mTNF and 1 ng mL $^{-1}$ mIFN-γ for 12 hours. The positive control Yumm1.7 cells have 100% positivity of H-2K^{b} expression and H-2K^{b} negative cells from the treated groups were sorted.

3.4 Lentiviral cloning, production and infection

To generate *HIF1α*-shRNA HCT-116 cells, oligonucleotides were cloned into pLKO.1 between the *AgeI* and *EcoRI* sites. To generate uORF mutant cells, oligonucleotides were cloned into lentiCRISPR v2 between the *BsmBI* sites. Lentiviral packaging plasmids psPAX2 and pMD2.G were co-transfected with the backbone plasmid into HEK293T cells for 48 hours for lentivirus production. Target cells were infected with the virus together with 8 μg mL $^{-1}$ polybrene for 24 hours and then selected by 1 μg mL $^{-1}$ puromycin in culture media.

3.5 Immunoblotting

Same numbers of cells were lysed in lysis buffer (1× loading buffer diluted by 1% SDS <weight/volume>) and immediately heated at 100 ℃ for 15 minutes. Equivalent volumes

were subjected to SDS-PAGE and transferred to nitrocellulose membranes, then blocked with 5% (weight/volume) non-fat milk or 1% (weight/volume) BSA for 1 hour at room temperature. Membranes were then incubated with the indicated primary antibodies overnight at 4 ℃, followed by the appropriate HRP-conjugated secondary antibodies. Immunoreactive bands were visualised with chemiluminescence kits.

3.6 Immunofluorescence

Cells were fixed in 4% (volume/volume) formaldehyde (in PBS) for 15 minutes at room temperature, and then permeabilised with 0.1% (volume/volume) Triton X-100 together with DAPI at 4 °C. After blocking in goat serum for 30 minutes, cells were incubated with anti-RelA (1:400, Cell Signalling, 8242, clone D14E12) for 1 hour at room temperature, then washed three times with PBS and incubated with FITC-conjugated secondary antibodies for 1 hour at room temperature. The slides were then washed three times with PBS and mounted. Cell images were captured with ZEISS LSM 710 confocal microscope.

3.7 RNA isolation, cellular fractionation and quantitative real-time PCR

Total RNA and fractionated RNA were extracted and purified using RNase Mini kit (Qiagen, 74106) according to manufacturer's instructions. cDNA was synthesised by reverse transcription using anchored Oligo-dT(20), random primers and RevertAid Reverse Transcriptase (Thermo Fisher Scientific, EP0441). Quantitative real-time PCR was performed using SYBR™ Select Master Mix (Thermo Fisher Scientific, 4472908) on a LightCycler 480 Real-Time PCR System (Roche). Relative mRNA abundance was calculated by normalisation to *B2M* mRNA. Where indicated, relative gene expression was further normalised to expression in control group in the same experiment and represented as fold change.

3.8 Click chemistry labelling

Cells were grown at 80% confluence, washed three times with PBS and replaced with L-

methionine- and FBS-free media (Merck Life Science, R7513) containing 0.2 mM L-Cystine-2HCl (Merck Life Science, 57579) and 1 × L-Glutamax (ThermoFisher, 35050061), then incubated for additional 30 minutes. Dialysed FBS (Life Technologies, A3382001) was added to reach a final concentration at 10% together with 50 μM L-methionine (Sigma-Aldrich, M5308) or 50 μM L-Azidohomoalaine (Merck Life Science, 900892) and incubated for additional 4 hours. Cells were washed 2 times with ice-cold PBS, harvested and lysed with lysis buffer (1% <volume/volume> NP-40 and 0.1% <weight/volume> SDS in PBS). Cell lysates were centrifuged and supernatants were collected. For 200 μL reaction volume, 1 μL Biotin-PEG4-Alkyne (4 mM stock solution) (Merck Life Science, 764213), 10 uL THPTA (100 mM stock solution) (Merck Life Science, 762342), 4 uL CuSO4 (50 mM stock solution) (Jena Bioscience, CLK-MI004-50) and 10 uL Sodium Ascorbate (300 mM stock solution) (Merck Life Science, A7631) were added and briefly vortexed to mix well. Then the solution was added to 175 μL cell lysates (200 μL lysis buffer for each well of a 6-well plate) and continuously vortexed for 2 hours at room temperature. The 200 μL solution was diluted with 800 μL 0.1% (weight/volume) SDS in PBS and subjected to PD10 Column (GE Healthcare, GE17-0851-01) for desalting according to manufacturer's instructions. 3.5 mL desalted solutions were purified by 50 μL Pierce™ Streptavidin Magnetic Beads (ThermoFisher, 88817) at 4 ℃ overnight, washed three times with 0.1% (weight/volume) SDS in PBS and eluted by heating at 100 ℃ 5 minutes with 100 μL 1× loading buffer diluted by 1% (weight/volume) SDS. 5 μL of each sample was loaded into gel and detected by western blot.

3.9 Cell viability assay

Cells were grown in 96-well plate at 80% confluency. Cell viability was measured by CellTiter-Glo® 2.0 Cell Viability Assay kit (Promega, G9242) based on the total ATP levels. The result represents the net result of cell proliferation and cell death.

3.10 Purification of endogenous ubiquitin conjugates

Ubiquitin conjugates were purified through the use of a GST-1 × UBA^{ubq}. 30 µg GST-1 × UBA^{ubq} proteins were pre-bound to 15 µL GSH-Sepharose 4B beads per sample and incubated at 4 ℃ on a rotor for 2 hours. Cells from a 10 cm dish with 90% confluency per sample were lysed with 500 µL lysis buffer (20 mM sodium phosphate ,pH 7.4, 1% (volume/volume) NP-40, 2 mM EDTA,1 mM DTT, 10mM N-Ethylmaleimide and protease inhibitor cocktails), centrifuged and supernatants were collected. 50 µL volumes from each sample were collected as input, the rest of samples were incubated with Sepharose beads at 4 ℃ on a rotor overnight. The beads were washed four times with lysis buffer and heated at 100 ℃ for 5 minutes with 40 µL 1× loading buffer diluted in 1% (weight/volume) SDS. 20 µL of each sample was loaded into gel and analysed by western blot.

3.11 Allograft tumour model

Experiments were carried out 7 days after the mice were brought in the animal facility. Mice were anesthetised with isoflurane in a plastic desiccator. Mouse melanoma Yumm1.7 cells (1×10^5 in 100 µl FBS-free DMEM/F-12 media) were injected subcutaneously at the flank of eight-week-old female C57BL/6J mice. Tumour size was measured every 2–3 days one week after the implantation and tumour volume was analysed by using the formula $V = 0.5 \times L \times W^2$ (V: volume, L: length, W: width). The mice were euthanised 16 days after implantation and the subcutaneous tumours were surgically removed and weighed. A pilot experiment was performed to predetermine the tumour growth timing as 16 days and the sample size was calculated as 10 mice for each group with the power 0.8 and type I error rate 5% by using the calculation tool (http://powerandsamplesize.com). The mice were randomly allocated into four groups for the implantation of four different cell lines. Due to the requirement of blind experiment, tumour implantation and tumour volume measurement were carried out by another investigator, who was blinded to the allocation of cell lines.

3.12 Flow cytometry analysis

For isolation of Yumm1.7 tumour infiltrating immune cells, extracted tumours were minced and digested by Miltenyi mouse tumour dissociation kit (Miltenyi biotec, 130-096-730) according to manufacturer's instructions. 1.5×10^6 live cells were used per sample and cell suspensions were first blocked with anti-mouse CD16/CD32 antibody (1:100, BioLegend, 156604, clone S17011E) at room temperature for 10 minutes prior to staining. For surface staining, cells were stained with antibodies and Fixable Viability Dye eFluor™ 506 (Thermo Fisher Scientific, 65-0866-14) for 20 minutes on ice. For intracellular staining, cells were fixed with fixation buffer (BioLegend, 420801) at room temperature for 15 minutes and permeabilised using Perm/Wash Buffer (BD Biosciences, 554723), then incubated with antibodies at room temperature for 30 minutes. The following antibodies were used in flow cytometry analysis: PE anti-mouse CD45 (1:200, BioLegend, 103106, clone 30-F11), APC anti-mouse CD3 (1:200, BioLegend, 100236, clone 17A2), Alexa Fluor 488 anti-mouse CD4 (1:200, BioLegend, 100425, clone GK1.5), PE-CY7 anti-mouse CD8a (1:200, BioLegend, 100722, clone 53-6.7), BV650 anti-mouse NK1.1 (1:100, BioLegend, 108736, clone PK136), BV785 anti-mouse F4/80 (1:200, BioLegend, BM8, clone 123141), APC anti-mouse TNFR1 (1:100, BioLegend, 113006, clone 55R-286), anti-human TNFR1 (1:100, R&D Systems, MAB225, clone 16803), PE anti-mouse H-2Kb (1:100, BioLegend, 116508, clone AF6-88.5), APC anti-mouse I-A/I-E (1:100, BioLegend, 107614, clone M5/114.15.2), FITC anti-mouse Fas (1:100, BioLegend, 152606, clone SA367H8), PE anti-mouse TRAIL-R2 (1:100, BioLegend, 119906, clone MD5-1), APC anti-mouse PD-L1 (1:100, BioLegend, 124312, clone 10F.9G2) and APC anti-human IL8 (1:100, BioLegend, E8N1, clone 511410). Flow analysis was performed in a BD LSRFortessa™ X-20 Flow Cytometer and data processing was performed using FlowJo v10 software (FlowJo, LLC).

3.13 3'mRNA Sequencing (services provided by Oxford Genomic Centre)

Material was quantified using RiboGreen (Invitrogen) on the FLUOstar OPTIMA plate reader (BMG Labtech) and the size profile and integrity analysed on the 2200 or 4200 TapeStation (Agilent, RNA ScreenTape). RIN estimates for all samples were between 9.8 and 10. Input material was normalised to 400 ng prior to library preparation. Strand specific library preparation was completed using QuantSeq 3'mRNA-Seq kit (Lexogen) using forward read directions following manufacturer's instructions. Libraries were amplified (13 cycles) on a Tetrad (Bio-Rad). Individual libraries were normalised using Qubit, and the size profile was analysed on the 2200 or 4200 TapeStation. Individual libraries were normalised and pooled together accordingly. The pooled library was diluted to 10 nM for storage. The 10 nM library was denatured and further diluted prior to loading on the sequencer. Single end sequencing was performed using a NextSeq 500 platform (Illumina, NextSeq 500/550 High Output Kit v2.5, 75 Cycles), generating a raw read count of >15 million reads per sample.

Trimming and mapping were carried out using Cutadapt 2.10 and STAR 2.7.8a against GrCm39 or UCSC mm10. The reference genome sequence and GTF used to generate STAR index for UCSC mm10 was from iGenome, while GrCm39 from gencode Release M27. Feature count against supplied GTF was carried out with quantMode of STAR for 1st read strand. A Bioconductor package erccdashboard v 1.20.0 was used to calculate lower limits of detection. CPM was calculated after removing genes whose counts across all samples is less than 3, then library normalisation is applied using edgeR v3.22.3.

3.14 Bioinformatics analysis

Single cell RNA-seq dataset GSE72056 from the Gene Expression Omnibus (GEO) database were analysed by Gene Ontology (GO) term enrichment using the Gene Set Enrichment Analysis (GSEA) algorithm. Ribo-seq data for detection of initiation sites from datasets GSE87328, GSE131650, GSE58207, GSE65885, SRA160745, GSE94460,

GSE74279 and GSE75290 were analysed by using GWIPS-viz Genome Browser (https://gwips.ucc.ie/index.html). Translation efficiency and total mRNA levels under normoxia and hypoxia in U87MG cells from polysome profiling dataset GSE128547 were calculated based on the definition previously reported [268, 269]. SKCM-TCGA dataset downloaded from cBioPortal was used for gene expression correlation analysis and survival analysis. Hypoxia score was calculated by obtaining the mean expression value (log2) of hypoxia signature with 51 genes reported previously [270]. TNF and IFN-γ signature scores were calculated by using the mean value of gene set M5890 and M5913, respectively. Overlapping genes between the datasets M5890 and M5913 were not included. Antigen presentation signature score was calculated by using the mean value of marker genes (*PSMB5*, *PSMB6*, *PSMB7*, *PSMB8*, *PSMB9*, PSMB10, *TAP1*, *TAP2*, *ERAP1*, *ERAP2*, *CANX*, *CALR*, *PDIA3*, *TAPBP*, *B2M*, *HLA-A*, *HLA-B* and *HLA-C*) reported previously [271, 272]. Differentially expressed genes from RNA-seq data in Yumm1.7 cell were analysed using Idep.93 (http://bioinformatics.sdstate.edu/idep/). TCGA Pan-cancer Atlas datasets were used to analysis the genetic alteration ratio and methylation levels by using cBioPortal and SMART [273], respectively.

3.15 Quantification and statistical analysis

Where indicated, all error bars indicate standard error of the mean. Statistical analyses were performed using Excel and GraphPad Prism 9 software. Sample size, statistical parameters, P values and methods are mentioned within the figures and legends. Briefly, when comparing two datasets, F-test was first used to test the variance of the datasets and then use t-test to calculate the P values by using assumption of homoscedasticity or heteroscedasticity accordingly. Mann-Whitney U test was used to compare differences between two independent groups when the dependent variable is not normally distributed. Normal distribution and variance similarity were assessed with D'Agostino and Pearson

omnibus normality test. For comparison of datasets more than two groups, one-way ANOVA or two-way ANOVA with corresponding corrections was used. Where indicated, the experiments were repeated at least three times and the investigators were not blinded to allocation during experiments and outcome assessment.

4

Mechanism of hypoxia-induced repression of immune receptor signalling

4.1 Hypoxia inhibits TNF-, IL-1β- and L18-MDP-mediated signalling

Considering immune tolerance is important in the gastro-intestinal tract, particularly in the intestine where there are thousands of different microorganisms exist in a hypoxic microenvironment [182, 274], I wondered whether a hypoxic microenvironment would directly affect immune signalling. To investigate this, I first tested the activity of surface receptor TNF Receptor 1-, IL-1β receptor- and cytosolic receptor NOD2-mediated signalling under hypoxia in the HCT-116 colorectal cancer cell line. This cell line resembles intestine epithelial cells and has intact components of all these three receptor-mediated signalling pathways [24, 275-277]. I first tested the inducibility of Interleukin-8 (IL-8) as a readout of NF-κB activation when stimulated with TNF, IL-1β and L18-MDP under hypoxic conditions. I used 1% oxygen as the condition of hypoxia treatment considering the oxygen level is between 0.2%- 2% in colon and also it is an average tumour hypoxia level [182, 274]. Hypoxia significantly inhibited the induction of IL-8 mediated by these stimulations following 24- and 48-hour hypoxia (Figure 4.1).

During normoxia, the activated NF-κB translocated from cytoplasm to nucleus (Figure 4.2) to initiate the transcription of NF-κB target genes. Consistent with hypoxic inhibition of IL8 production, the nuclear translocation of the NF-κB subunit RelA induced by these ligands was also inhibited under hypoxic conditions (Figure 4.2). These data indicated that hypoxia impairs immune receptor signalling.

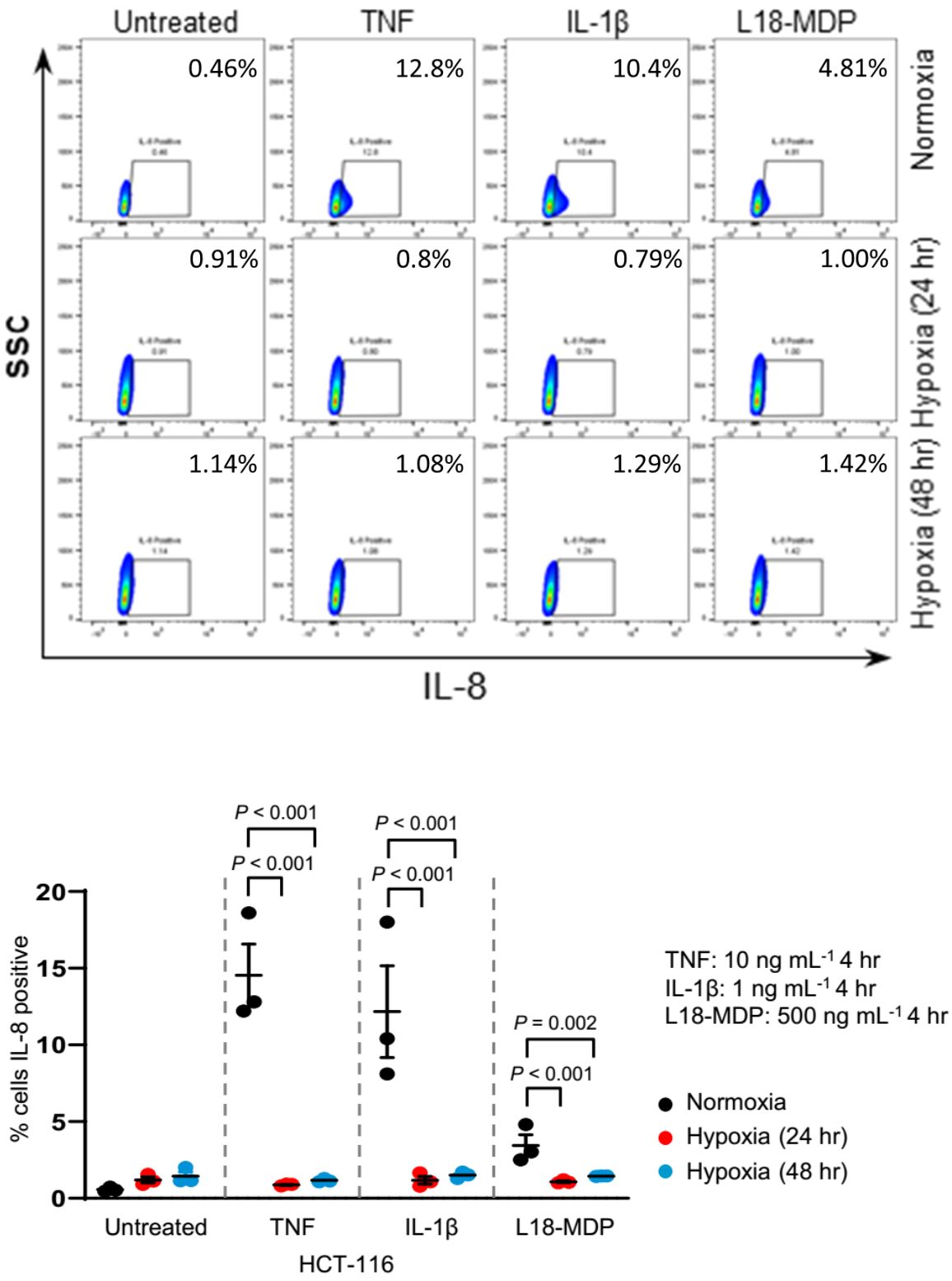


Figure 4.1 Hypoxia inhibits TNF-, IL-1β- and L18-MDP-induced IL-8 expression. HCT-116 cells were cultured under normoxia or hypoxia for 20 hr or 44 hr followed by treatment with TNF (10 ng mL^{-1}), IL-1β (1 ng mL^{-1}) or L18-MDP (500 ng mL^{-1}) for additional 4 hr, stained with anti-IL-8 antibody and analysed by flow cytometry. Representative (top) and quantification analysis (bottom) of IL-8 positive cells was showed. Data are shown mean ± SEM of three independent experiments. Statistical significance was determined by two-way ANOVA with Dunnett's correction.

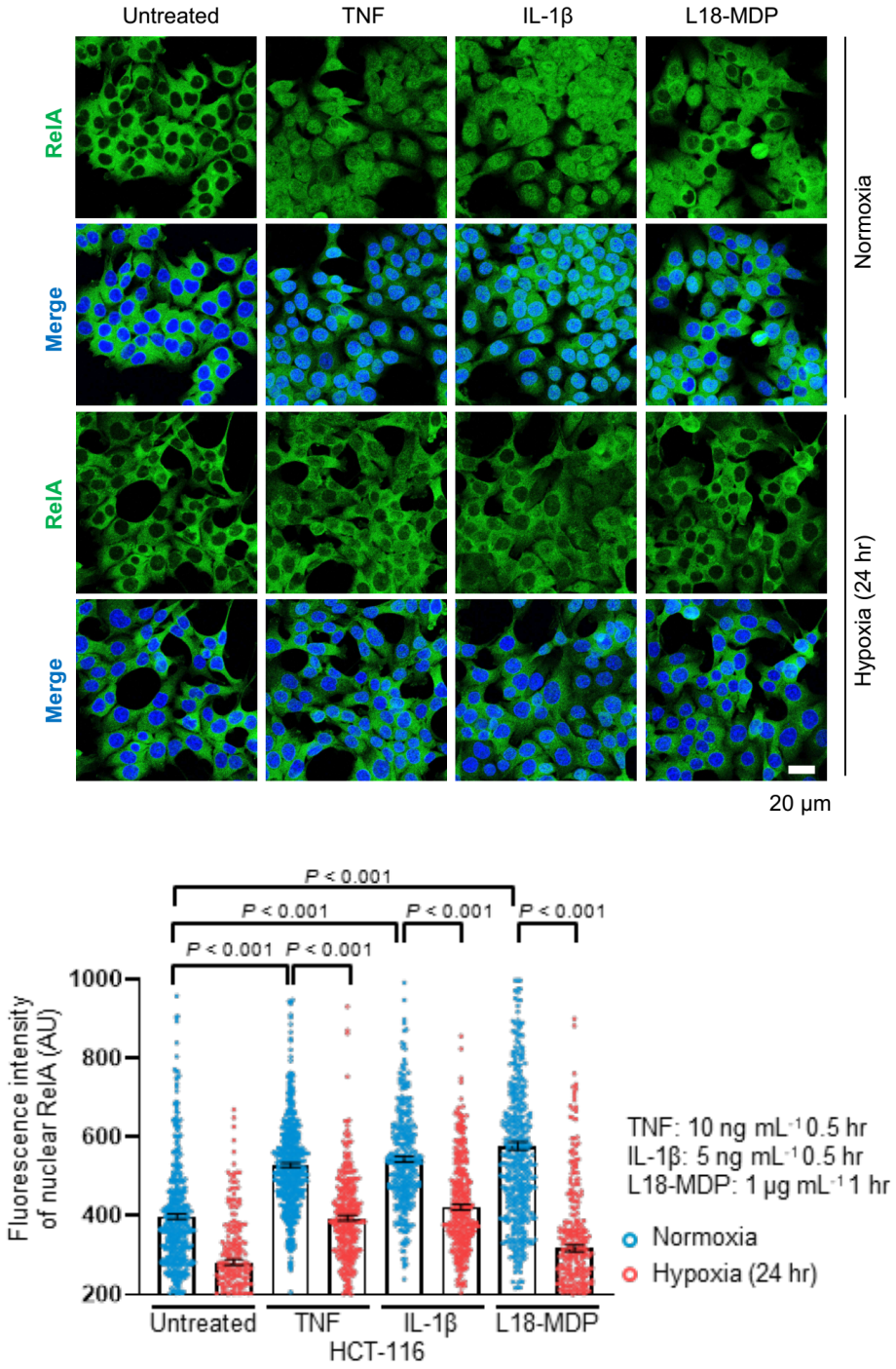


Figure 4.2 Hypoxia inhibits TNF-, IL-1β- and L18-MDP-induced RelA nuclear translocation. HCT-116 cells were cultured under normoxia or hypoxia for 24 hr followed by treatment with TNF (10 ng mL^{-1}; 0.5 hr), IL-1β (1 ng mL^{-1}; 0.5 hr) or L18-MDP (500 ng mL^{-1}; 1 hr), stained with anti-RelA antibody (green) and DAPI (blue). Scale bar, 20 μm (top). Quantification analysis of fluorescence intensities of nuclear localised RelA (bottom) in each condition. AU, arbitrary units. Data are shown mean ± SEM of individual cells (bottom) and one representative of three independent experiments with similar results (top). Statistical significance was determined by one-way ANOVA with Bonferroni's correction.

To elucidate the underlying molecular mechanism, I analysed the activation of these receptors by pulldown of ubiquitinated conjugates [278]. The activation of TNFR1, IL1β receptor and NOD2 by their corresponding ligands requires poly-ubiquitination on their respective adaptor proteins (RIPK1, IRAK1 and RIPK2 respectively). During normoxia, the activation of these receptors triggers the degradation of IκBα and phosphorylation of RelA on Ser536, an activation marker of NF-κB (Figure 4.3A-C). However, hypoxia inhibited TNF-, IL-1β- and L18-MDP-induced ubiquitination on these adaptor proteins and consequently, the degradation of IκBα and the phosphorylation of RelA on Ser536 were also inhibited (Figure 4.3A-C). These data indicated that hypoxia represses the activation of these innate immune receptors.

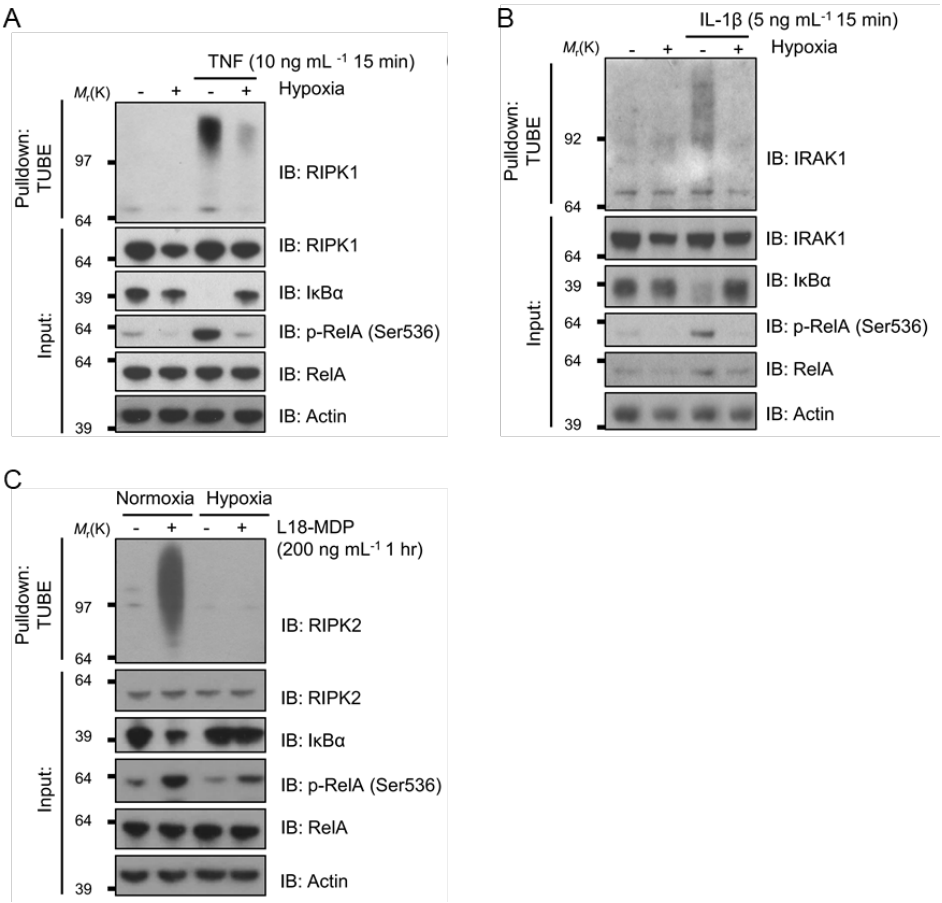


Figure 4.3 Hypoxia represses the activation of innate immune receptors Purification of endogenous ubiquitin conjugates from HCT-116 cells. Cells were cultured under normoxia or hypoxia for 24 hr, then stimulated with TNF (10 ng mL^{-1}; 15 min) (A), IL-1β (5 ng mL^{-1}; 15 min) (B) or L18-MDP (200 ng mL-1; 1 hr) (C) before harvest. Data were shown as one representative of three independent experiments with similar results.

4.2 Hypoxia downregulates TNF receptor 1 (TNFR1)

I wondered whether hypoxic inhibition of these receptor-mediated innate immune responses shared a common mechanism since the activation of these receptors were all inhibited under hypoxia. Considering the complexity of these receptor-mediated immune responses, I focused on TNF signalling to seek for the answer. By the time-course analysis of hypoxia-treated HCT-116 cells, I found that TNF receptor TNFR1 was markedly reduced after 24 hours cultured under hypoxia, while other components within TNF signalling pathway were largely retained (Figure 4.4).

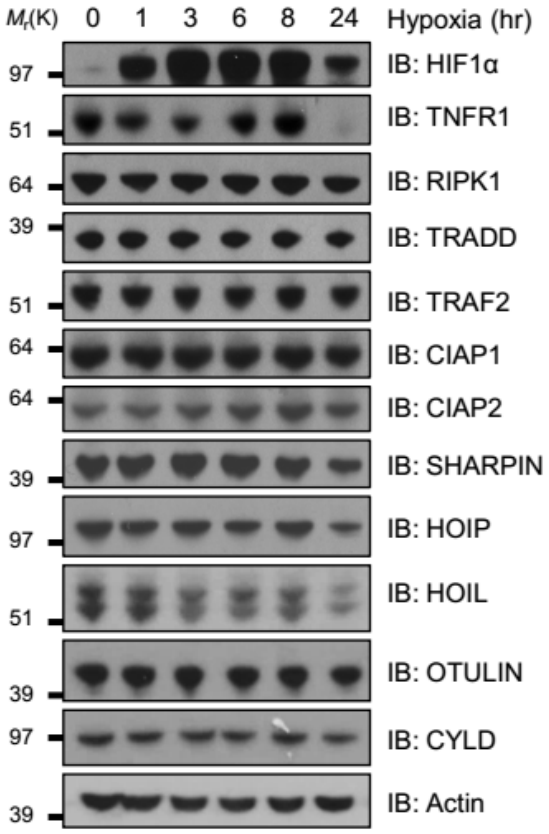


Figure 4.4 TNFR1 is reduced under hypoxia. Analysis of protein levels determined by immunoblotting using the indicated antibodies at the indicated time points in HCT-116 cells cultured under hypoxia. Data were shown as one representative of three independent experiments with similar results.

This result was consistent with my previous data that hypoxia inhibited the activation of TNF receptor. TNFR1 was reduced after 24 hours of hypoxia treatment concomitantly with repressed activation of TNF signalling, as indicated by the stabilisation of IκBα and reduced phosphorylation of RelA (Figure 4.5A). I wondered whether this process could be oxygen dependent, then I cultured the hypoxia-pre-treated cells under normoxia for 6, 12 and 24 hours. The data showed that 12 hours reoxygenation restored TNF signalling by rescuing TNFR1 expression, as indicated by the restoration of IκBα degradation and RelA phosphorylation (Figure 4.5B). TNFR2 is also involved in regulating TNF signalling, although its expression is more restricted in immune cells and endothelial tissues [46]. To exclude the possibility that TNFR2 was involved, I generated *TNFRSF1A* knockout HCT-116 cells and showed that *TNFRSF1A* knockout completely abrogated TNF responsiveness and mirrored the hypoxia-induced phenotype, as indicated by the abrogation of IκBα degradation and phosphorylation of RelA in the presence of TNF (Figure 4.5C). Additionally, hypoxia inhibited TNF-induced expression of NF-κB target genes, which was similar to *TNFRSF1A* knockout cells (Figure 4.5D). Taken together, these data indicated that 1% oxygen causes a strong reduction of TNFR1, resulting in loss of TNF signalling.

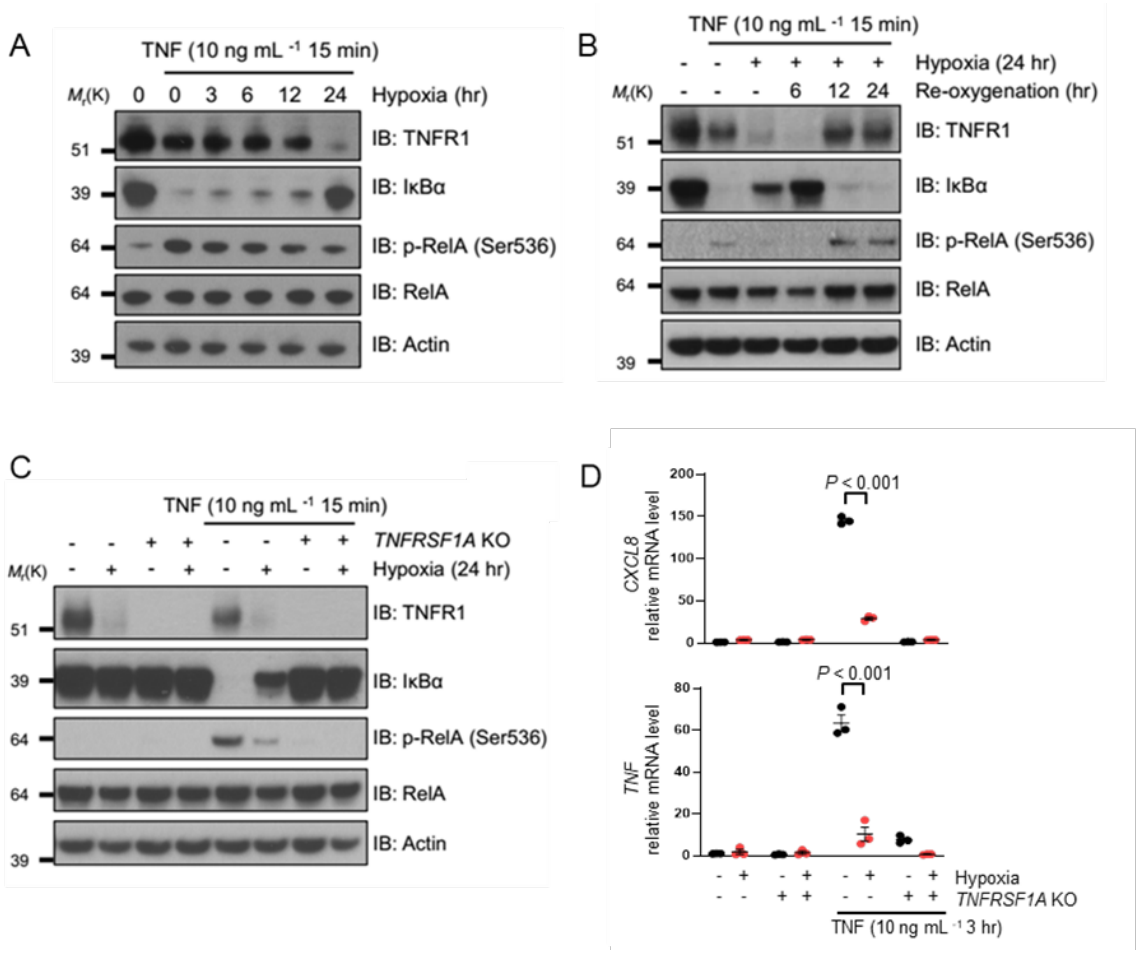


Figure 4.5 Hypoxia mimics *TNFRSF1A* knockout. (A) Analysis of protein levels determined by immunoblotting using the indicated antibodies at the indicated time points in HCT-116 cells cultured under hypoxia followed by stimulation with TNF (10 ng mL-1; 15 min). (B) HCT-116 cells were cultured under hypoxia for 24 hr followed by re-oxygenation for the indicated time points, then stimulated with TNF (10 ng mL^{-1}; 15 min). (C and D) WT or TNFRSF1A knockout HCT-116 cells were cultured under normoxia or hypoxia for 24 hr. Cells were stimulated with TNF (10 ng mL^{-1}; 15 min) and subjected to immunoblotting with the indicated antibodies (C) or stimulated with TNF (10 ng mL^{-1}; 3 hr) and analysed by qRT-PCR. *CXCL8* and *TNF* mRNA were determined by qRT-PCR (D). qRT-PCR results were normalised to the housekeeping gene *B2M*. Data are shown mean ± SEM of three independent experiments or one representative of three independent experiments with similar results. Statistical significance was determined by one-way ANOVA with Bonferroni's correction.

To test if the observations from HCT-116 would apply also to other similar cell lines, I tested Caco-2, SW48, GP2d and LS-174T (Figure 4.6A), which all consistently showed hypoxic inhibition of TNFR1 expression and of activation of TNF signalling, as indicated by the status of IκBα and phosphorylation of RelA.

It is difficult to test the impact of hypoxia on the immune signalling in the gut *in vivo*. However, organoids are 3D cell culture systems that mimic some of the structural and

functional characteristics of an organ, allowing me to test the role of hypoxia on immune signalling in intestine organoids. Therefore, I cultured organoids that derived from the human duodenum under hypoxia to simulate the hypoxic microenvironment. Consistent with the cell line data, hypoxia also inhibited TNF-induced NF-κB target genes expression including *CXCL8*, *TNF* and *TNFAIP3* in these organoids (Figure 4.6B), suggesting that hypoxia plays an immune-regulatory role not only in transformed cells, but also in primary cells.

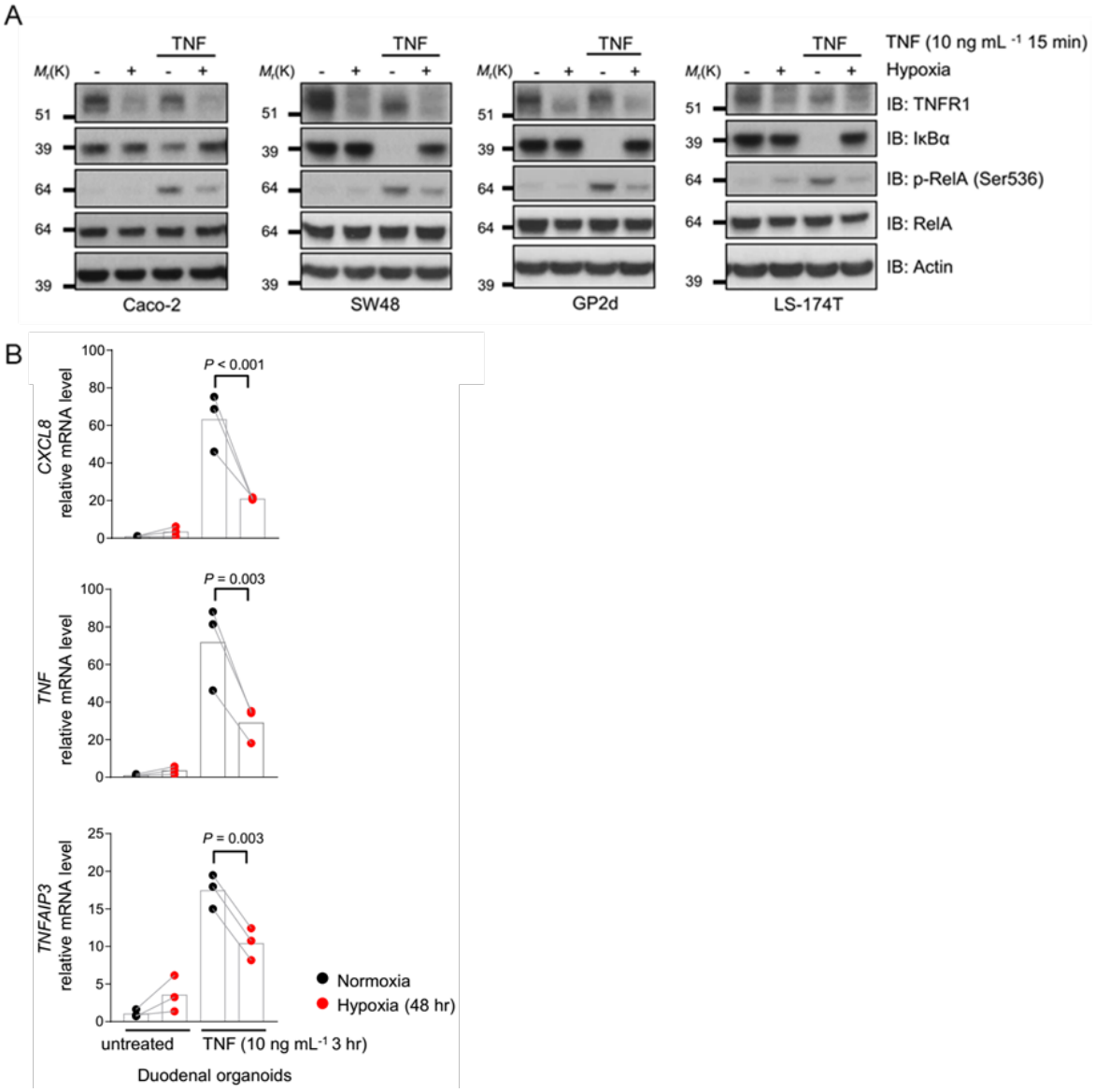


Figure 4.6 Hypoxia inhibits TNF signalling in multiple cell lines and in duodenal organoids. (A) The indicated cell lines were cultured under hypoxia for 24 hr followed by stimulation with TNF (10 ng mL^{-1}; 15 min). (B) Human duodenal organoids derived from 3 donors were culture under normoxia or hypoxia for 48 hr followed by stimulation with TNF (10 ng mL^{-1}; 3 hr). *CXCL8*, *TNF* and *TNFAIP3* mRNA were determined by qRT-PCR. qRT-PCR results were normalised to the housekeeping gene *B2M*. Data are shown mean as one representative of three independent experiments with similar results. Statistical significance was determined by one-way ANOVA with Bonferroni's correction.

4.3 Hypoxia inhibits TNF-induced cell death

Apart from the role of TNF in activation of inflammatory response, it also regulates cell death (Figure 1.5). Therefore, I tested the effect of hypoxia on TNF-induced cell death in HT-29 cells, which are sensitive to TNF-mediated killing [72]. From a time-course experiment, I found that total TNFR1 was substantially reduced after 24 hours of hypoxia treatment (Figure 4.7A). However, the degradation of IκBα was still sensitive in response to TNF, this probably due to the remaining TNFR1 on the cell surface as membrane localised TNFR1 is also regulated by membrane trafficking [279, 280]. The accumulation of IκBα started to be obvious after 48 hours of hypoxia (Figure 4.7A). Therefore, I pre-treated the HT-29 cells under hypoxia for 48 hours and then tested TNF-induced cell death. The cells were treated with TNF alone or together with SMAC mimetics Compound A (CpA) to induce RIPK1-dependent apoptosis or treated additional with pan-Caspase inhibitor zVAD to induce RIPK1-dependent necroptosis (Figure 1.5). Hypoxia significantly inhibited TNF-mediated apoptosis (CpA treated) and necroptosis (CpA+zVAD treated), which mirrored RIPK1 inhibitor Necrostatin-1 (Nec1s)-mediated blockade of cell death (Figure 4.7B). These data indicated that hypoxia-mediated TNFR1 reduction is not only capable of inhibiting TNF-induced inflammatory signalling, but also sufficient to block TNF-induced cell death.

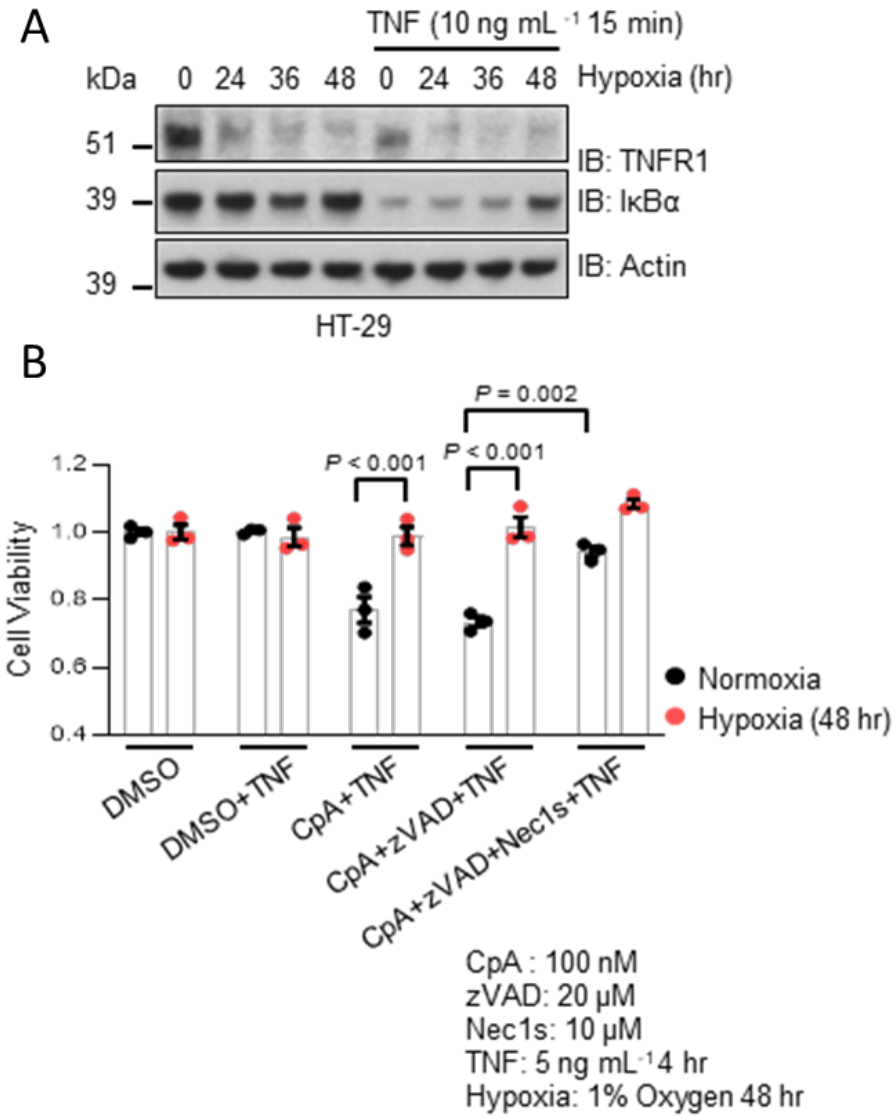


Figure 4.7 Hypoxia inhibits TNF-induced cell death. (A) HT-29 cells were cultured under hypoxia for the indicated time points followed by stimulation with TNF (10 ng mL^{-1}; 15 min). (B) HT-29 cells were cultured under hypoxia for 48 hr followed by the indicated treatments for additional 4 hr. Cell viability was determined by CellTiter-Glo. TNF (5 ng mL^{-1}), Compound A (CpA, 100 nM), zVAD (20 μM), Necrostatin-1 (Nec1s, 10 μM). Data are shown mean ± SEM of three independent experiments (B) or one representative of three independent experiments with similar results (A). Statistical significance was determined by one-way ANOVA with Bonferroni's correction.

4.4 Hypoxia-induced TNFR1 reduction is regulated at translational level

The reduced protein expression could be either due to increased protein degradation, reduced mRNA or reduced protein translation. To explore the mechanisms behind the reduced level of TNFR1 during hypoxia, I first tested the half-life of TNFR1 under hypoxia by cycloheximide chase. Although hypoxia downregulated TNFR1, the half-life seemed not shortened by hypoxia (Figure 4.8A-C). This probably was caused be detection limits as basil level of TNFR1 under hypoxia was low, whereas background signals were getting high.

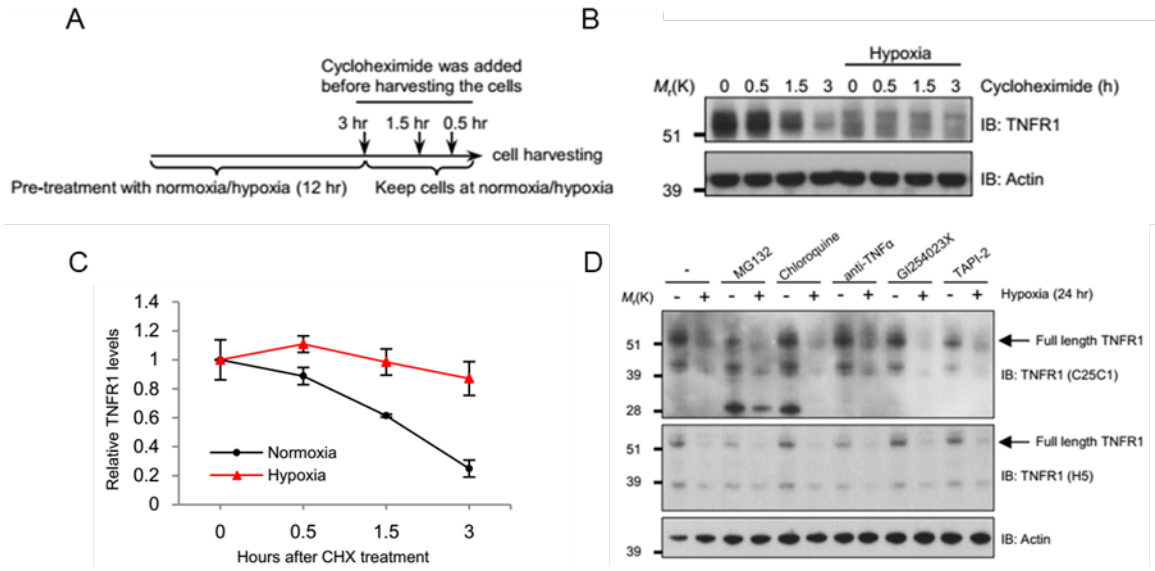


Figure 4.8 The half-life of TNFR1 is not shortened under hypoxia. (A) Schematic overview of the experimental strategy. (B) HCT-116 cells were treated with 100 μg ml^{-1} cycloheximide (CHX) for the indicated time points under normoxia or hypoxia. (C) Quantification analysis of TNFR1 protein levels in (B). (D) HCT-116 cells were treated with the indicated inhibitors and cultured under hypoxia for 24 hr. TNFR1 protein levels were determined by immunoblotting with two different monoclonal antibodies against TNFR1. MG132 (20 μM), Chloroquine (60 μM), neutralising antibody against TNF (1 μg mL^{-1}), G1254023X (10 μM) and TAPI2 (100 μM). Data are shown mean ± SEM of three independent experiments (C) or one representative of three independent experiments with similar results (B and D).

To further validate this result, I treated the cells with multiple inhibitors or neutralising antibody including the proteasome inhibitor MG132, the lysosome inhibitor Chloroquine, the inhibitors of the previous reported TNFR1 peptidases ADAM10/17 [281, 282] G1254023X [283] and TAPI2 [284] and the neutralising antibody of TNF [285] (Figure

4.8D). I also tested TNFR1 expression with different TNFR1 antibodies, which recognise the N-terminus and C-terminus, respectively, just in case of antigen lost due to protease-mediated cleavage on TNFR1. However, none of these treatments blocked hypoxia-induced reduction of TNFR1. In addition, *TNFRSF1A* mRNA level was slightly reduced under hypoxia (Figure 4.9A), but this cannot explain the robust reduction of TNFR1 under hypoxia, implying that the reduction of TNFR1 is more likely due to the reduction of protein translation.

Hypoxia-inducible factor 1α (HIF1α) is stabilised under hypoxia and plays important roles during cellular hypoxia response. Therefore, I tested whether hypoxia-mediated reduction of TNFR1 was due to the accumulation of HIF1α. Two shRNAs against HIF1α were deployed, which successfully inhibited the induction of HIF1α under hypoxia. However, in HIF1α knockdown cells, TNFR1 levels were still reduced under hypoxic conditions and showed no obvious difference compared with the wild-type cells (Figure 4.9B), indicating that HIF1α is not involved in hypoxia-mediated reduction of TNFR1.

The regulatory components of translation within mRNAs locate at the 5'- and 3'-UTR. To compare the contributions of 5'- and 3'-UTR of *TNFRSF1A* in regulation of translation during hypoxia, I cloned its 5'-UTR and 3'-UTR and inserted them into corresponding GFP-expressing vectors, respectively (Figure 4.10A). To test the *de novo* synthesised GFP during hypoxia, I co-transfected the GFP reporters with a transfection control RFP vector and maintained under normoxia for only 2 hours to ensure sufficient transfection efficiency before culturing the cells under hypoxia. Surprisingly, I found that the expression of 5'-UTR-containing reporter was dramatically reduced under hypoxia (Figure 4.10B and 4.10C).

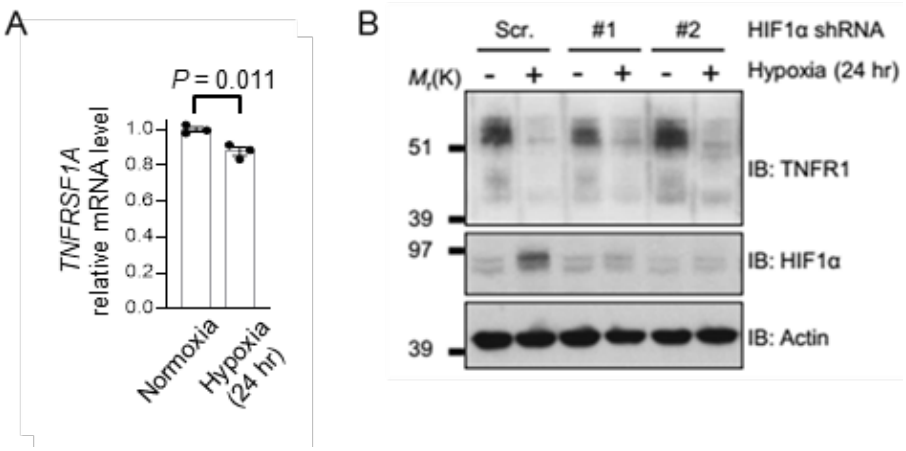


Figure 4.9 Hypoxia-induced TNFR1 reduction is independent of HIF1α. (A) *TNFRSF1A* mRNA was determined by qRT-PCR. qRT-PCR results were normalised to the housekeeping gene *B2M*. (B) Wild type and stable *HIF1α*-knockdown HCT-116 cells were cultured under hypoxia for 24 hr and analysed by immunoblotting with the indicated antibodies. Data are shown mean ± SEM of three independent experiments (A) or one representative of three independent experiments with similar results (B). Two-tailed unpaired ratio t-test was used.

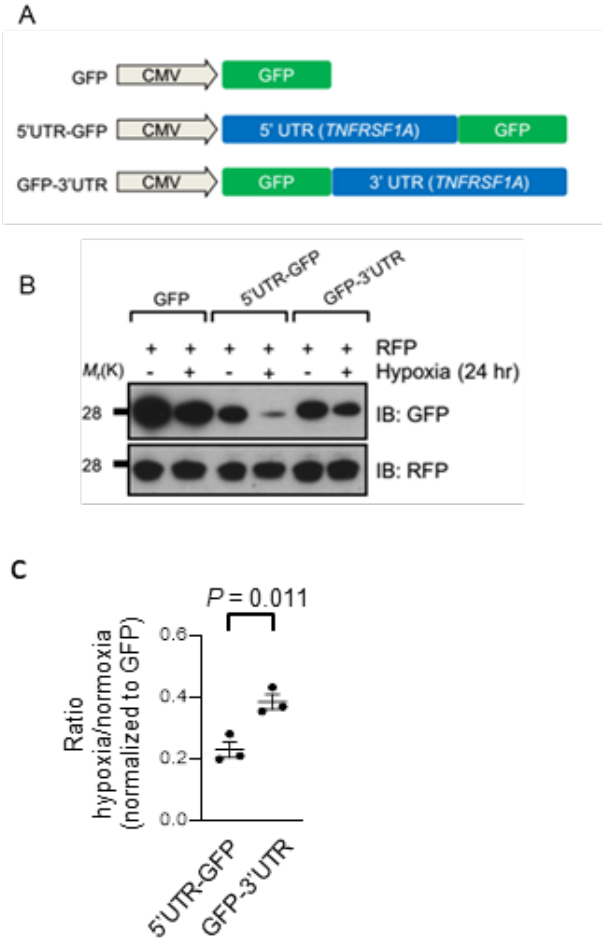


Figure 4.10 Hypoxia downregulates TNFR1 translation via 5'UTR. (A) Schematic drawing of GFP reporter constructs. (B) HCT-116 cells were transfected with the indicated constructs 2 hr before culturing under hypoxia for additional 24 hr. (C) GFP and RFP reporters were quantitatively analysed. Data are shown as one representative of three independent experiments with similar results.

Further analysis of human 5'-UTR of *TNFRSF1A* revealed two uORFs (hereafter defined by ATG as the start codon) overlapped with each other in different frames (Figure 4.11A) and both of them located in the upstream of the CDS. The sequence of uORF2 was identified to be highly conserved comparing with uORF1 among different species (Figure 4.11A), implying that the existence of uOFR2 may be crucial for fine-tuning TNF signalling. Recognition of the start codon is crucial for translation. Hence, to test whether these uORFs were recognisable by ribosomes, I analysed the ribosome footprint data derived from multiple cell lines [286-293]. The data showed that both start codons of these uORFs were translation initiation sites (Figure 4.11B). However, in these studies, to grasp the initiation

sites, the cells need to be treated by elongation inhibitors [294, 295], thus it was difficult to compare the initiation efficiencies of these uORFs as inhibitor-induced ribosome stalling at uORF1 could block ribosome scanning of uORF2. To compare the initiation strength of uORF1 and uORF2, I generated two GFP reporters, which expressions were either initiated by the start codon of uORF1 or uORF2 (Figure 4.12A). Intriguingly, I found that uORF2 was highly translated comparing with uORF1 (Figure 4.12C). In addition, the expression of uORFs in mouse *TNFRSF1A* also showed similar pattern as humans (Figure 4.12B and 4.12D), indicating that the translational regulation of *TNFRSF1A* is conserved similar between species.

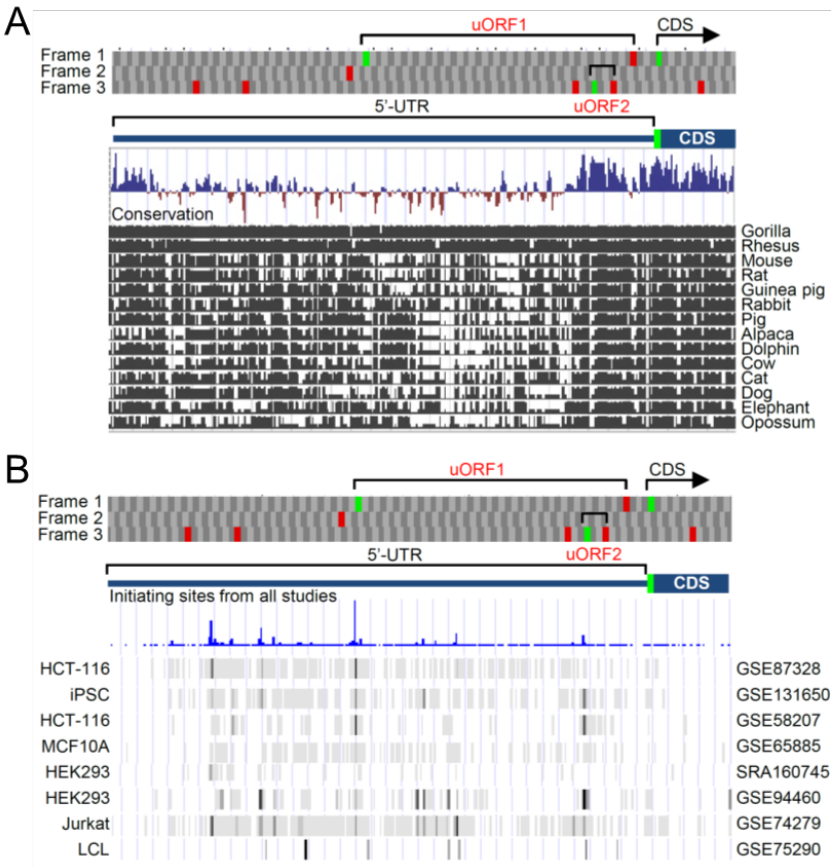


Figure 4.11 Identification of uORFs in the 5'UTR of *TNFRSF1A*. (A) Analysis of evolutionary conservation of uORF2 among species by UCSC Genome Browser. The conservation scores of all species (blue) and individual specie (grey) were shown. Start codon (green) and stop codon (red) were indicated on each frame. (B) Ribo-seq data analysis of ribosome initiation sites of human *TNFRSF1A* in the indicated cells derived from indicated studies.

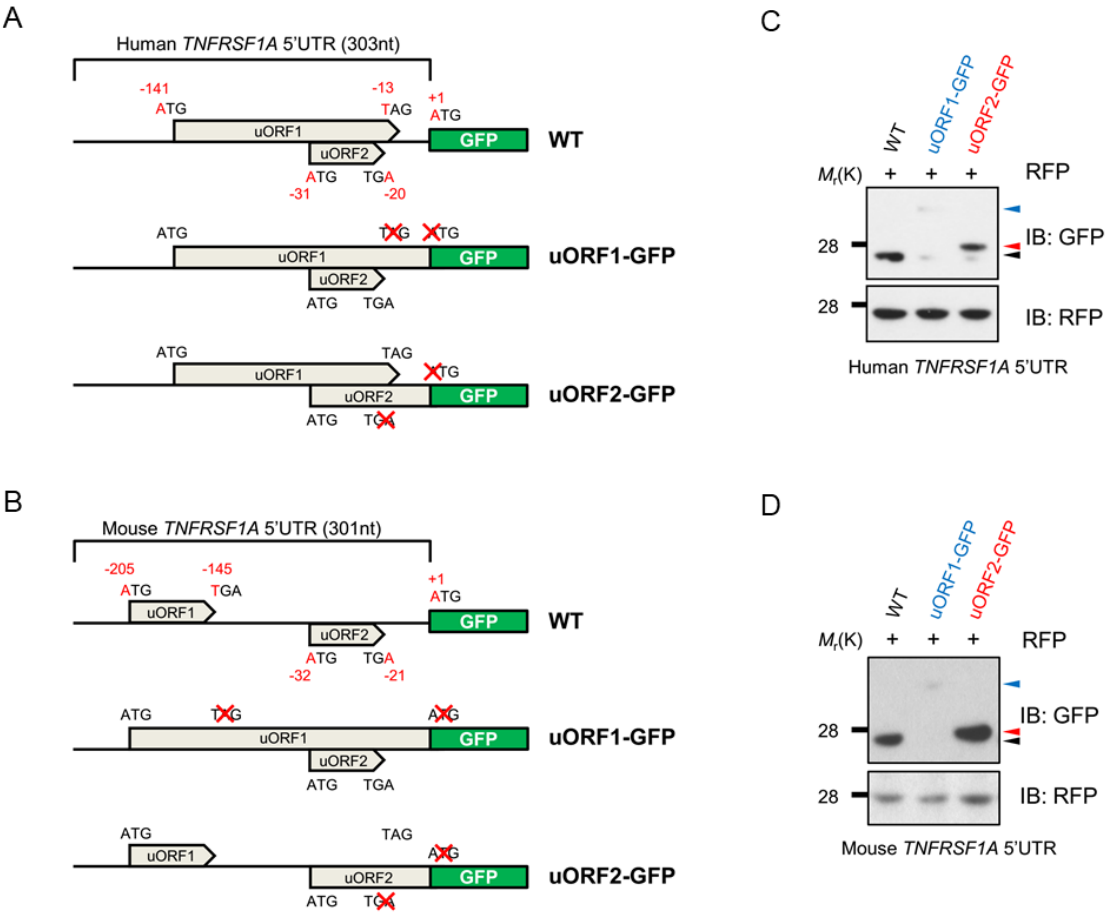


Figure 4.12 The conserved uORF2 is highly used for translation. (A-B) Schematic drawing of human (A) and mouse (B) *TNFRSF1A* 5'-UTR GFP reporter constructs. (C-D) HCT-116 cells were transfected with the indicated constructs 2 hr before culturing under hypoxia for additional 24 hr. Human (C) or mouse (D) *TNFRSF1A* 5'-UTR GFP reporters were analysed by immunoblotting. Data are shown as one representative of three independent experiments with similar results (C and D).

4.5 uORF2 of *TNFRSF1A* inhibits TNFR1 translation under hypoxia

uORF2 is very short, it only contains 12 nucleotides, which encode a peptide that only has 3 amino acids. To explore whether uORF2 affected the expression of TNFR1 under hypoxia, I generated a series of constructs that were mutated of either the start codon or the stop codon of uORF2 (Figure 4.13A). All the start codon mutations enhanced the expression of GFP in HCT-116 (Figure 4.13B) and HEK293T cells (Figure 4.13D) under both normoxia and hypoxia, indicating that the recognition of the start codon of uORF2 is important to constantly inhibit GFP expression. Then I generated three mutants at the stop codon, including two alternative stop codons (-21G>A and -20A>G/-21G>A) and one readthrough mutant (-20A>T) to test the impact of the stop codon of uORF2 on GFP expression. Two alternative stop codon mutants -21G>A and -20A>G/-21G>A showed very similar expression pattern as wild-type (Figure 4.13C), indicating that stop codon preference has on impact on GFP expression. However, the stop codon mutant -20A>T substantially inhibited the expression of GFP under both normoxia and hypoxia (Figure 4.13C). This mutant generated a new uORF2 that overlapped with the CDS of GFP, which was very similar to the uORF2 of ATF4 (Figure 1.15). These data showed that translation termination at the stop codon of uORF2 was essential for GFP translation, indicating that the expression of GFP depends on ribosome reinitiation after translation of uORF2. Previous studies showed that the reinitiation efficiency of downstream CDS depends on the length of uORF [296]. To test this, I enlarged the length of uORF2 by fusing it with a RFP-coding CDS, which generated a RFP-fusion open reading frame upstream of GFP by using the start codon from the CDS of RFP and the stop codon from uORF2 (Figure 4.13E). The expression of GFP was completely inhibited by the translation of this long uORF (Figure 4.13F), suggesting the notion that TNFR1 expression is controlled by reinitiation.

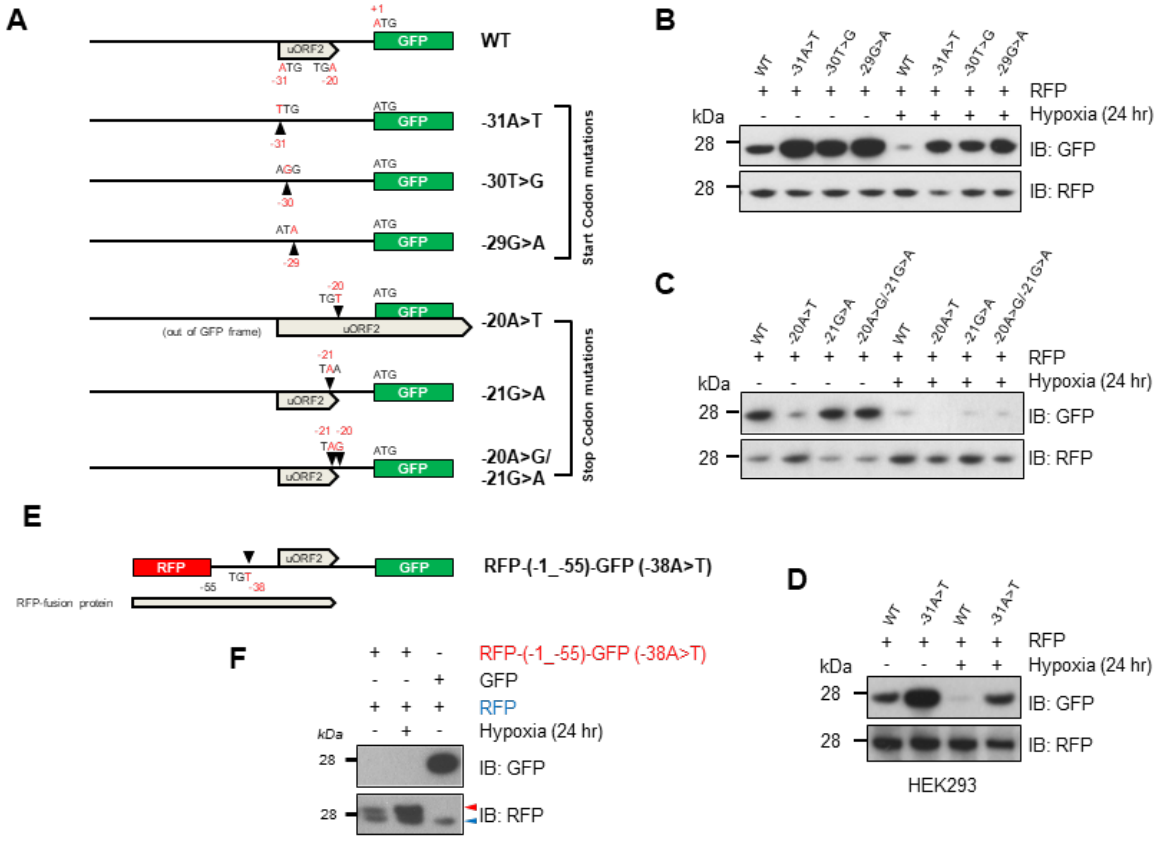


Figure 4.13 uORF2 restricts translation of TNFR1 under both normoxia and hypoxia. (A) Schematic drawing of the GFP reporter constructs with mutations of the start codon or stop codon. (B-C) HCT-116 cells were transfected with the indicated constructs 2 hr before culturing under hypoxia for additional 24 hr. Start codon (B) and stop codon (C) mutant GFP reporters were analysed by immunoblotting. (D) HEK-293T cells were transfected with the indicated constructs 2 hr before culturing under hypoxia for additional 24hr. GFP and RFP reporters were analysed by immunoblotting. (E) Schematic drawing of the RFP-5'-UTR (Human *TNFRSF1A* -1_-55)-GFP fusion reporter construct. RFP coding sequence was fused with 5'UTR (-1_-55 of Human *TNFRSF1A*) at the 5' end. A point mutation (-38A>T) was introduced to ensure RFP and uORF2 were in a single reading frame. (F) HCT-116 cells were transfected with the indicated constructs 2 hr before culturing under hypoxia for additional 24hr. GFP and RFP reporters were analysed by immunoblotting. Data are shown as one representative of three independent experiments with similar results (B-D and F).

Similar to ATF4 (Figure 1.15), the stop codon mutant -20A>T generated a protein encoded by a long uORF2. Translation of this long uORF2 bypassed the start codon of GFP during ribosome scanning, resulting in low GFP expression, which mirrored hypoxia-induced inhibition of GFP expression in the wild-type (Figure 4.13C). Previous studies showed that decreased hydroxylation on ribosome proteins and termination factor eRF1 can induce stop codon readthrough, which process is also affected during hypoxia [242, 259]. To test whether hypoxia can mediate stop codon readthrough at uORF2, I generated a series of constructs by inserting a Flag-coding sequence into 3'-end of the start codon of uORF2 (or relevant uORF2 mutant), allowing me to examine the uORF2-coding product by detecting Flag if there were stop codon readthrough. Among these GFP reporters (Figure 4.14A), the stop codon mutant -20A>T mimicked the product of uORF2 stop codon read-through and was used as a positive control. The insertion of Flag-tag did not affect the inhibitory role of uORF2 in GFP expression and no stop codon read-through was found under hypoxia (Figure 4.14B), since there was no flag-tagged protein expression in the wild-type group under either normoxic or hypoxic conditions.

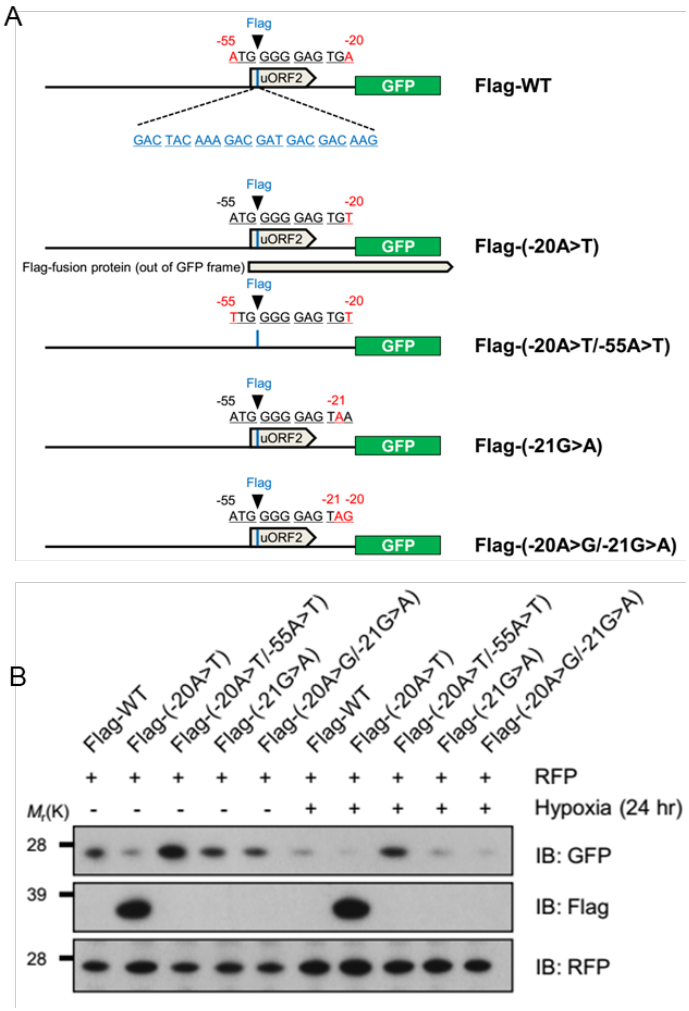


Figure 4.14 Hypoxia-induced reduction of TNFR1 is not due to stop codon read-through. (A) Schematic drawing of the GFP reporter constructs with an insertion of Flag-sequence. (B) HCT-116 cells were transfected with the indicated constructs 2 hr before culturing under hypoxia for additional 24hr. GFP and RFP reporters were analysed by immunoblotting. Data are shown as one representative of three independent experiments with similar results (B).

By using a plate reader, I also quantified the potential sequence-effect of uORF2 on GFP expression (Figure 4.15). I used Renilla luciferase to normalise the transfection efficiency because small amount of RFP plasmid transfection was less sensitive to be detected by fluorescence. The result showed that except for the start codon mutations enhanced GFP expression and the stop codon mutant -20A>T inhibited GFP expression, all other mutations, including sequence alterations within uORF2 (-26G>C/-27G>C/-28G>C), sequence alterations adjacent to uORF2 (-34C>G/-35C>G/-36>G) and a shorter form of uOFR2 (-25G>T), which just encoded 2 amino acids, largely maintained suppression of GFP

expression as the wild-type (Figure 4.15), indicating that the inhibition of GFP expression by uORF2 is depending on its translation.

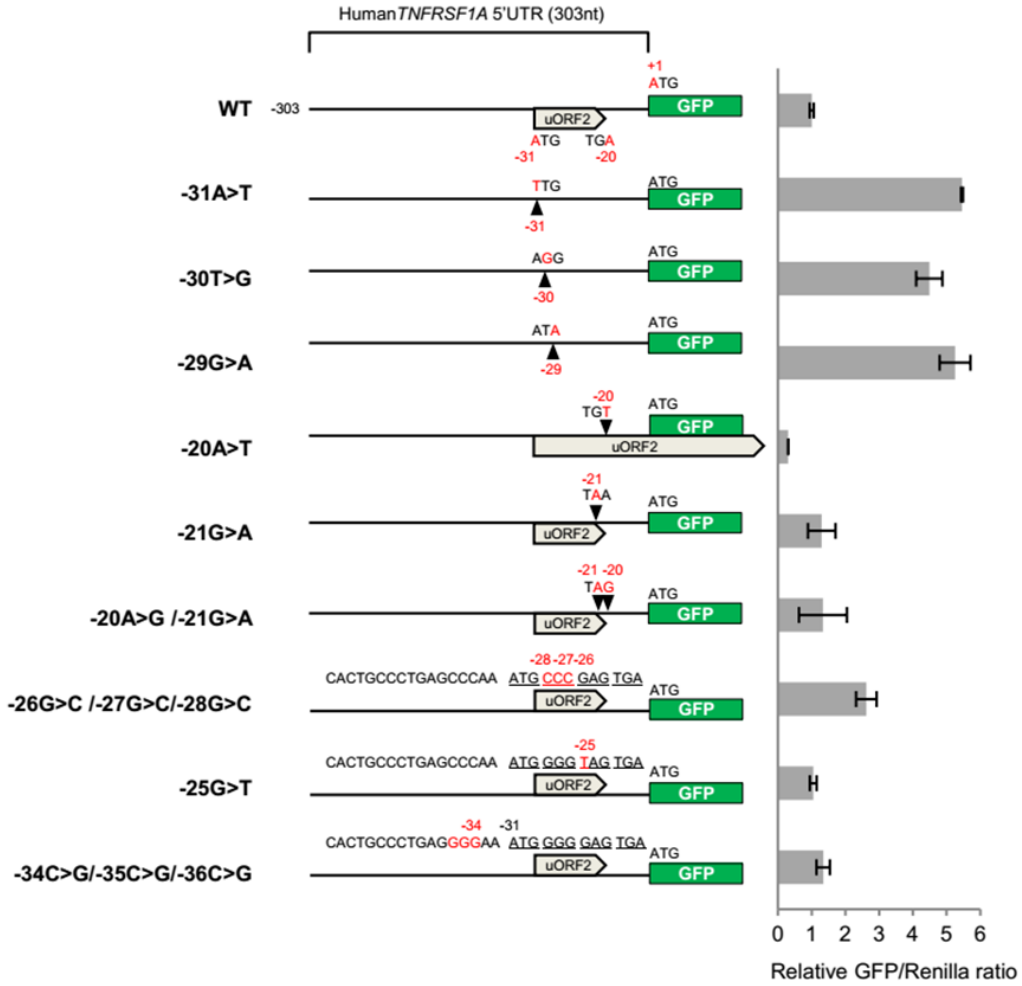


Figure 4.15 The sequence of uORF2 barely has influence on reinitiation efficiency. Schematic drawing of various Human *TNFRSF1A* 5'-UTR-GFP reporters. The corresponding reporter expression levels were showed on the right. GFP expression levels were determined by fluorescence reader and normalised to Renilla luciferase levels. Data are shown mean ± SEM of three independent experiments.

4.6 Deleting uORF2 of *TNFRSF1A* increases TNFR1 translation and amplifies TNF sensitivity

To test the endogenous function of uORF2 in regulation of TNFR1 expression and potentially TNF signalling, I designed a sgRNA that specifically target to uORF2 of *TNFRSF1A*. A protospacer adjacent motif (PAM) was found in the complementary strand of uORF2 (Figure 4.16A), making it possible to evaluate the impact of uORF2 on the regulation of endogenous TNFR1 expression by CRISPR-Cas9. The location of the cutting site by Cas9 protein was designed within the start codon of uORF2 (between T and G), resulting in higher efficiency of mutating the start codon of uORF2 after non-homologous end joining repair. By using this method, I successfully generated uORF2 mutated polyclones and they were resistant to hypoxia-induced TNFR1 reduction (Figure 4.16B), resulting in higher TNF-induced NF-κB target gene expression comparing with the wild-type (sg_GFP) during hypoxia (Figure 4.16C).

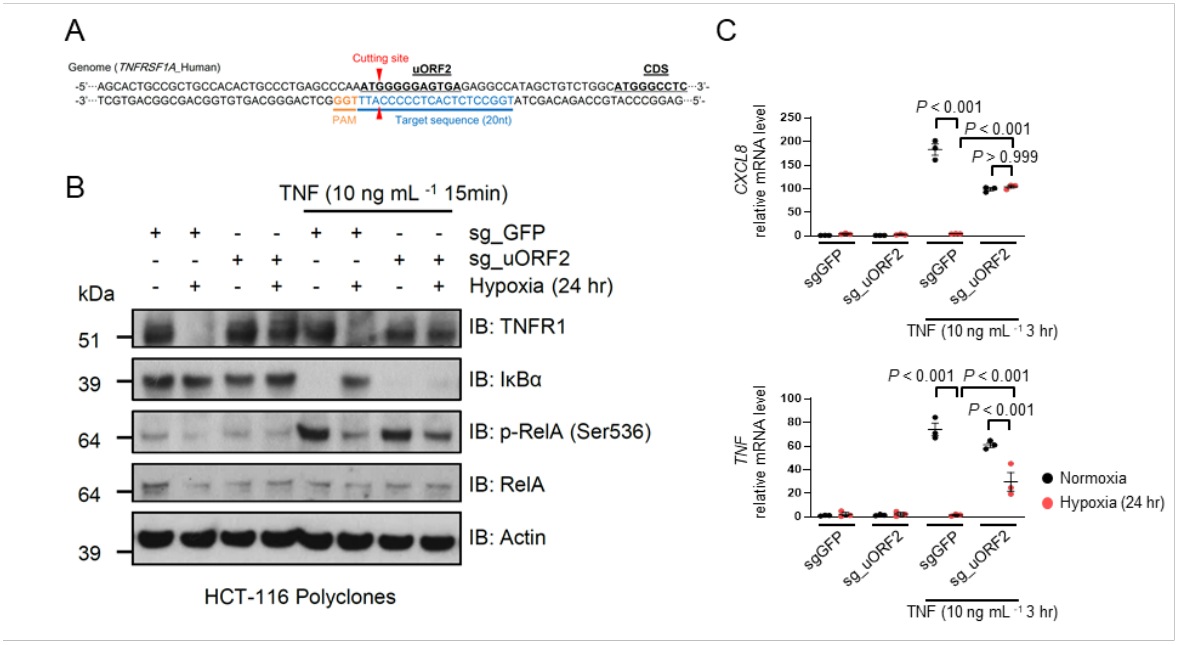


Figure 4.16 Generation of uORF2 mutant polyclones (A) The CRISPR -CAS9 target sequence and cutting site on uORF2 of human *TNFRSF1A*. (B and C) Wild-type and uORF2 mutant HCT-116 cells (polyclones) were cultured under normoxia or hypoxia for 24 hr. Cells were stimulated with TNF (10 ng mL^{-1}; 15 min) and subjected to immunoblotting with the indicated antibodies (B) or stimulated with TNF (10 ng mL^{-1}; 3 hr) and analysed by qRT-PCR. *CXCL8* and *TNF* mRNA (C) were determined by qRT-PCR. qRT-PCR results were normalised to the housekeeping gene *B2M*. Data are shown mean ± SEM of three independent experiments (C) or one representative of three independent experiments with similar results (B). Statistical significance was determined by one-way ANOVA with Bonferroni's correction.

Two monoclonal cell lines were randomly separated from the polyclones (Figure 4.17A). As expected, both clones showed increased surface (Figure 4.17B) and total (Figure 4.17C) TNFR1 expression comparing with wild-type control, resulting in increased sensitivity to low concentrations of TNF (Figure 4.17C and 4.17D). It is worthy to notice that Clone #1 was homozygous with complete uORF2 loss in both alleles, whereas clone #2 was heterozygous with uORF2 loss only in allele 1 and one frame shift mutation in allele 2 (Figure 4.17A), which generated a larger uORF2 that blocked the translation of TNFR1 on the mRNA transcribed from allele 2. As a consequence, the expression level of TNFR1 and TNF sensitivity were lower in clone #2 comparing with clone #1, but still higher than wild-type (Figure 4.17B-D), suggesting that deletion of uORF2 in only one allele is sufficient to

increase TNFR1 expression and subsequent TNF signalling. However, the expression of *CXCL8* and *TNF* in these clones showed some differences, which could be due to different sensitivities of transcription of *CXCL8* and *TNF* to the activation of NF-κB.

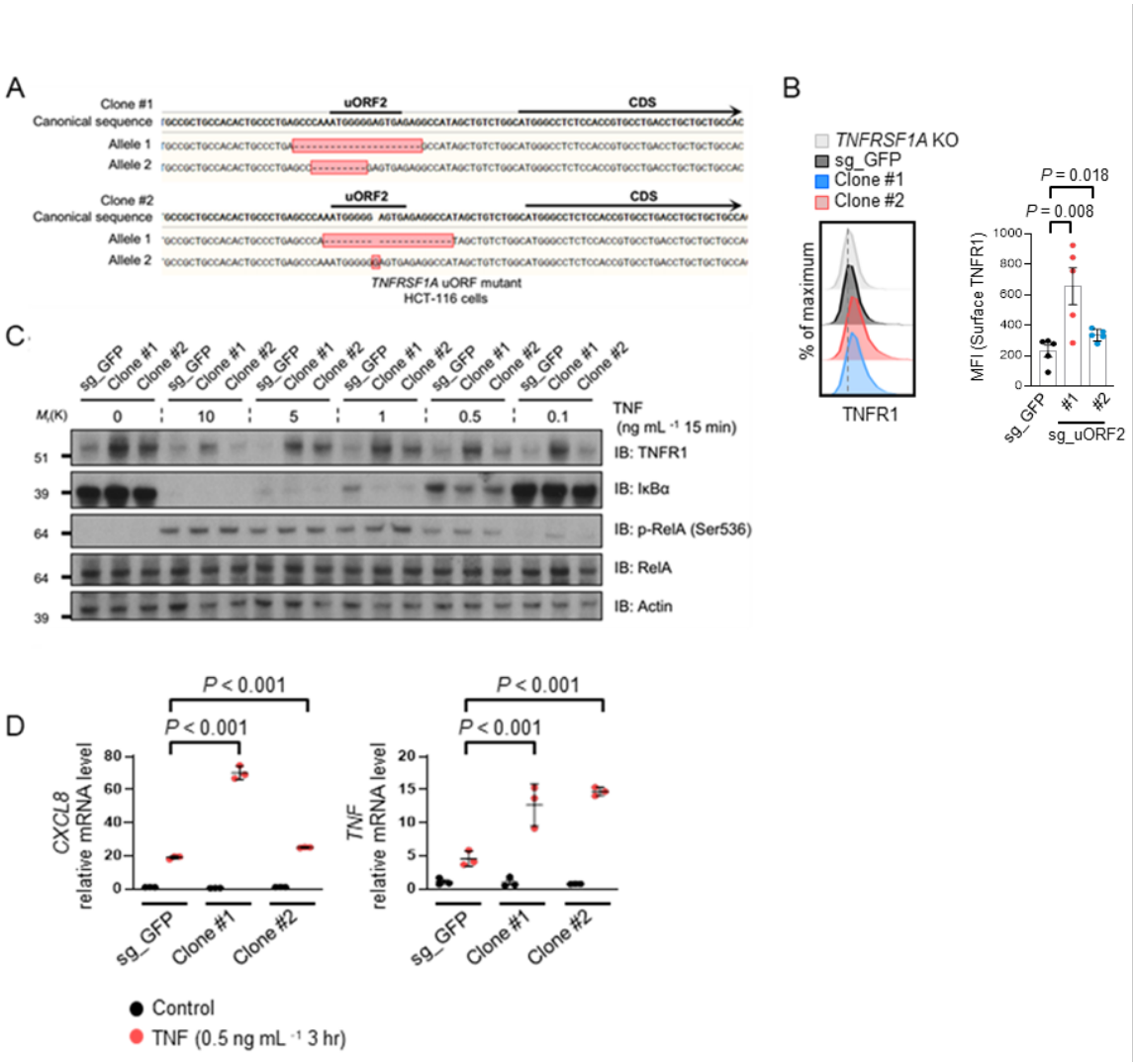


Figure 4.17 Deleting uORF2 increases TNF sensitivity. (A) Genomic sequences of alleles in uORF2 mutants. (B) Wild type, *TNFRSF1A* knockout and uORF2 mutant HCT-116 cells were surface stained with anti-TNFR1 antibody and analysed by flow cytometry. (C) Wild type and uORF2 mutant HCT-116 cells were stimulated with the indicated concentrations of TNF for 15 min and then analysed by immunoblotting with the indicated antibodies. (D) Wild type and uORF2 mutant HCT-116 cells were stimulated with TNF (0.5 ng mL^{-1}; 3 hr). *CXCL8* and *TNF* mRNA were determined by qRT-PCR. qRT-PCR results were normalised to the housekeeping gene *B2M*. Data are shown mean ± SEM of three independent experiments (B and D) or one representative of three independent experiments with similar results (C). Statistical significance was determined by one-way ANOVA with Dunnett's correction (B) and one-way ANOVA with Bonferroni's correction (D).

In addition, although both clones showed reduced *TNFRSF1A* mRNA levels (Figure 4.18A), they still restored TNFR1 expression (Figure 4.18B) and NF-κB target genes expression (Figure 4.18C) under hypoxia, supporting the notion that the presence of uORF2 regulates the threshold of TNF sensitivity under hypoxia.

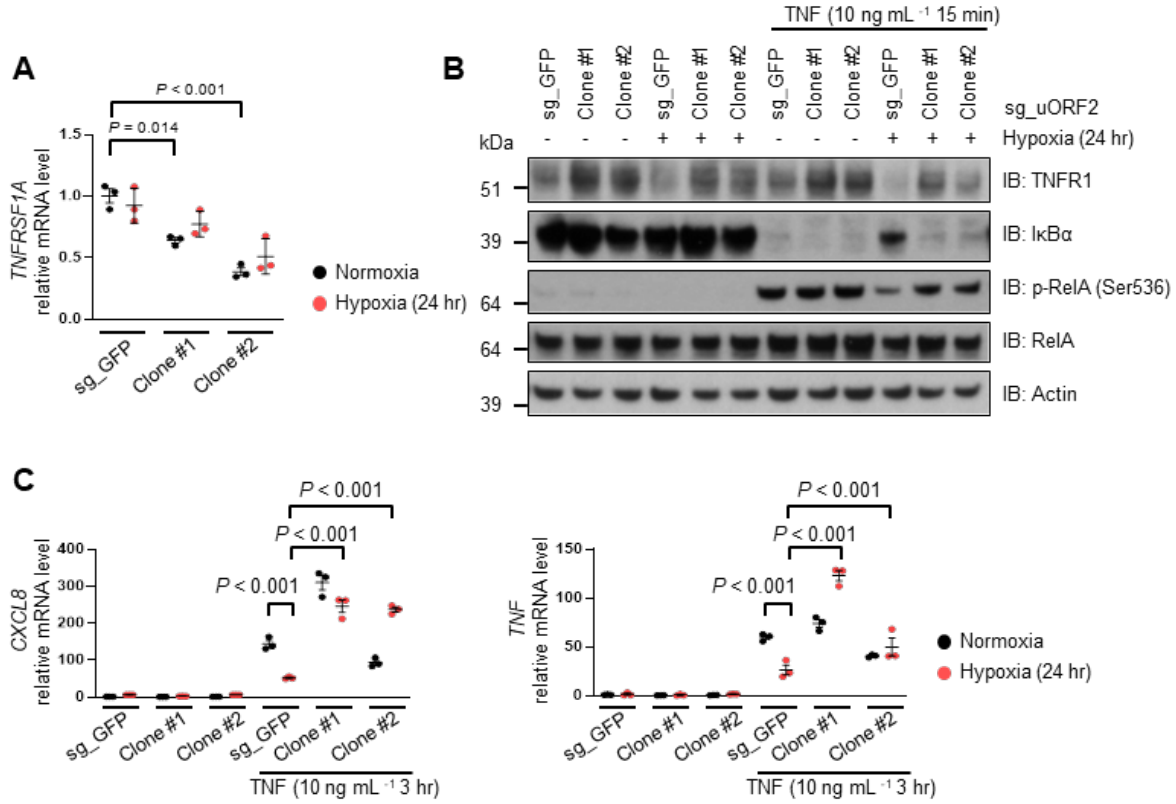


Figure 4.18 Deleting uORF2 maintains TNF signalling under hypoxia. (A-C) Wild type and uORF2 mutant HCT-116 cells were cultured under normoxia or hypoxia for 24 hr. *TNFRSF1A* mRNA levels were analysed by qRT-PCR or stimulated with TNF (10 ng mL^{-1}; 15 min) and subjected to immunoblotting with the indicated antibodies (B) or stimulated with TNF (10 ng mL^{-1}; 3 hr) and *CXCL8* and *TNF* mRNAs (C) were determined by qRT-PCR. qRT-PCR results were normalised to the housekeeping gene *B2M*. Data are shown mean ± SEM of three independent experiments (A and C) or one representative of three independent experiments with similar results (B). Statistical significance was determined by one-way ANOVA with Bonferroni's correction.

To show that the elevated expression of TNFR1 is due to uORF2 mutation, I utilised click chemistry to check the *de novo* synthesised TNFR1 under both normoxia and hyppxia. The principle of this method is by using L-methionine surrogate L-Azidohomoalanine (L-AHA) to label all *de novo* synthesised proteins. The L-AHA incorporated proteins can be further labelled with biotin through azide-alkyne Huisgen cycloaddition reaction and be purified by streptavidin-beads (Figure 4.19A). In the experiment, I utilised *TNFRSF1A* knockout and L-AHA non-treated cells as negative controls and the data indicated that mutations of uORF2 can indeed enhance the *de novo* protein synthesis of TNFR1 under both normoxia and hypoxia (Figure 4.19B), whereas other proteins such as RelA and S6 are largely not affected.

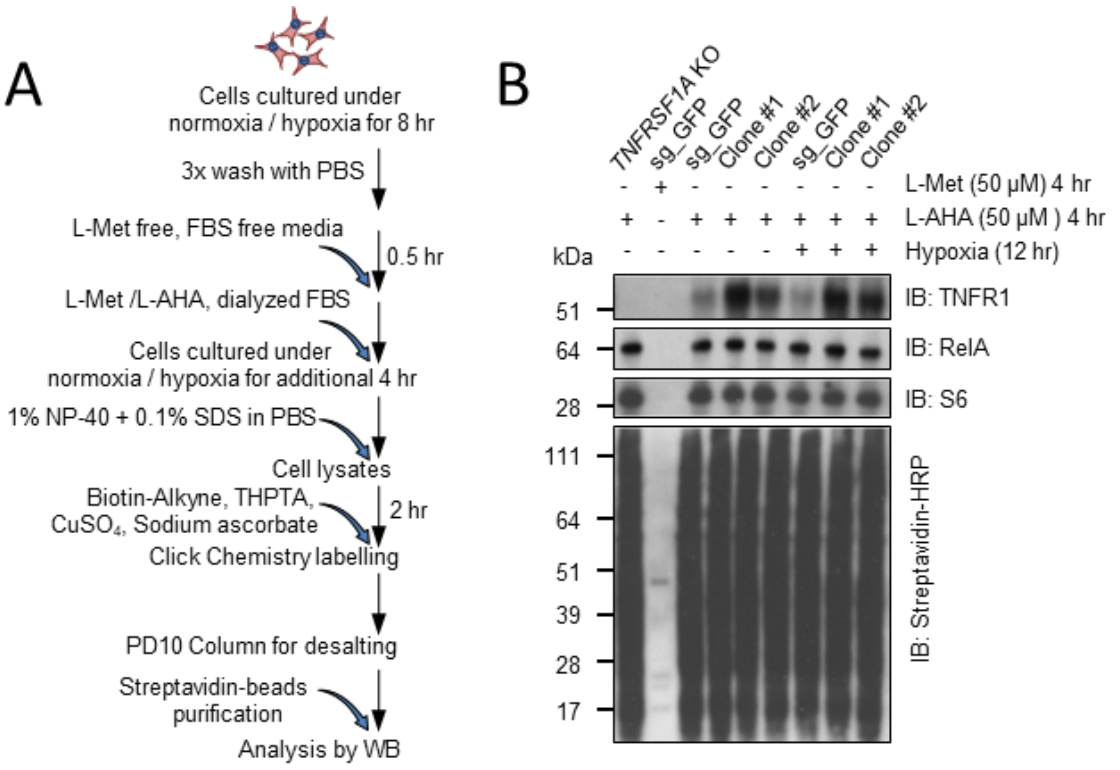


Figure 4.19 Deleting uORF2 increases TNFR1 *de novo* protein synthesis. (A) Workflow of click-chemistry based labelling of *de novo* synthesised proteins. (B) Biotin-labelled *de novo* synthesised proteins were purified with streptavidin beads and analysed by immunoblotting with the indicated antibodies. Data are shown as one representative of three independent experiments with similar results.

4.7 Downregulation of eIF4G1 mirrors hypoxia and partially reduces TNFR1 and TNF signalling

I wondered what was the mechanism regulating the different translational patterns of uORF-containing and non-uORF containing *TNFRSF1A*. Considering the initiation is the rate-limiting step in protein translation and its complexity [224, 225], I analysed the proteins (Figure 4.20) and mRNAs (Figure 4.21) of the main initiation factors. As expected, AMPK was activated and mTOR signalling was inhibited during hypoxia, as indicated by the increased phosphorylation of AMPK and reduced phosphorylation of P70S6K, S6 and 4E-BP1, respectively (Figure 4.20). The inactivation of mTOR was expected to inhibit general translation. However, hypoxia-mediated translational inhibition of the CDS seemed more sensitive than of uORF2 (Figure 4.14B). I hypothesised that there could be additional regulations on initiation factors by hypoxia, which could affect the reinitiation process. Surprisingly, I found that the protein levels of eIF1 and eIF4G1, as well as the core components of eIF3 complex eIF3A/B/C were reduced under hypoxia (Figure 4.20 and 4.21). Although the mRNA levels of *EIF1A*, *EIF4A1*, *EIF4E1*, *EIF4E2*, *EIF4G2* and *EIF4G3* were reduced during hypoxia, their protein levels were largely retained (Figure 4.20 and 4.21). In addition, analysis of the mRNAs of eIF3 components showed that the mRNA levels of *EIF3A*, *EIF3B*, *EIF3D*, *EIF3G*, *IEF3I*, *EIF3J* and *EIF3M* were significantly downregulated during hypoxia (Figure 4.21). The loss of eIF3 complex was reported as one mechanism of reduced reinitiation efficiency after translation of a long uORF [296]. The eIF3A/B/C are the core components of eIF3 complex, they regulate the assembly of eIF3 complex and also stabilities of eIF3 components [297]. The reduced protein levels of eIF3A/B/C were probably due to reduced transcriptions of *EIF3A* and *EIF3B*, resulting in reduced eIF3A and eIF3B protein levels, and consequently reduced the stability of the whole complex.

Previous studies showed that eIF4E2 together with HIF2α and eIF4G3 forming a hypoxia-induced initiation complex and is responsible for m^7GTP cap-dependent translation during hypoxia, whereas eIF4F is disassembled due mTOR inactivation [170, 298]. However, I did not observer the formation of such an initiation complex mediated by m^7GTP in HCT-116 cells during hypoxia. Reversely, the binding between m^7GTP and eIF4E2 was inhibited during hypoxia as well as other initiation factors, including eIF4A1, eIF4A2, eIF4G1, and eIF3A/B (Figure 4.22). The different result may be due to the different cell lines used in the studies. However, these data still supported that hypoxia inhibits the formation of eIF4F complex at m^7GTP cap.

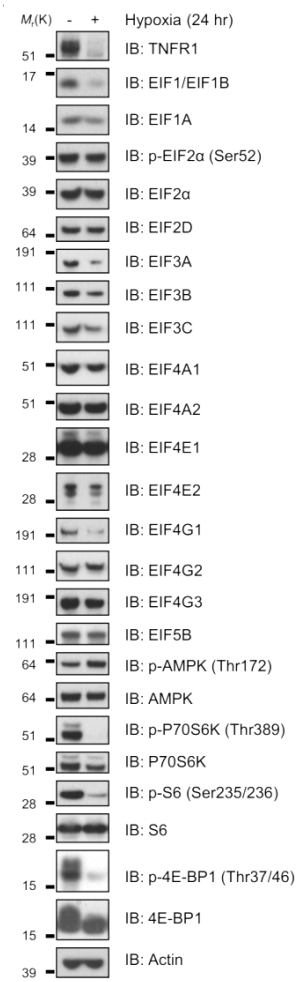


Figure 4.20 eIF1, eIF4G1, eIF3A/B/C proteins were reduced under hypoxia. HCT-116 cells were cultured under normoxia or hypoxia for 24 hr and subjected to immunoblotting with the indicated antibodies. Data are shown as one representative of three independent experiments with similar results.

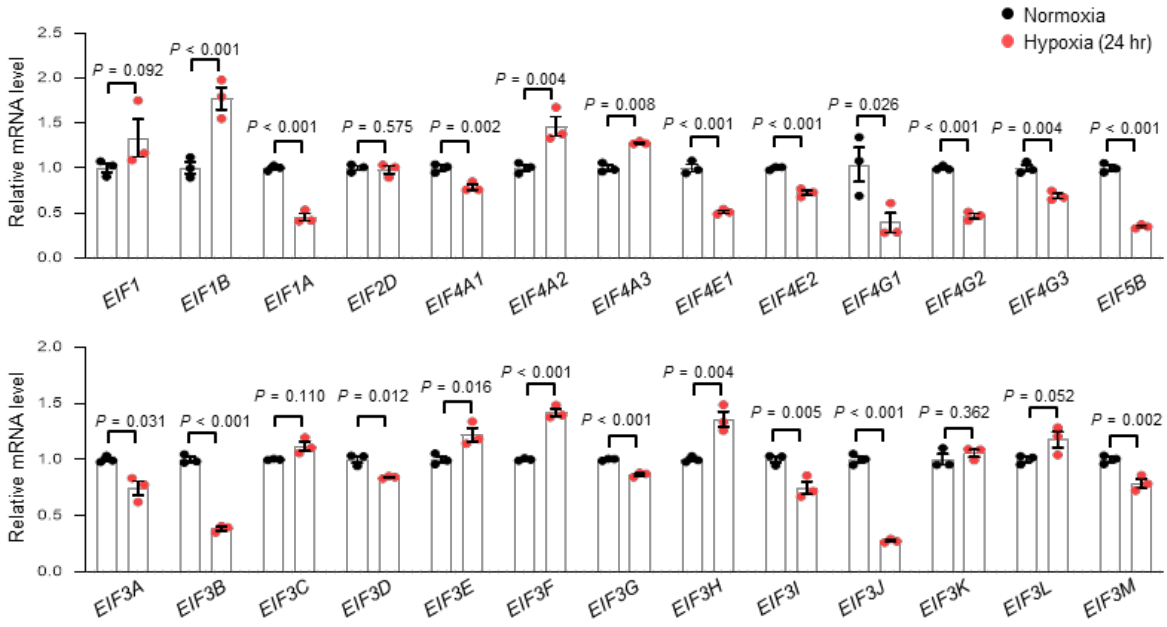


Figure 4.21 The transcription of initiation factors were regulated under hypoxia. HCT-116 cells were cultured under normoxia or hypoxia for 24 hr. The indicated genes were determined by qRT-PCR. qRT-PCR results were normalised to the housekeeping gene *B2M*. Data are shown mean ± SEM of three independent experiments. Statistical significance was determined by Two-tailed unpaired student t-test.

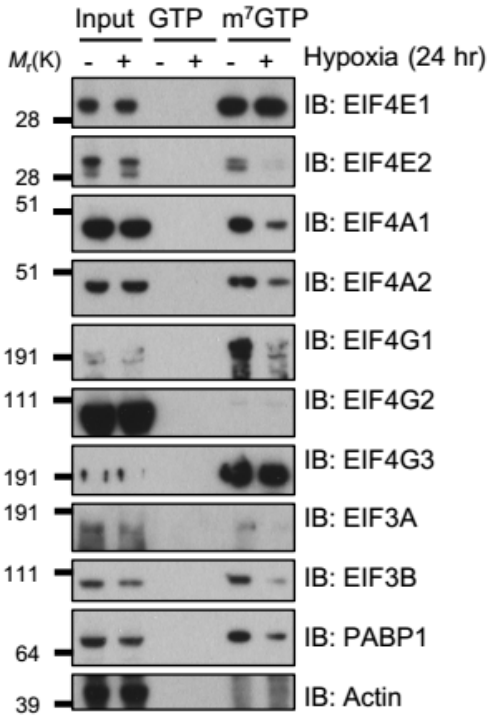


Figure 4.22 Hypoxia inhibits initiation complex formation. HCT-116 cells were cultured under normoxia or hypoxia for 24 hr. The cell lysates were subjected to affinity pulldown by GTP- or m^{7}GTP-lablled beads and analysed by immunoblotting with the indicated antibodies. Data are shown as one representative of three independent experiments with similar results.

To test the impact of hypoxia-induced reduction of eIF4G1 and eIF1 on TNFR1 expression, two specific siRNAs against *EIF1* and *EIF4G1* were deployed. The data indicated that knockdown of *EIF4G1* alone downregulates TNFR1 as well as general translation comparing with scramble siRNA control (Figure 4.23), whereas *EIF1* knockdown had no effect either on TNFR1 expression or general translation, as indicated by incorporated puromycin levels. Similar with my previous data that the uORF2 mutant was hypoxia-resistant (Figure 4.18B), uORF2 mutation was also resistant to *EIF4G1* knockdown. Knockdown of *EIF4G1* reduced TNFR1 and inhibited TNF signalling, as indicated by the accumulation of IκBα and reduced *CXCL8* mRNA levels when treated with TNF (Figure 4.24A and 4.24B). However, in the uORF2 mutant cells, the degradation of IκBα and induction of *CXCL8* induced by TNF were not affected by *EIF4G1* knockdown (Figure 4.24A and 4.24B).

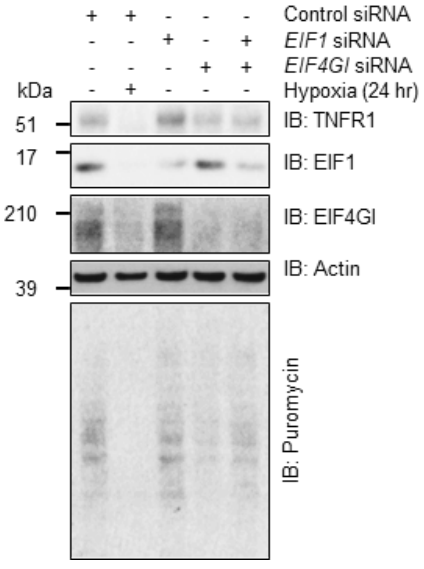


Figure 4.23 Knockdown of eIF4G1 reduces TNFR1 expression. HCT-116 cells were transfected with scramble control siRNA or siRNAs against *EIF1*, *EIF4G1* or in combination for 24 hr before culturing under normoxia or hypoxia for additional 24 hr. Protein levels were analysed by immunoblotting with the indicated antibodies. Data are shown as one representative of three independent experiments with similar results.

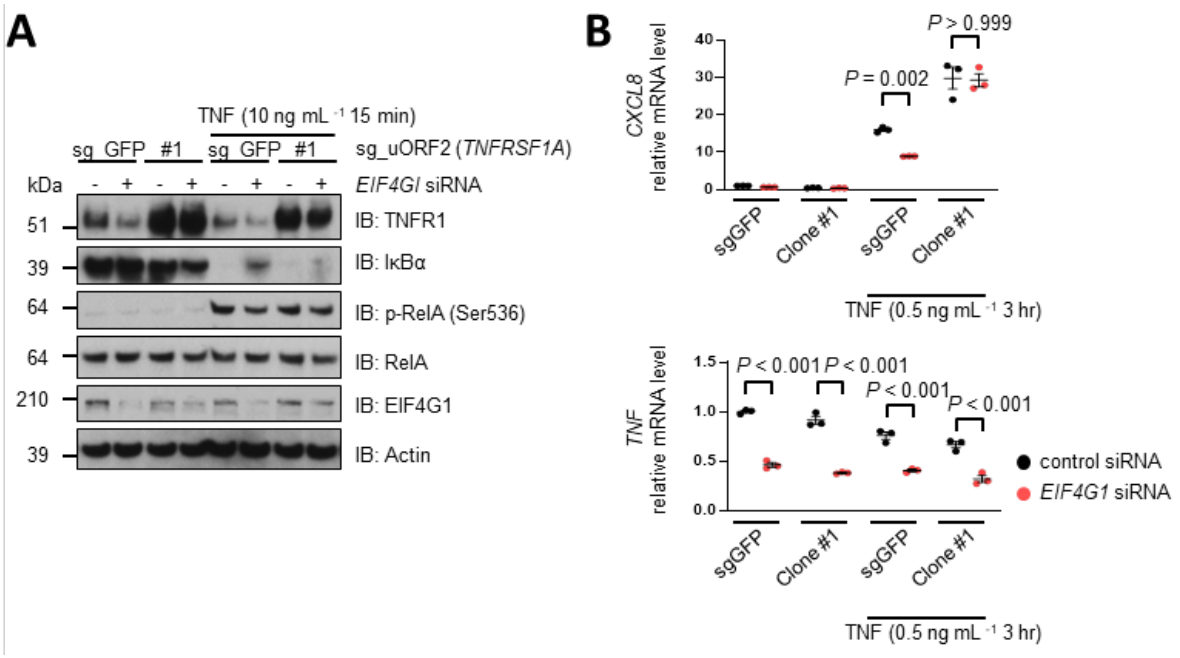


Figure 4.24 uORF2 mutation is resistant to eIF4G1 knockdown. (A and B) sgGFP control or uORF2 mutant (clone #1) HCT-116 cells were transfected with control siRNA or siRNAs against *EIF4G1* for 48 hr. The cells were then stimulated with TNF (10 ng mL^{-1}; 15 min) and subjected to immunoblotting with the indicated antibodies (A) or stimulated with TNF (0.5 ng mL^{-1}; 3 hr) and analysed by qRT-PCR. *CXCL8* and *EIF4G1* mRNA (B) were determined by qRT-PCR. qRT-PCR results were normalised to the housekeeping gene *B2M*. Data are shown mean ± SEM of three independent experiments (B) or one representative of three independent experiments with similar results (A). Statistical significance was determined by one-way ANOVA with Bonferroni's correction.

Not only *EIF4G1* mRNA was downregulated during hypoxia, but also its translation. Similar to *TNFRSF1A*, two uORFs were found in the 5'UTR of *EIF4G1*. Intriguingly, based on the data derived from the GFP reporter bearing the 5'UTR of *EIF4G1* (Figure 4.25A), hypoxia downregulated GFP expression in wild-type reporter. However, after mutated all the (potential) start codons, the expression of GFP was stabilised under hypoxia (Figure 4.25A and 4.25B). These data suggested the notion that the translation of eIF4G1 could also be regulated by its uORFs and its downregulation could partially explain the hypoxic inhibition of protein translation.

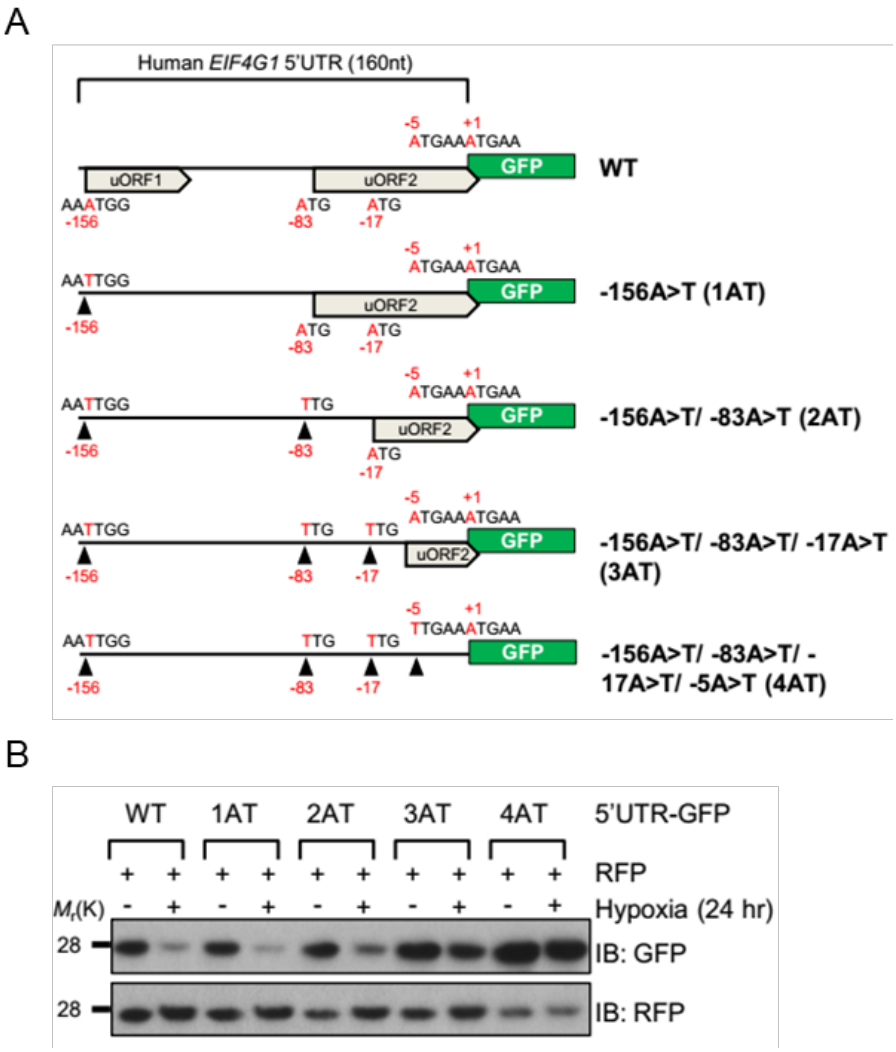


Figure 4.25 Deleting uORFs of EIF4G1 inhibits its reduction under hypoxia. (A) Schematic drawing of human *EIF4G1* 5'-UTR-GFP reporter constructs. (B) HCT-116 cells were transfected with the indicated constructs 2 hr before culturing under hypoxia for additional 24hr. The reporters were analysed by immunoblotting. Data are shown as one representative of three independent experiments with similar results (B).

4.8 uORFs regulate the expression of multiple immune receptors under hypoxia

I wondered whether the presence of uORFs could be a general mechanism to regulate the expression of other immune receptors under hypoxia, since various numbers of uORFs were found in these genes (Table 4.1). However, the number of uORFs was defined by the number of their open reading frames at their 5'UTRs, whether they are recognisable by ribosome was not clear. Surprisingly, the expressions of uORF-containing reporters were largely reduced under hypoxia except the reporters of *IFNGR1* and *RIG-I*, which had no uORFs at their 5'UTRs (Figure 4.26). In addition, the reduction of GFP in *STING* reporter seemed to be mild during hypoxia. This might be related to the recognition efficiency of its start codon(s) in the uORFs by ribosomes.

Table 4.1 Summary of the number of uORFs in the indicated genes

Gene (*Homo sapiens*)	Number of uORF(s)
TNFRSF1A	2
NOD2	3
IL1R1	4
IFNGR1	0
IFNGR2	1
IL6ST	2
TLR4	1
IFNAR1	1
STING	2

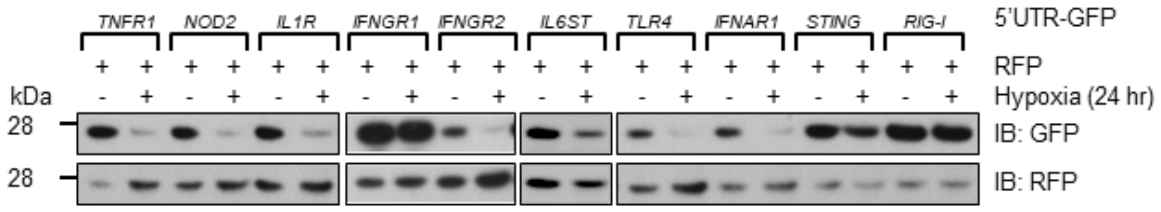


Figure 4.26 The presence of uORF negatively correlates with protein expression under hypoxia. HCT-116 cells were transfected with the indicated constructs 2 hr before culturing under hypoxia for additional 24 hr. The reporters were analysed by immunoblotting. Data are shown as one representative of three independent experiments with similar results.

To further test if this effect was uORF dependent, I used four single-uORF-containing reporters *TNFRSF1A*, *TLR4*, *IFNAR1* and *IFNGR2* and one non-uORF-containing reporter *RIG-I* (Figure 4.27) to statistically analysis the fold change of GFP expression in wild-types and their uORF mutant counterparts between hypoxia and normoxia. Mutation of the start codons of the uORFs in *TNFRSF1A*, *TLR4*, *INGAR1* and *IFNGR2* substantially enhanced GFP expression under both normoxia and hypoxia, whereas the insertion mutant of *RIG-I* bearing uORF2 (*TNFRSF1A*) sensitised GFP expression to hypoxia comparing with the wild-type (Figure 4.27). The fold-changes of GFP expression between hypoxia and normoxia were both decreased in uORF-containing and non-uORF-containing reporters, which was consistent with hypoxic-inhibition of translation [245, 299]. However, hypoxia has a more pronounced negative effect on the translation of uORF-containing reporters as the ratios of uORF-containing reporters between hypoxia and normoxia were significantly reduced comparing with non-uORF containing reporters. This suggested that translation reinitiation is more sensitive to hypoxic inhibition than translation initiation.

Ribosome profiling or Ribo-seq is a high-throughput method to detect ribosome occupancy on mRNAs. The ribosome binding mRNAs are protected by RNase when preparing the samples before sequencing. The relative mRNA levels have been used to indirectly reflect translating mRNAs. However, this method has its limitation as it cannot tell whether the ribosome is stalled on the mRNA or it is translating. Therefore, polysome profiling is introduced to separate polysome from monosome by ultracentrifugation and then the separated fractions can be sequenced. The translating mRNAs and non-translating mRNAs are in the polysome fraction and in the monosome fraction, respectively. The ratio (P/M) of mRNA levels in polysome fraction versus monosome fraction is defined as translation efficiency. I then analysed a group of polysome profiling datasets that derived from normoxia/hypoxia-treated U87MG cells [268]. I focused on the receptors of the major

pro-inflammatory cytokines IL-1, IL-6 and TNF, as well as other TNFR family receptors, interferon receptors, TGF receptors and pathogen recognition receptors that the cells expressed. Consistent with the reporter data, those uORF-containing mRNAs were generally more sensitive to hypoxic inhibition of translation, as indicated by the reduced polysome-to-monosome (P/M) ratios (Figure 4.28), an indicator of active translation [300].

In summary, hypoxia is a complicated physiological and pathophysiological condition. Hypoxic inhibition of translation reinitiation may be caused by multiple factors, including the reduced initiation factors such as EIF3A/B/C and EIF4G1 (Figure 4.20), inhibited mTOR activity (Figure 4.20) or there could be additional mechanisms. However, the higher sensitivity of reinitiation to hypoxia may explain why the presence of uORF2 in *TNFRSF1A* suppresses TNFR1 expression and consequently inhibits the TNF signalling under hypoxia. In addition, this mechanism also provides a potential explanation of how other uORF-containing mRNA-encoded immune receptor-mediated signalling pathways are suppressed during hypoxia (Figure 4.1-4.3).

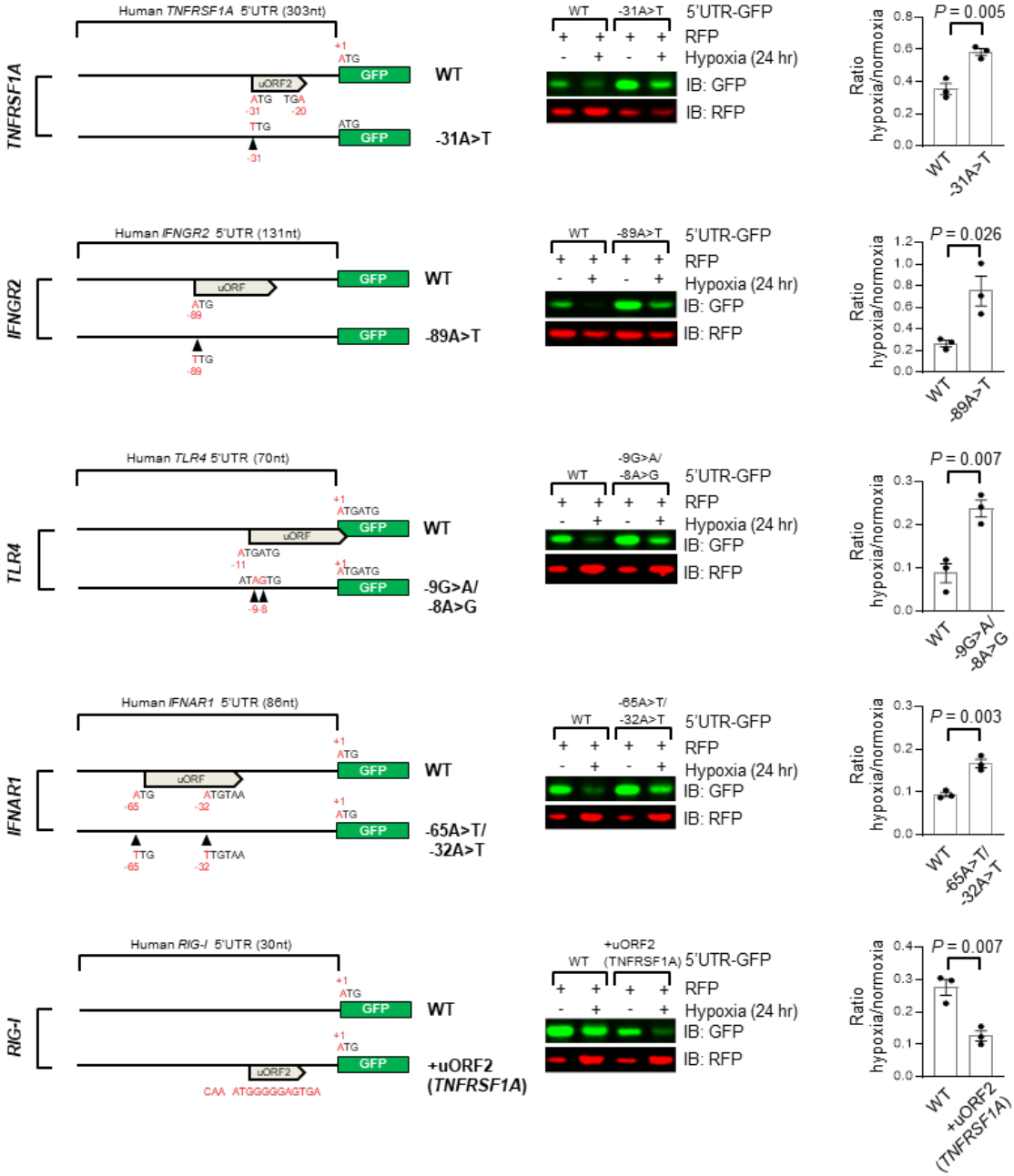
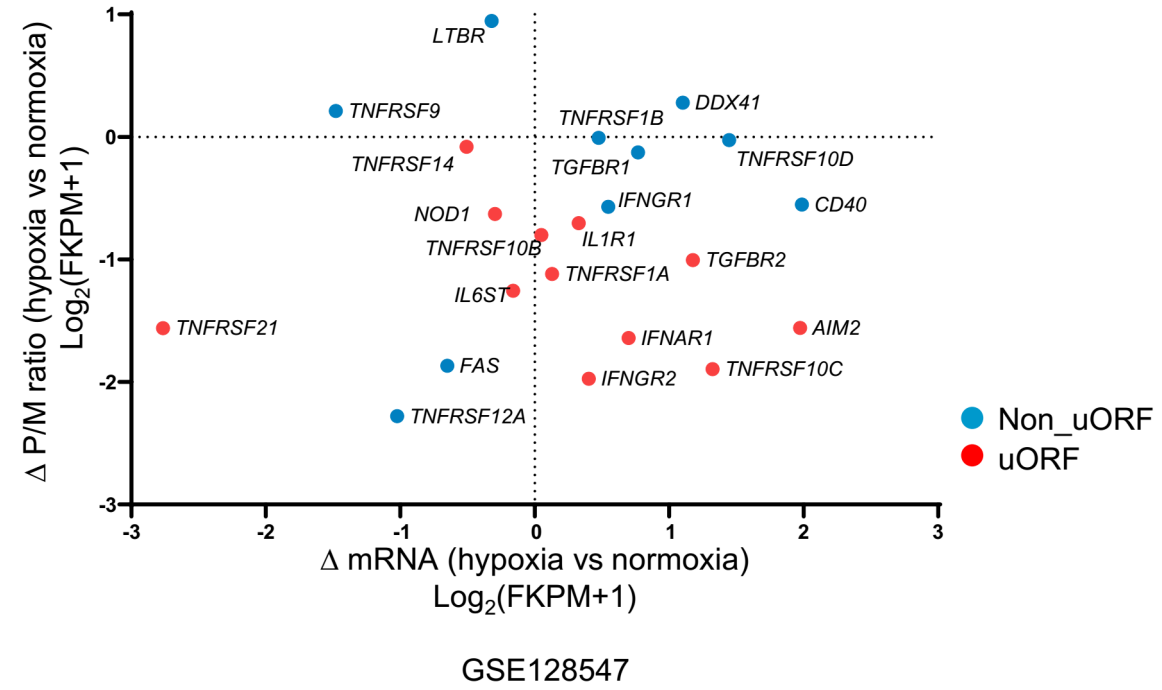


Figure 4.27 uORFs negatively regulate the translation of several immune receptors under hypoxia. HCT-116 cells were transfected with the indicated constructs 2 hr before culturing under hypoxia for additional 24 hr. The reporters were analysed by immunoblotting. Schematic drawing of the indicated GFP reporter constructs (left). GFP expression ratios of the indicated reporters between hypoxia and normoxia were statistical analysed (right). Data are shown mean ± SEM of three independent experiments (B) or one representative of three independent experiments with similar results (A). Two-tailed paired student t-test was used.



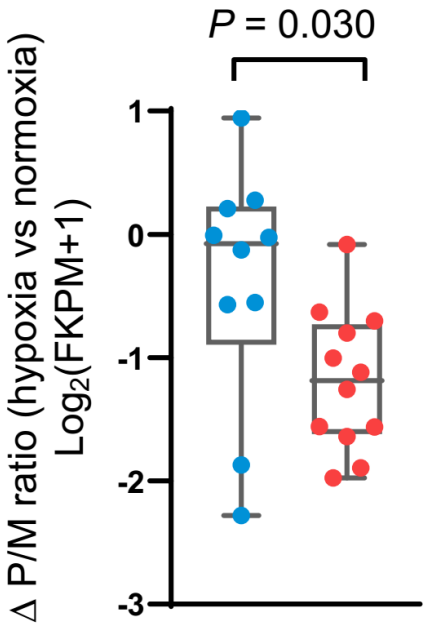


Figure 4.28 Hypoxia natively regulates the translation of receptors encoded by uORF-containing mRNAs. Top: Plots of fold changes in polysome-to-monosome (P/M) ratios and fold changes in total mRNA levels of the indicated genes between hypoxia and normoxia in U87MG cells. Bottom: The box and whisker plot (minimum to maximum values with individuals) represents P/M ratio fold changes. The receptor genes were grouped based on the presence of ATG-initiated uORF(s) in their mRNAs. Red: uORF-containing mRNAs. Blue: non-uORF containing mRNAs. Dataset were derived from GSE128547.

5

Translated uORFs promote tumour immune evasion

5.1 TNF and IFN-γ synergistically induce MHC-I expression

Given that TNF and IFN-γ were key cytokines produced by activated T cells [32] and the translations of TNFR1 and IFN-γR2 were regulated by uORFs under hypoxia (Figure 4.26 and 4.27). I hypothesised that the uORFs could have a role in regulating tumour immune evasion. Additionally, TNF receptor and IFN-γ receptor are two major receptors engaged in the anti-tumour immunity [32, 301, 302]. However, less is known about how these receptors are regulated in a tumour microenvironment.

Production of TNF and IFN-γ are two markers of activated T cells [303] and responsiveness to TNF and IFN-γ from surrounding cells including cancer cells is crucial for further T cell activation and infiltration [32, 301, 302]. The tumour microenvironment can be divided into "hot" and "cold" according to the presence of infiltrated T cells. The hot tumours are characterised by highly infiltrated T cells and with signatures of immune activation, whereas cold tumours are defined by the absence of T cells [304]. Enhanced infiltration of T cells has been shown to be beneficial for immunotherapy and increased survival [130]. MHC-I-mediated tumour antigen presentation is crucial for T cells infiltration and T cell-mediated immune responses [111, 305] and upregulation of MHC-I expression in cancer cells requires functional IFN-γ signalling [108]. Deficiency in tumour antigen presentation machinery or downregulation of MHC-I expression has been found in 40–90% of human tumours [129], suggesting that the IFN-γ signalling may not function properly. However, comparing with the mutation rate of *TP53* (36%), genetic mutation rates of the genes within antigen presentation machinery and of components in IFN-γ signalling were relatively low in cancer patients (Figure 5.1). There are various mechanisms in regulating tumour antigen presentation, for example, methylations on the promoter and enhancer regions of MHC-I negatively regulates MHC-I expression (Figure 5.2) [306-309]. In this study, considering hypoxia is a common feature in solid tumours, I wondered how

hypoxic-inhibition of immune receptor signalling could affect tumour immunity.

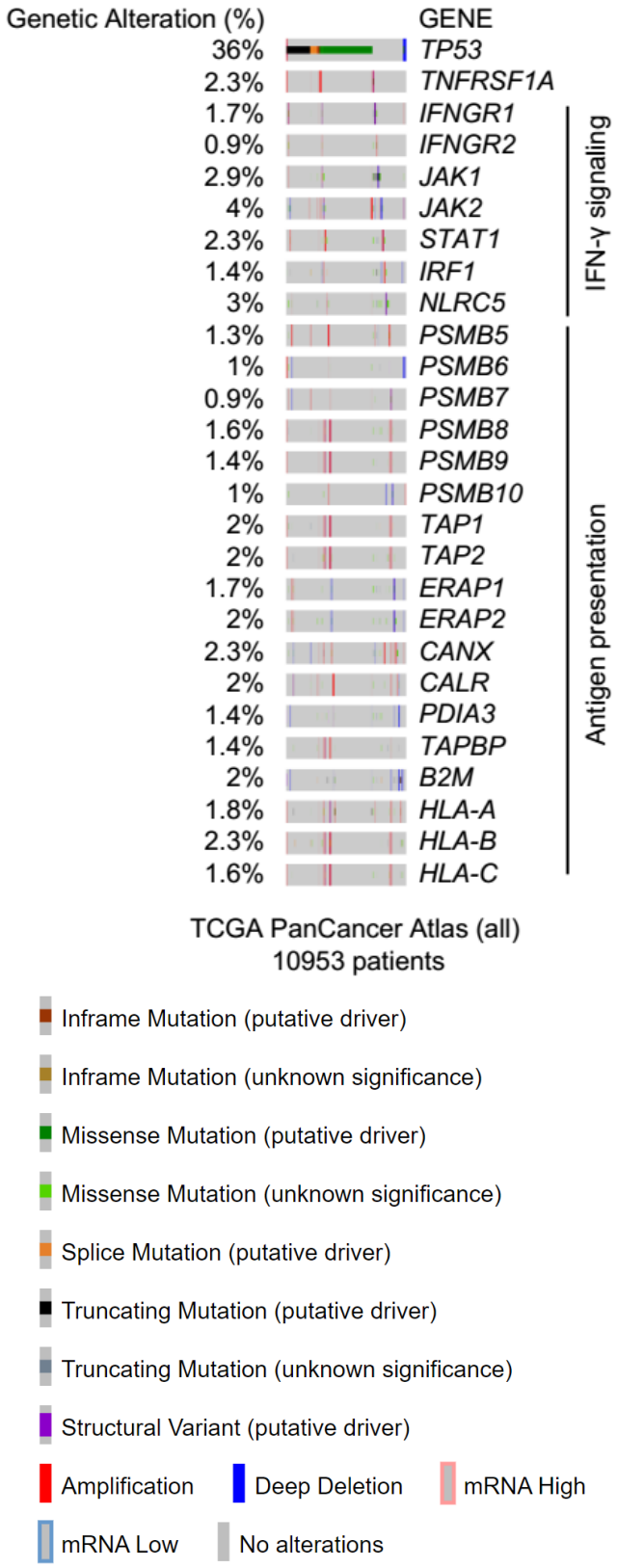


Figure 5.1 Genetic alteration rates of the indicated genes from 32 TCGA Pan-cancer Atlas Studies (10953 patients). The alterations include in-frame mutation, missense mutation, splice mutation, truncating mutation, structural variant, amplification and deep deletion.

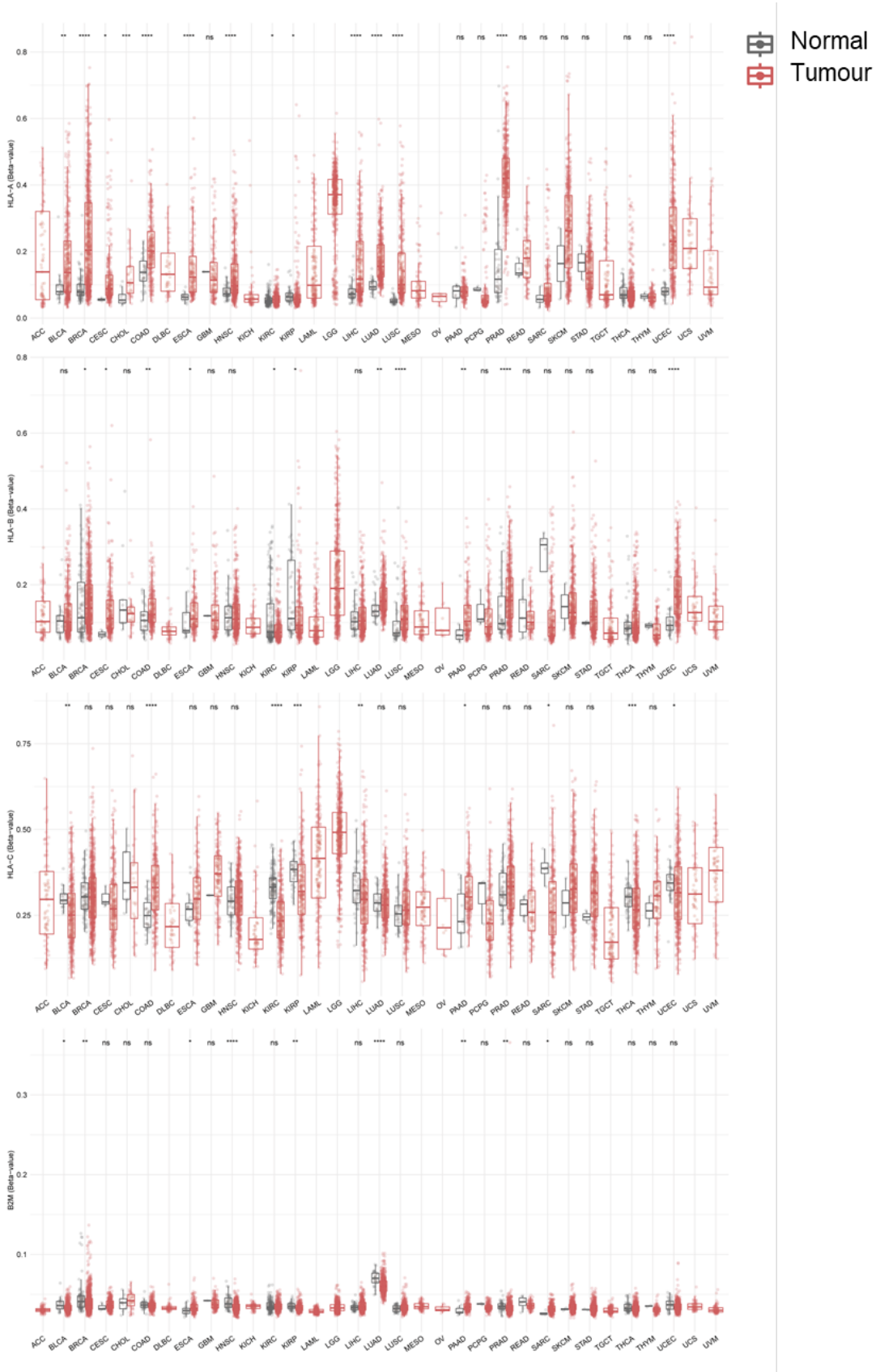


Figure 5.2 Methylation status of the indicated genes from 32 TCGA Pan-cancer Atlas Studies. Box plot of DNA methylation Beta-values of the indicated genes was shown. ns: p > 0.05; *: p <= 0.05; **: p <= 0.01; ***: p <= 0.001; ****: p <= 0.0001.

The expression of MHC-I and T cell infiltration are reciprocally regulated [108]. To characterise the immune receptor signalling in regulating the expression of MHC-I and T cells infiltration, I analysed the single cell data derived from melanoma patients [310]. The reason why I utilised datasets from melanoma was because I focused on the signalling, which I was able to test them in an established Yumm1.7 mouse melanoma model (described in later section). I divided the tumour cells into two groups (T cell high and T cell low) based on the median value of the ratio of CD3 versus CD45 from the tumours. I found that tumours with fewer infiltrated T cells showed lower mRNA levels of MHC-I and negatively correlated with IFN-γ signalling and TNF signalling (Figure 5.3A and 5.3B).

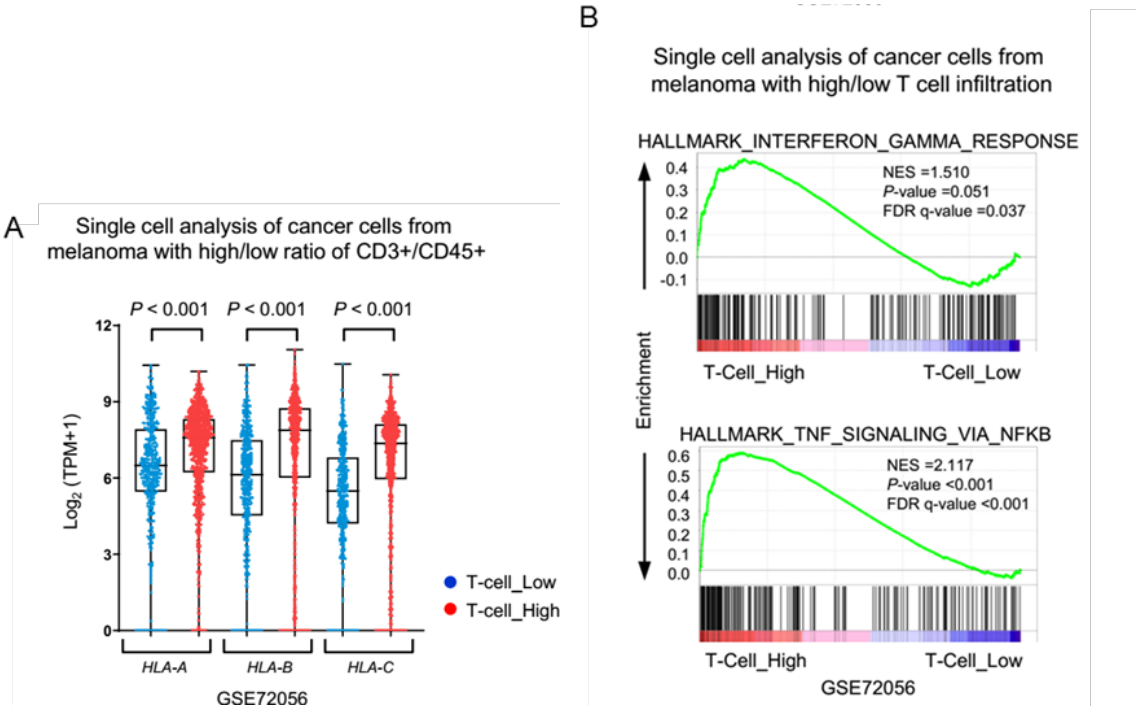


Figure 5.3 T cells infiltration correlates with MHC-I expression, TNF and IFN-γ signalling. (A) The box and whisker plot (minimum to maximum values with individuals) represents median values of HLA-A, HLA-B and HLA-C from cancer cells that derived from melanoma with high or low CD3+/CD45+ ratio. (B) Gene set enrichment analysis of single melanoma cells derived from tumours with high or low CD3+/CD45+ ratio, with a false discovery rate (FDR) of <25%. Dataset were derived from GSE72056. Statistical significance was determined by Mann-Whitney U test.

Considering the hypoxic tumour microenvironment, I wondered whether hypoxia could regulate antigen presentation by inhibiting TNF and IFN-γ signalling. I planned to utilise a "cold" mouse tumour cell line to test MHC-I induction by TNF and IFN-γ and *in vivo* mouse model afterwards. Mouse melanoma Yumm1.7 cells have been previously categorised as an immunologically cold tumour model. They are syngeneic to C57BL/6, have well-defined human-relevant driver mutations (BrafV600E Cdkn2a-/- Pten-/-) and are genomically stable [311]. Therefore, Yumm1.7 cells were used in the experiments. Treating the cells with IFN-γ induced the expression of MHC-I (Figure 5.4A) and the combination treatment with TNF and IFN-γ showed synergistic effects on induction of MHC-I (Figure 5.4A). MHC-II expression was not observed by treating the cells with either TNF or IFN-γ alone, or in combination (Figure 5.4B).

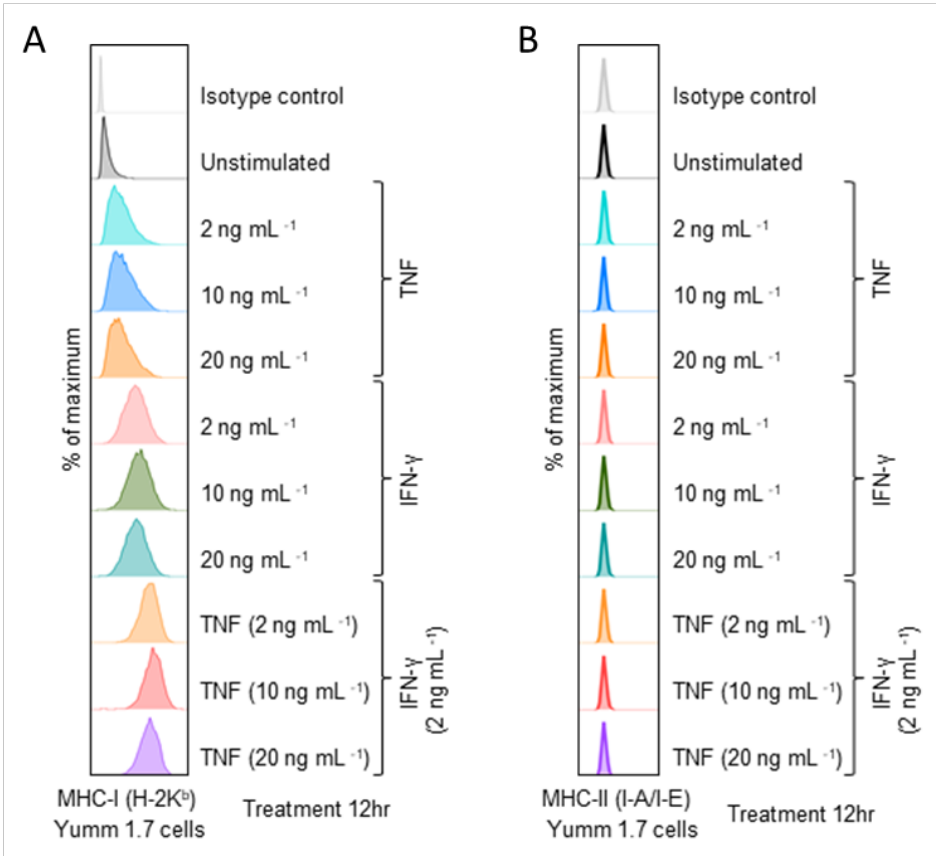


Figure 5.4 TNF and IFN-γ synergistically induce MHC-I expression (A and B) Yumm1.7 cells were stimulated with TNF or IFN-γ alone or in combination with TNF and IFN-γ for 12 hr. H-2K^b (A) and I-A/I-E (B) positive cells were analysed by flow cytometry. Data are shown as one representative of three independent experiments with similar results.

5.2 Hypoxia inhibits MHC-I expression induced by TNF and IFN-γ

Next, cells were cultured under normoxia and hypoxia for 24 and 48 hours and both TNFR1 and IFN-γR2 were reduced (Figure 5.5A), whereas IFN-γR1 was retained. These data were in line with my previous data that the presence of uORF in *TNFRSF1A* and *IFNGR2* inhibited their translation during hypoxia, whereas the translation of non-uORF containing *IFNGR1* was less affected (Figure 4.26). Indeed, IFN-γR1 was quite stable across multiple cell lines under hypoxia, whereas IFN-γR2 expression levels were varied among different cell lines and relatively sensitive to hypoxia comparing with IFN-γR1 (Figure 5.5B).

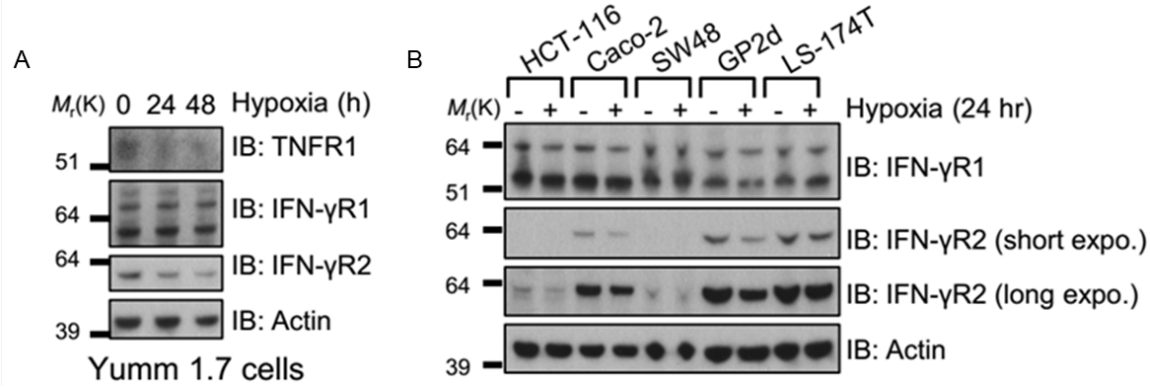


Figure 5.5 Hypoxia downregulates TNFR1 and IFN-γR2 (A) Yumm1.7 cells were cultured under normoxia and hypoxia for 24hr or 48 hr and subjected to immunoblotting with the indicated antibodies. (B) The indicated cell lines were cultured under normoxia and hypoxia for 24hr and subjected to immunoblotting with the indicated antibodies. Data are as one representative of three independent experiments with similar results (B and C).

To evaluate the impacts of TNF signalling and IFN-γ signalling on clinical outcomes of melanoma patients, I analysed the RNA sequencing data from TCGA database. The mRNA levels of downstream target genes of TNF signalling and IFN-γ signalling, *HLA–A*, *HLA–B* and *HLA–C* were positively correlated with disease specific survival rates (Figure 5.6), whereas the mRNA levels of *TNFRSF1A* and *IFNGR2* did not (Figure 5.6). These data suggested the notion that increased activity of TNF signalling and IFN-γ signalling is beneficial for restricting the tumour progression. However, transcriptional regulation of *TNFRSF1A* and *IFNGR2* might not be a major contributor in disease progression, this was

possibly due to their translational regulations.

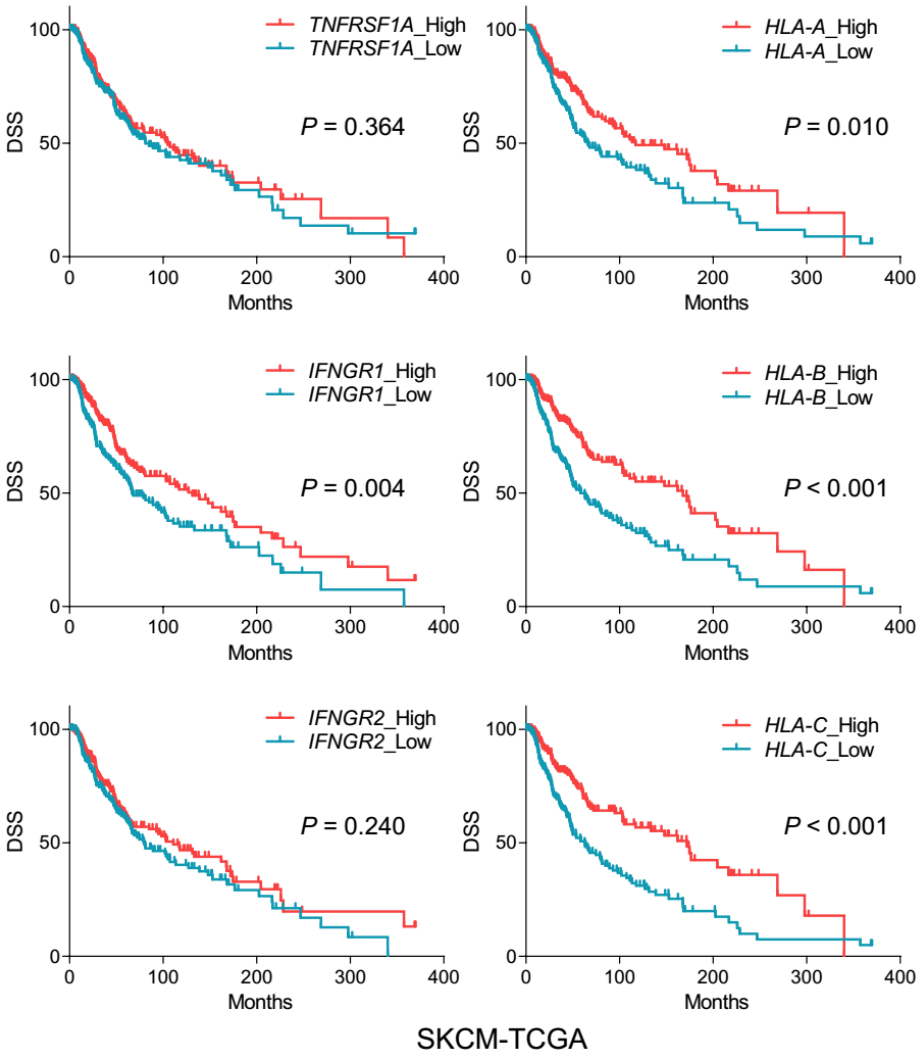


Figure 5.6 Analyses of the correlations between disease specific survival rates (DSS) and the expressions of indicated genes in melanoma patients from SKCM-TCGA dataset. n= 420 patients were divided into two groups (high and low) based on the median expression value of each gene. Statistical significance was determined by Gehan-Breslow-Wilcoxon test.

5.3 Deleting uORFs of *TNFRSF1A* and *IFNGR2* sustains TNF- and IFN-γ-induced MHC-I expression under hypoxia

To test the impact of hypoxia on TNF and IFN-γ signalling in Yumm1.7 cells, I used CRISPR-Cas9 to mutate both uORFs in *TNFRSF1A* and *IFNGR2* simultaneously (Figure 5.7A). In line with *TNFRSF1A* uORF2 mutation in HCT-116 cells, the uORFs double mutant monoclonal Yumm1.7 cells (Figure 5.7B) also showed increased TNFR1 surface

expression without upregulating its mRNA level (Figure 5.7C and 5.7D). The surface expression of TNFR1 was significantly reduced under hypoxia in the wild-type cells. Although it was also downregulated in the uORFs double mutant cells, its expression was still much higher than the wild-type. The surface expression of IFN-γR2 was slightly increased in this mutant and this difference was more evident after hypoxia treatment (Figure 5.7C). Thereby, the predominant effect of the uORFs mutation was increased protein levels of TNFR1 and IFN-γR2, which was irrespective of culturing under normoxia or hypoxia. Additionally, the mRNA level of *IFNGR2* was statistically significantly downregulated in the uORFs double mutant cells (Figure 5.7D), consistent with the previous reported cellular intrinsic feedback mechanism [78, 107].

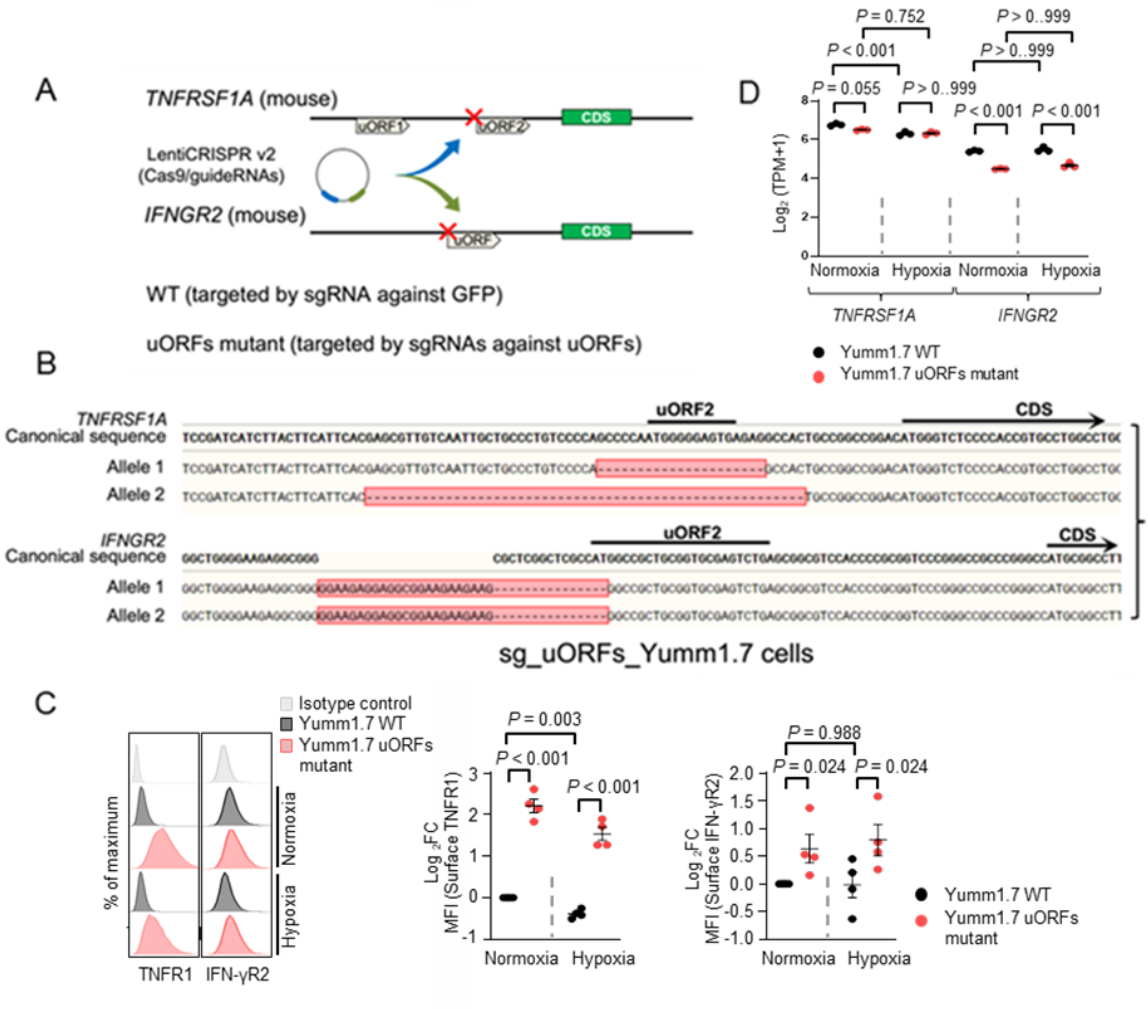


Figure 5.7 Characterisation of uORFs double mutant cells. (A) Targeting the uORFs of mouse *TNRSF1A* and *IFNGR2* by CRISPR -Cas9. (B) Genomic sequences of alleles in the uORFs double mutant Yumm1.7 cells. (C and D) Wild-type and uORFs double mutant Yumm1.7 cells were cultured under normoxia or hypoxia for 24 hr, then subjected to immunoblotting with the indicated antibodies (C) or analysed by RNA-seq (D). Data are shown mean ± SEM of four independent experiments (D) or one representative of three independent experiments with similar results (C). Statistical significance was determined by one-way ANOVA with Bonferroni's correction.

I confirmed that the uORFs double mutant has higher TNF (Figure 5.8A) and IFN-γ (Figure 5.8B) signalling signatures under both normoxia and hypoxia when treated with TNF and IFN-γ. Importantly, the uORFs double mutant was resistant to the hypoxic inhibition of MHC-I expression induced by TNF and IFN-γ and showed much higher responsiveness than the wild-type cells (Figure 5.8C). This could be due to synergistic effects of both pathways in the uORFs mutant cells as they showed higher TNF and IFN-γ signalling signatures (Figure 5.8A and 5.8B).

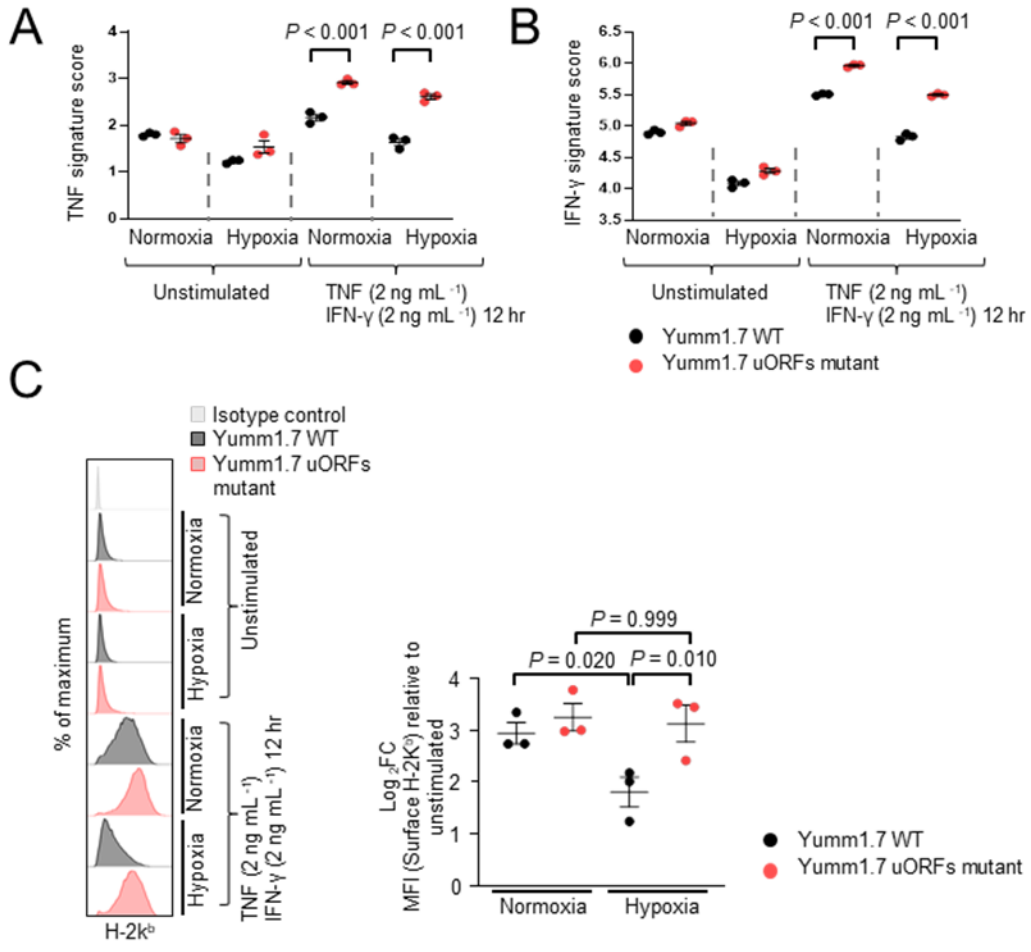


Figure 5.8 Deleting uORFs of *TNFRSF1A* and *IFNGR2* sustains TNF- and IFN-γ-induced MHC-I expression under hypoxia. (A and B) Gene expressions were analysed by RNA-seq. Signature scores were calculated by using the mean value of *TRAF1*, *JUN*, *CXCL1*, *CCL20*, *IL6* and *NFKBIE* for TNF signature (A) and of gene set M5913 for IFN-γ signature (B), respectively. (C) Wild-type and uORFs double mutant Yumm1.7 cells were cultured under normoxia or hypoxia for 24 hr followed by stimulation with TNF (2 ng mL^{-1}) and IFN-γ (2 ng mL^{-1}) for additional 12 hr. The cells were surface stained with anti- $H\text{-}2K^b$ antibodies and analysed by flow cytometry. Data are shown mean ± SEM of three independent experiments. Statistical significance was determined by

one-way ANOVA with Bonferroni's correction.

To further test the effect of TNF and IFN-γ on the uORFs mutant cells, I tested their viabilities under different time points in the presence of TNF, IFN-γ or in combination. The double mutant cells showed no difference in viability under normal culture conditions comparing with wild-type control cells (Figure 5.9A). Treatment with TNF or IFN-γ alone or in combination neither had any effect on the cell viability of the uORFs double mutant cells (Figure 5.9B).

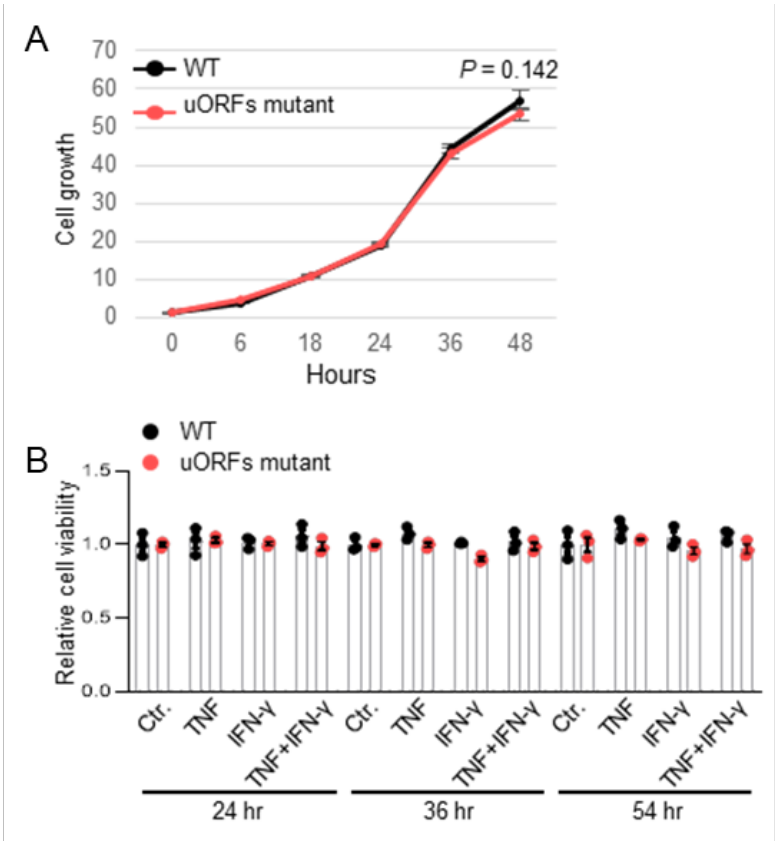


Figure 5.9 Mutation of uORFs in *TNFRSF1A* and *IFNGR2* does not affect cell viability. (A) Cell growth curves of wild-type control and uORFs double mutant Yumm1.7 cells were determined by CellTiter-Glo. (B) Wild-type control and uORFs double mutant Yumm1.7 cells were stimulated with TNF (2 ng mL^{-1}), IFN-γ (2 ng mL^{-1}) or in combination with TNF (2 ng mL^{-1}) and IFN-γ (2 ng mL^{-1}) for the indicated time points. Cell viability was determined by CellTiter-Glo. Data are shown mean ± SEM of three independent experiments. Statistical significance was determined by two-way ANOVA with Bonferroni's correction.

5.4 Deleting uORFs of *TNFRSF1A* and *IFNGR2* upregulates anti-tumour signatures

To further elucidate the impact of deleting uORFs in *TNFRSF1A* and *IFNGR2* in Yumm1.7 cells, I analysed the RNA sequencing data of wild-type and the uORFs double mutant cells cultured under normoxia or hypoxia in the presence or absence of TNF and IFN-γ (Figure 5.10A). The data showed that genes regulated by hypoxia were not affected by the mutation of both uORFs, as indicated by the similar gene clustering between wild-type and the uORFs mutant cells. However, a subset of genes involved in immune responses (yellow cluster) was upregulated (Figure 5.10A and 5.10B). These included the genes involved in promoting T cell chemotaxis (*CXCL9*/*10*/*11*/*16* and *CCL5*/*7*/*8*) [312-315], T cell co-stimulation (*ICAM1* and *CD40*) [316-318] and transcription regulation (*STAT1* and *NLRC5*) [319]) of MHC-I antigen presentation (*H2-K1*, *H2-D1*). Those genes were substantially upregulated in the uORFs mutant cells treated with TNF and IFN-γ during hypoxia comparing with wild-type cells (Figure 5.11A). In addition, a subset of genes involved in cell migration and motility was downregulated in the uORFs mutant cells (green cluster) (Figure 5.10A and 5.10B).

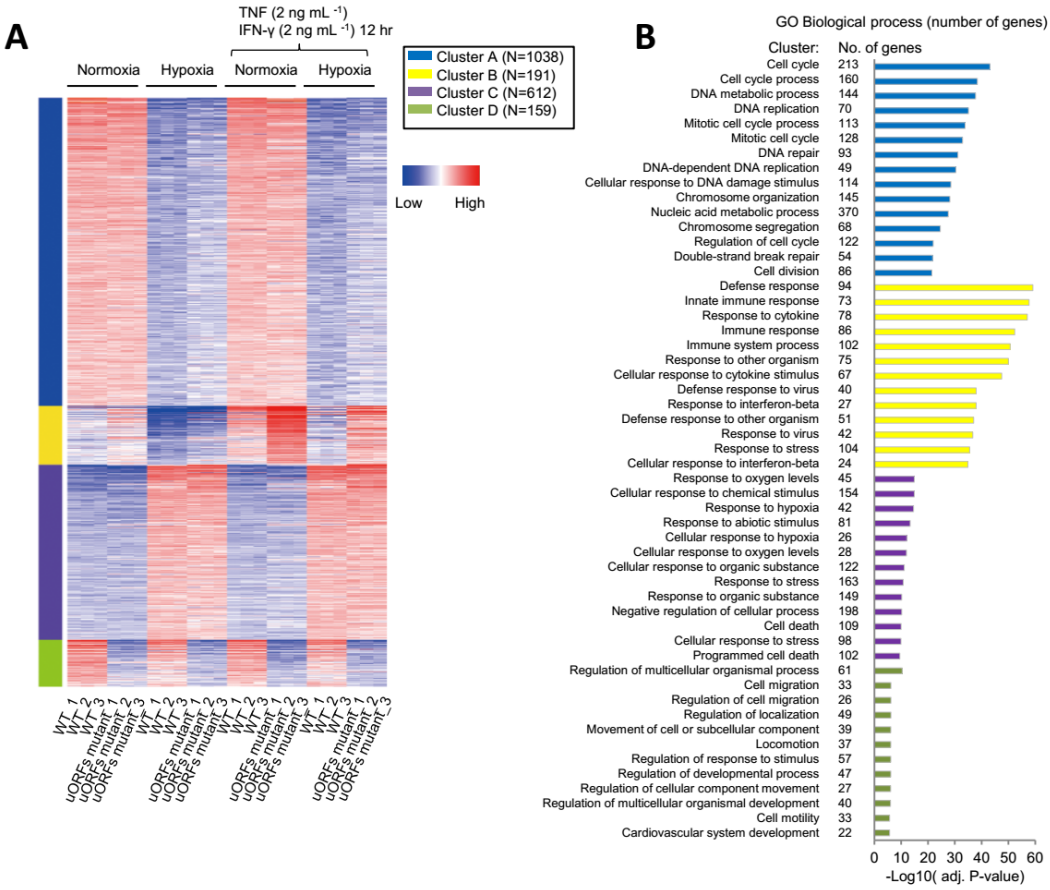


Figure 5.10 k-means clustering analysis of the uORFs double mutant cells. (A) Heatmap of the enriched pathways by k-means clustering of the indicated uORF modified Yumm1.7 cells cultured under normoxia or hypoxia for 24 hr then treated with TNF and IFN-γ for additional 12 hr. Blue: downregulated genes. Red: upregulated genes. (B) GO analysis of enriched pathways from (A) was shown. RNA-seq was performed by using three biological replicates.

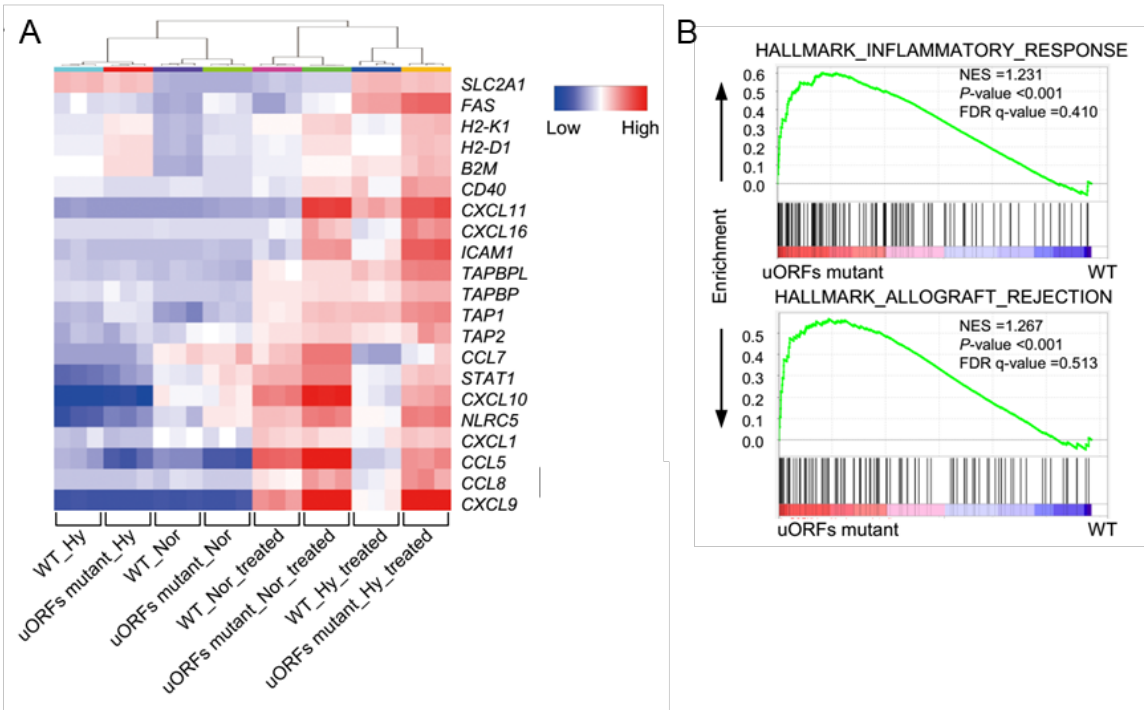


Figure 5.11 uORFs double mutation enhances anti-tumour immune signatures (A) Heatmap of the expression of indicated genes under indicated conditions. Complete-linkage clustering was applied with distance = 1-pearson's correlation. (B) Gene set enrichment analysis of the gene expression of the TNF-/IFN-γ-treated uORFs double mutant cells and sgGFP control cells cultured under hypoxia, with a false discovery rate (FDR) of <25%. RNA-seq was performed by using three biological replicates.

Next, I compared the gene expression profiles of both cell lines that cultured under hypoxia and treated with TNF and IFN-γ. Gene enrichment analysis showed that mutation of both uORFs can substantially upregulate the gene signatures for "inflammatory response" and "allograft rejection" (Figure 5.11B), supporting the notion that enhanced TNF and IFN-γ signalling may facilitate anti-tumour immune responses under hypoxic microenvironment.

5.5 Deleting uORFs in *TNFRSF1A* and *IFNGR2* enhances immune control of melanoma tumour growth

To test the impact of deleting uORFs in *TNFRSF1A* and *IFNGR2* on tumour growth *in vivo*, I employed an allograft tumour model by injecting the wild-type control and the uORFs double mutant cells into immune competent mice. Strikingly, the uORFs double mutation significant affected tumour growth *in vivo*, as indicated by the reduced tumour

volume (Figure 5.12A) and tumour weight (Figure 5.12B) of the uORF double mutant tumours. The activation of CD8 T cells requires the engagement between T cell receptor (TCR) on T cells and MHC-I on target cells. Therefore, mutating the genes in MHC-I complex can abrogate CD8 T cell-mediated cytotoxicity. B2M is a core component within MHC-I complex that shared by different MHC-I genes (H2 class I genes in mouse) and it is essential for assembling of MHC-I complex [320]. Therefore, I generated *B2M* knockout cells from both wild-type and uORFs double mutant cells. Loss of *B2M* abrogated MHC-I surface expression, allowing me to sort *B2M* knockout polyclones by surface staining of MHC-I (detailed sorting procedures described in methods). In addition, using polyclones also helped to minimize clone effects from using *B2M* knockout monoclones.

These polyclones which had no detectable MHC-I (Figure 5.12C) were injected into immune competent mice. The loss of MHC-I substantially rescued the growth retardation phenotype of the uORF double mutant tumours and showed similar tumour growth curve and tumour weight as wild-type control tumours (Figure 5.12A and 5.12B), indicating that CD8 T cells may be directly involved in controlling the tumour growth of the uORF double mutant tumours. This was further confirmed by flow cytometry analysis showing that the population of CD8 T cell (Figure 5.12F) was significantly increased in the uORFs double mutant tumours, whereas other immune cells including CD3 total T cells and CD4 T cells were not significantly changed in the uORFs double mutant tumours (Figure 5.12D, 5.12E and 5.12G). As expected, CD8 T cell population is substantially decreased in the *B2M* knockout groups (Figure 5.12F), resulting in increased CD4/CD8 ratios (Figure 5.12G). The observation that highly infiltrated CD8 T cells in the uORFs double mutant tumours was consistent with my previous data that the uORFs double mutant cells expressed higher T cell chemoattractant and MHC-I (Figure 5.8C and 5.11A).

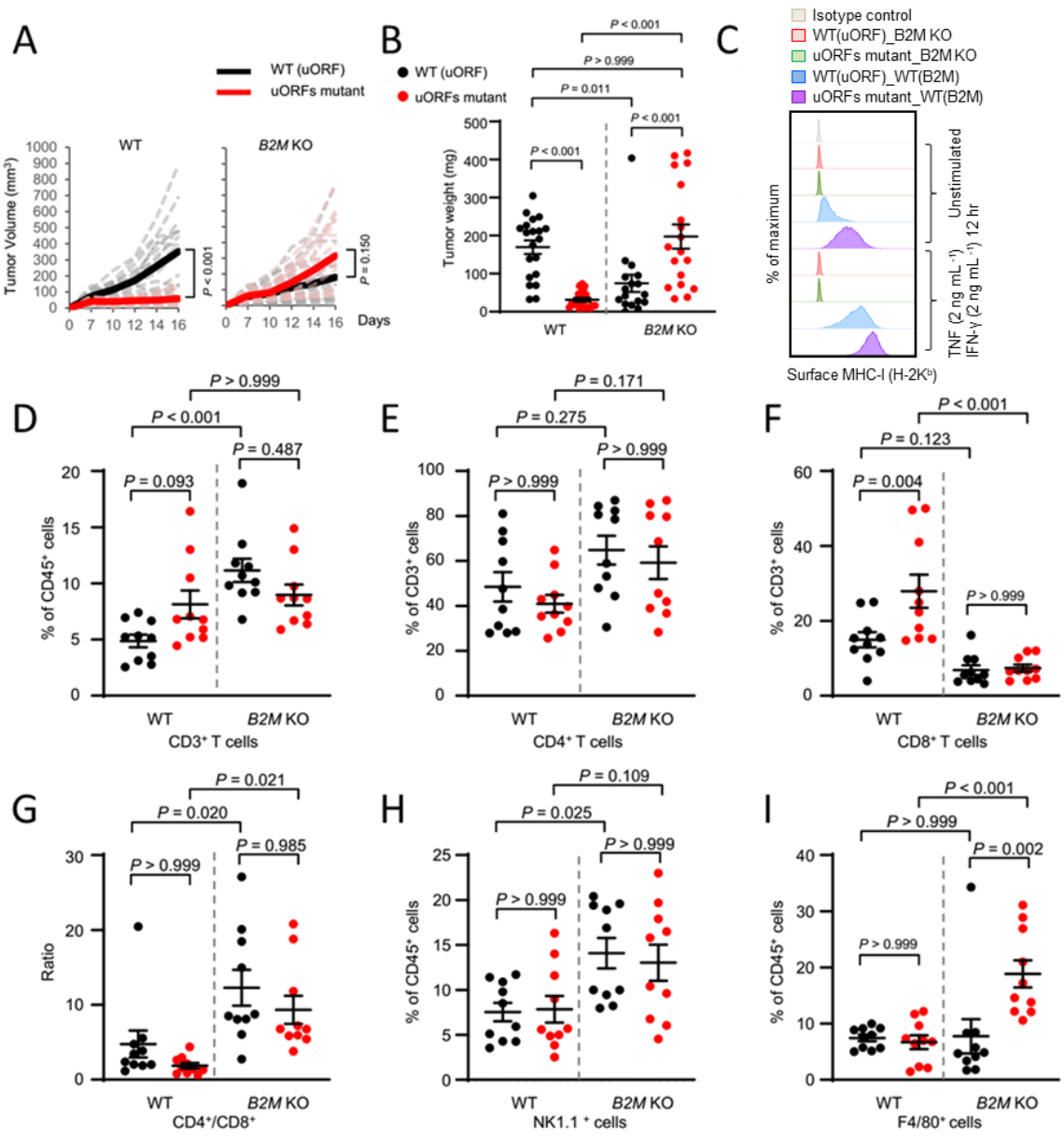


Figure 5.12 Mutation of uORFs in *TNFRSF1A* and *IFNGR2* enhances immune control of melanoma tumour growth. (A and B) Growth curves (A) and weight (B) of allograft tumours derived from wild-type control, uORFs double mutant and corresponding *B2M* knockout polyclone Yumm1.7 cells. The dashed line indicates each individual growth curve and the solid line is the mean value of each individuals. n= 10 mice per group per independent experiment. Summarised data of two independent experiments were shown. Tumours were established in mice by subcutaneous injection of cells. (C) Characterisation of *B2M* knockout polyclones of sgGFP control and uORFs double mutant Yumm1.7 cells. Cells were stimulated with or without TNF (2 ng mL $^{-1}$) and IFN-γ (2 ng mL $^{-1}$) for 24 hr. H-2K^{b} positive cells were analysed by flow cytometry. (G-I) Five tumours from each group per independent experiment were analysed by flow cytometry for the populations of CD3+ (D), CD4+ (E), CD8+ (F), NK1.1+ (H) and F4/80+ (I) among CD45+ or CD3+ cells. CD4/CD8 ratios were shown in (G). Data are shown mean ± SEM. Summarised data of two independent experiments were shown. Statistical significance was determined by two-way ANOVA with Tukey's correction (A) and one-way ANOVA with Bonferroni's correction (B and D-I). n=10 mice per group per experiment.

In addition, *B2M* knockout reduced tumour growth in the wild-type tumours (Figure 5.12A and 5.12B). This phenotype is probably caused by the increased infiltration of NK cells in the *B2M* knockout tumours (Figure 5.12H) as MHC-I are inhibiting molecules of NK cells [321]. However, knockout of *B2M* showed no inhibition on the growth of the uORFs double mutant tumours, albeit the population of NK cells was increased (Figure 5.12H). I speculated that this phenotype may be due to the immunosuppressive macrophages [322] as there is significantly increased infiltration of macrophages specifically in the *B2M* knockout uORFs double mutant tumours (Figure 5.12I). The higher infiltration of macrophages may be due to the higher pro-inflammatory activity of the uORFs double mutant cells (Figure 5.10A, 5.10B and 5.11B). It is possible that, in the absence of MHC-I, CD8 T cells were unable to eliminate tumour cells, whereas macrophage accumulated within the tumour and inhibited the activity of NK cells.

CD8 T cells play an important role in anti-tumour immunity [80, 323] and their dependency on MHC-I is crucial for their activation. As long as MHC-I expression and antigen presentation pathway are functional, TNF and IFN-γ induced expression of MHC-I, T cell chemoattractant and T cell co-stimulating factors should be beneficial for CD8 T cell dependent anti-tumour immunity.

5.6 Melanoma patients with higher TNF and IFN-γ signatures have better clinical outcomes

To elucidate how TNF signalling and IFN-γ signalling affect the clinical outcomes in melanoma patients, I analysed the TCGA dataset. The data indicted that TNF and IFN-γ signalling signatures were highly correlated with each other and both of them were positively correlated with antigen presentation signatures (Figure 5.13A) in melanoma patients. In addition, higher TNF signatures, IFN-γ signatures and antigen presentation signatures predicted higher disease specific survival rates in melanoma patients (Figure 5.13B).

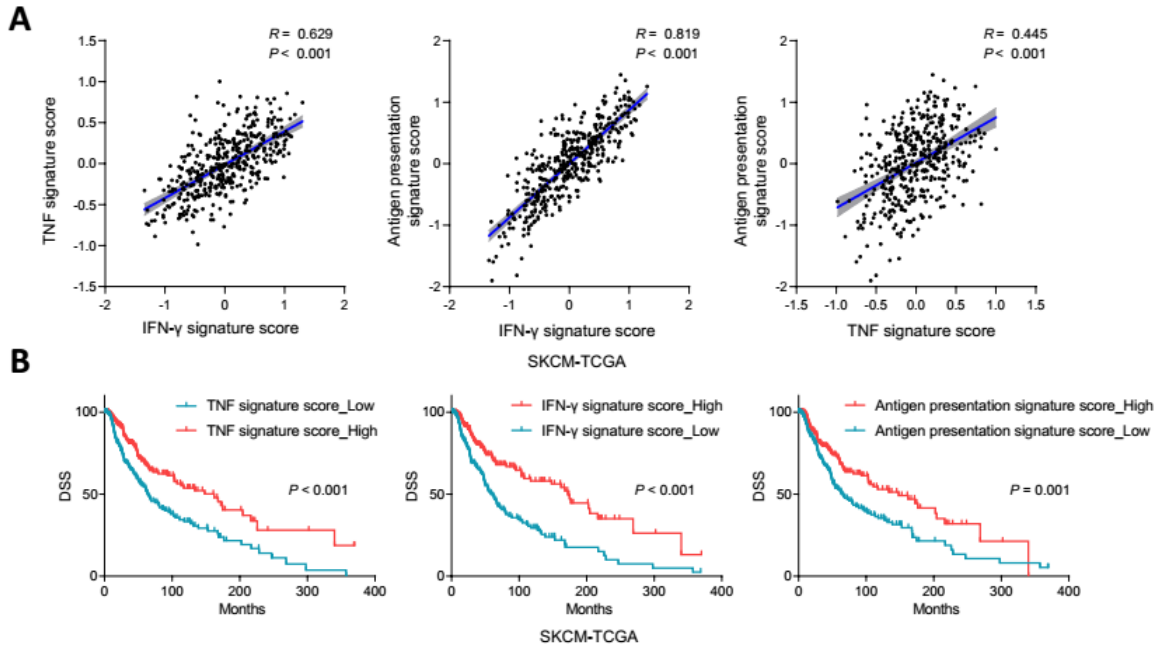


Figure 5.13 TNF and IFN-γ signatures predict better clinical outcomes. (A) Correlations among TNF signature score, IFN-γ signature score and antigen presentation signature score in SKCM-TCGA dataset. (B) Analysis of the correlations between disease specific survival rates (DSS) and TNF signature score, IFN-γ signature score or antigen presentation signature score in melanoma patients from SKCM-TCGA dataset. n= 420 patients were divided into two groups (high and low) based on the median value of each signature score. Statistical significance was determined by Chi-squared test (A) and Gehan-Breslow-Wilcoxon test (B).

To examine the expression of the target genes induced by TNF and IFN-γ on clinical outcomes, I analysed the human counterparts of the differentially expressed genes induced

by TNF and IFN-γ in the uORFs double mutant cells (Figure 5.11A). The expression of these genes is related to multiple aspects of anti-tumour immune responses, including T cell chemoattraction and activation (*CXCL9*, *CXCL10*, *CXCL11*, *CXCL16*, *CCL5*, *CCL7*, *ICAM1* and *CD40*), antigen presentation (*HLA-A*, *HLA-B*, *HLA-C*, *STAT1* and *NLRC5*) and cell death (*FAS*). Their expressions were positively correlated with *IFNG*, *TNF* and T cell infiltration (defined by the T cell marker gene *CD3D*) in melanoma patients (Figure 5.14). Notably, higher expression of these genes and higher T cells infiltration were beneficial for disease specific survival (Figure 5.15). To test the impact of hypoxia on the expression of these genes in patients, I gave a hypoxia score to each sample using Buffa hypoxia signature of 51 genes to reflect their hypoxic levels [270]. Consistent with our RNA-seq data, hypoxia negatively correlated with the expression of these genes (Figure 5.14) and it also had a negative impact on T cell infiltration (Figure 5.14 and 5.16) and disease specific survival in melanoma patients (Figure 5.15). These clinical data supported the role of hypoxia in negative regulation of anti-tumour immune response via inhibiting TNF and IFN-γ signalling.

In addition, by using a tumour mass spectrometry dataset derived from patients that underwent PD-1 immunotherapy [324], tumours that respond to PD-1 immunotherapy showed higher TNF and IFN-γ signatures (Figure 5.17A) and higher TNF and IFN-γ signatures were beneficial for better progression free survival (Figure 5.17B). These clinical data were consistent with our observations that enhanced TNF and IFN-γ signalling were beneficial for anti-tumour immunity. The data also suggested that higher TNF and IFN-γ signalling may enhance immunotherapy efficiency.

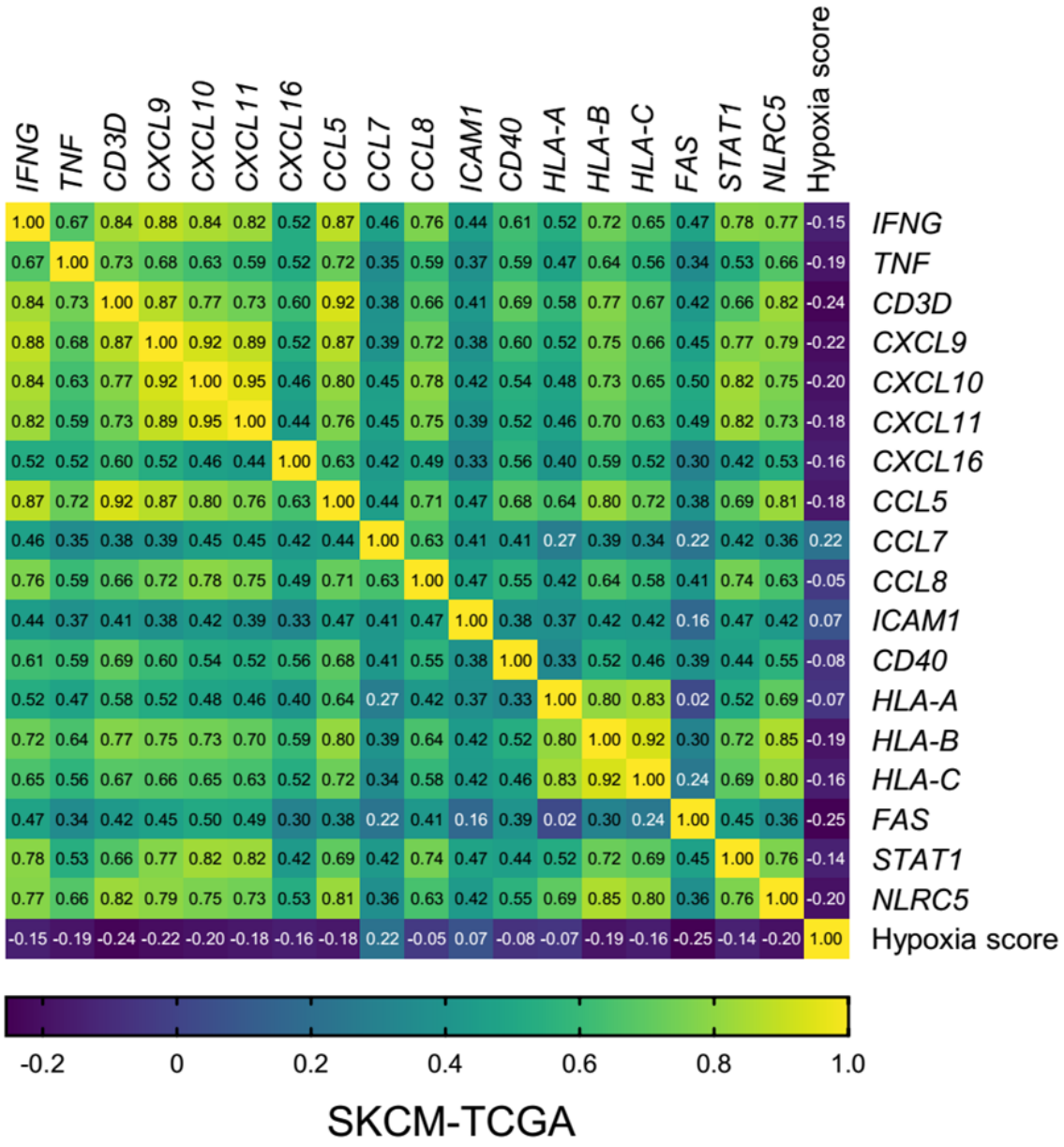


Figure 5.14 Correlation coefficients of the indicated genes from SKCM-TCGA dataset. Correlation analyses were performed to show the correlation coefficients among the indicated genes from SKCM-TCGA dataset. Pearson correlation coefficients between individual genes were shown by numbers and colours.

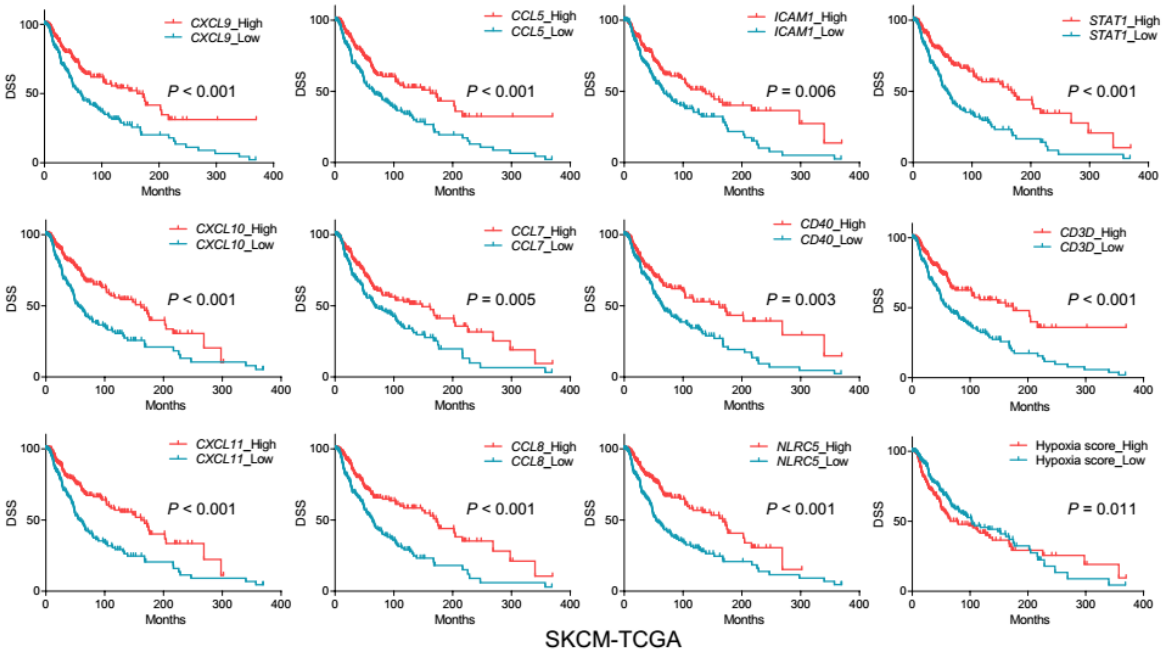


Figure 5.15 Analysis of the correlations between disease specific survival rates (DSS) and the expressions of indicated genes in melanoma patients from SKCM-TCGA dataset. n= 420 patients were divided into two groups (high and low) based on the median expression value of each gene. Statistical significance was determined by Gehan-Breslow-Wilcoxon test.

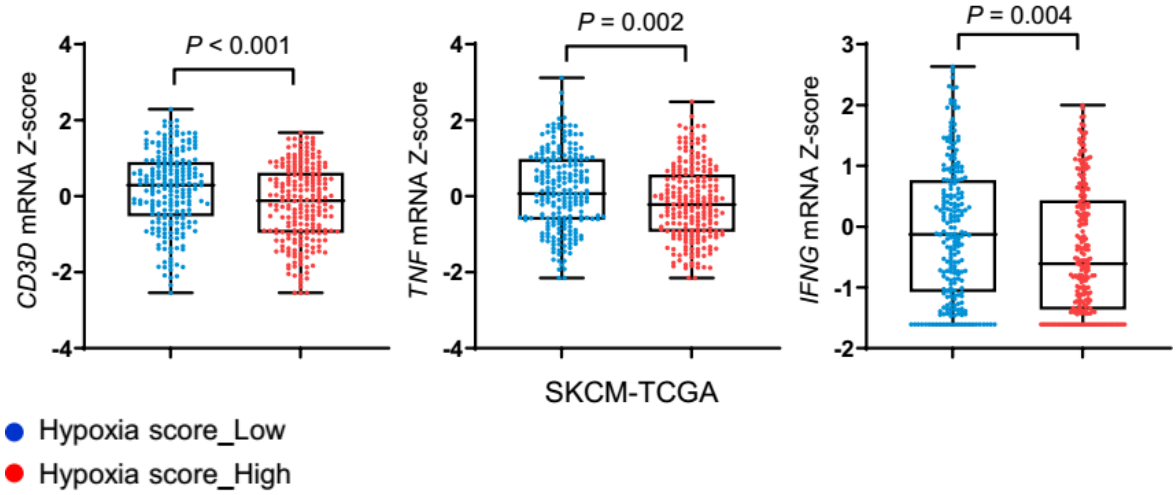


Figure 5.16 Hypoxia negatively correlates with T cell infiltration. The indicated genes from individual melanoma sample that derived from SKCM-TCGA dataset were analysed. Samples were grouped by the median value of hypoxia score. Statistical significance was determined by Mann-Whitney U test.

.

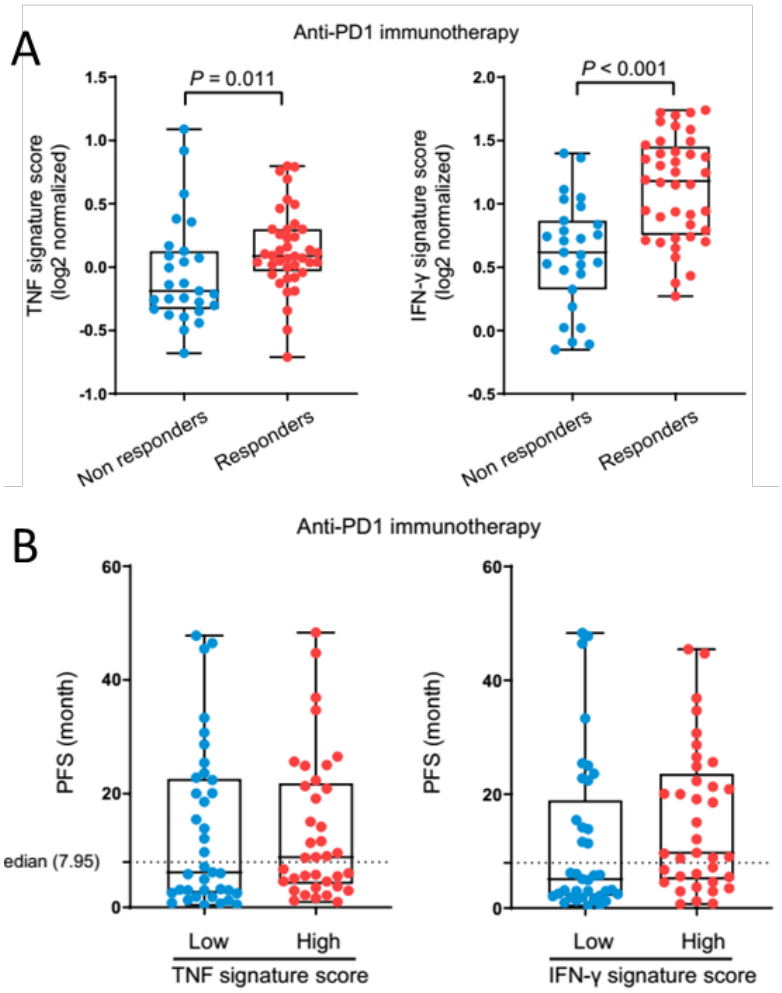


Figure 5.17 Higher TNF and IFN-γ signalling positively correlate with immunotherapy efficiency. (A) Analysis of the correlations between PD-1 immunotherapy responsiveness and TNF signature score or IFN-γ signature score from LC-MS/MS dataset derived from melanoma patients. PMID: 31495571. (B) Analysis of the correlations between progression free survival (PFS) and TNF signature score or IFN-γ signature score from LC-MS/MS dataset derived from melanoma patients. PMID: 31495571. Statistical significance was determined by Mann-Whitney U test.

Taken together, the reduction of TNFR1 and IFN-γR2 under hypoxia may play an important role for tumour escaping from T cell mediated immune surveillance. Targeting the uORFs of these genes upregulates the expression TNFR1 and IFN-γR2 irrespective of normoxia or hypoxia, however, this sustain their translation and functionally maintain TNF and IFN-γ signalling under hypoxic microenvironment, including promoting the expression of MHC-I, T cell chemoattractant and T cell co-stimulating factors, which may facilitate CD8 T cell dependent anti-tumour immunity.

6

Discussion

6.1 Regulation of immune receptor signalling

Innate immune receptors bind different microbial components, cytokines and chemokines to alert the immune system of an infection [2-4]. Each receptor recruits the corresponding adaptor proteins to transduce the signal to the downstream effectors. This process needs to be fine-tuned because the cells need to respond to the signal properly to avoid inflammation or autoimmunity. The activity of immune signalling can be regulated at different levels by various components, including adaptor proteins, ubiquitin ligases, deubiquitinating enzymes, kinases and phosphatases [63, 325]. In this thesis, I describe that translation of immune receptors via uORFs regulates immune receptor signalling during hypoxia, which provides evidence of how hypoxia has a direct inhibitory role on immune signalling.

6.2 Regulation of translation via uORFs during hypoxia

By using TNF signalling pathway as an example, I have uncovered a mechanism by which hypoxia regulates immune receptor signalling elicited by different types of receptor ligands, including L18-MDP-, TNF-, IL-1β- and IFN-γ (Figure 4.1, 4.2, 4.3 and 5.8B). I provide evidence that hypoxic inhibition of these signalling processes is, at least in part, mediated by the presence of uORF(s) in the mRNAs of the corresponding receptors. The uORF attenuates the translation of the CDS in the mRNAs encoding these receptors, which under hypoxic conditions led to a marked decrease in receptor levels and signalling responses (Chapter 4). Thus, although hypoxia has been found to suppress general protein synthesis due to various factors, such as the phosphorylation of eIF2α and PERK [245], and the inhibition of mTOR signalling [253], hypoxia may also regulate translation of a subset of mRNAs through a uORF-dependent mechanism (Figure 4.27 and Figure 4.28).

Recent studies showed that mutations in uORFs contribute to disease pathology by changing protein expression [326]. However, there are still outstanding questions in the field waiting to be answered: (1) How do uORFs dynamically regulate the translation of downstream

CDSs during various biological processes, such as under stress condition or during tumorigenesis? (2) How do uORFs cooperate with other cis- and trans-regulatory elements during mRNA translation? (3) Whether uORF-encoded polypeptides have biological functions and if so, what are their functions?

The presence of uORF2 attenuates the translation of TNFR1 during hypoxia. However, uORF2 is just a component of mRNA and it does not sense oxygen levels directly, thus it plays a passive role in hypoxia-mediated regulation of the translational process. The oxygen sensors [327-329], such as 2-oxoglutarate (2-OG)-dependent oxygenase family member, may play an active role in regulating the translation in response to hypoxia. To identify the genes involved in inhibiting translation during hypoxia, a targeted CRISPR screening against 2-OG-dependent oxygenase family or a genome-wide CRISPR screening could be performed. *De novo* protein synthesis activity during hypoxia can be visualised by click-chemistry labelling and cells with higher activity of *de novo* protein synthesis can be sorted by flow cytometry and sequenced by next generation sequencing, thereby candidate genes could be identified. Further investigations are needed to show how these candidate genes cooperate with uORFs in regulating the translational process during hypoxia.

My cell culture data show that the expression of TNFR1 is regulated by its uORF2 and also by hypoxia. It will be interesting to investigate the regulatory role of the uORF *in vivo*. For instance, generating a uORF2 (*TNFRSF1A*) genetically modified mouse may answer the question if hypoxia-mediated TNFR1 reduction contributes to immune tolerance in the intestine and other tissues, where there is physiological hypoxia [266]. In addition, it will also be interesting to investigate whether there are single nucleotide polymorphisms or mutations in uORFs (especially within start codons or stop codons) of the mRNAs encoding immune receptors or immune related proteins in the patients with autoimmune diseases. These experiments may further elucidate the physiological roles of uORFs and hypoxia-

mediated regulation of immune signalling and inflammation.

While my study is focussed on regulation of immune receptors, many other proteins are encoded by uORF-containing mRNAs and these may also be regulated during hypoxia via a uORF-dependent mechanism. For example, the translation initiation factor eIF4G1, encoded by uORF-containing mRNA may largely be regulated by hypoxia through uORF in a similar pattern (Figure 4.25). Intriguingly, proteins widely used as loading controls as they are stable under various conditions (alpha-Actin, beta-Actin, alpha-Tubulin, beta-Tubulin, GAPDH, Vinculin, Lamin B1, PCNA, Histone H1, Transferrin, VDAC1 and SDH) are encoded by mRNAs that do not contain uORFs (at least one transcript variant). The absence of uORFs might contribute to the abundance and stable level of these proteins.

uORFs have been identified in over 40% of human protein-coding genes and many of these uORFs have been found to be translated by mass spectrometry [238, 330]. These protein-coding uORFs may not only regulate the translation of the CDS, but the translated polypeptides have biological functions. Recent studies indicate that uORF-encoded peptides are involved in MHC-I mediated antigen presentation and recognition by T cells [249, 331]. Another study showed that a peptide MP31, encoded by a uORF in the 5'UTR of *PTEN*, regulates lactate-pyruvate conversion by competing with mitochondrial lactate dehydrogenase [332]. My work indicates that the translating uORFs of multiple immune receptor-coding genes attenuate the translation of the CDS during hypoxia (Figure 4.26 and 4.27). However, whether the uORF-encoded polypeptides have immune regulatory roles is entirely unknown. Further investigations are needed to investigate this possibility.

6.3 Hypoxia in regulation of inflammation

My work indicates that hypoxia-induced inhibition of translation leads to reduced expression of immune receptors and reduced immune signalling (Chapter 4 and Chapter 5). In support of this, previous studies have shown that chemical hypoxia mimetics have anti-

inflammatory roles in various animal models and in clinical trials (Table 1.2) [189]. However, the role of hypoxia in regulating immune response is still under debate. The role of hypoxia in promoting or inhibiting inflammation could be context dependent. For example, during acute ischemia, hypoxia may cause cell death, which facilitates the recruitment of immune cells and induce inflammation. Also, the expression of some of the pro-inflammatory target genes of NF-κB is also upregulated by HIF1α, such as *CXCL8* and *IL6* [333-336], and HIF1α itself is transcriptionally upregulated by NF-κB [337]. Recently, a study showed that knockdown of PHD2 in mouse promotes auto-inflammation in a HIF2α dependent manner [338]. However, due to complexity of *in vivo* studies, it is not clear whether the inflammation is caused directly by stabilisation of HIF2α or indirectly by HIF2α-induced cell death [338-340].

Recent *in vivo* studies found that targeting the HIF pathway with pharmacological hydroxylase inhibitors, such as dimethyloxallylglycine (DMOG), which stabilises and activates HIF1α, can have a broad anti-inflammatory effect such as in the mouse model of inflammatory bowel disease (IBD), ischemic acute kidney injury and sepsis [189, 341]. However, further studies are needed to determine whether the anti-inflammatory effect of hydroxylase inhibitors is directly mediated by HIF accumulation or PHD inhibition. There are possibilities that additional mechanisms may exist since hydroxylase inhibitors can also affect other oxygen sensors, such as TETs (Ten-eleven translocation enzymes) [342, 343].

Intriguingly, I obtained preliminary data indicating that treatment of HCT-116 cells with the hydroxylase inhibitor deferoxamine (DFO) reduced TNFR1 expression and inhibited the degradation of IκBα and the phosphorylation of NF-κB on Ser536 in the presence of TNF (Figure 6.1). Given that TNF is a driving force of inflammation and neutralising TNF antibody is widely used for treating inflammatory diseases [337], I speculate that the anti-inflammatory effect of hydroxylase inhibitors may be contributed by reduced TNFR1 levels

and consequently inhibition of TNF signalling. It will be interesting to investigate this further and to test if DMOG and other hydroxylase inhibitors also inhibit the expression of TNFR1 and other immune receptors.

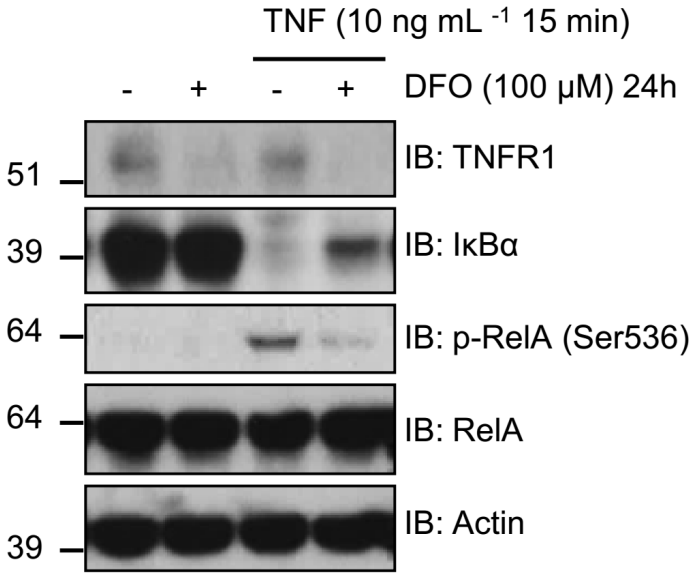


Figure 6.1 Hydroxylase inhibitor reduces TNFR1 and inhibits TNF signalling. HCT-116 cells were treated with 100 μM deferoxamine (DFO) for 24 hr. Cells were stimulated with TNF (10 ng mL^{-1}; 15 min) and subjected to immunoblotting with the indicated antibodies. Data are shown as one representative of three independent experiments with similar results.

6.4 Hypoxia inhibits a potential feedforward loop in T cell activation

Hypoxia is a common feature in solid tumours [344] and inhibition of immune receptor signalling can result in suppression of immune responses and tumour surveillance. My data suggest that the loss of TNF and IFN-γ signalling under hypoxia results in defective MHC-I-mediated antigen presentation, which is required for initiating CD8 T cell activation.

The basal expression of MHC-I on tumour cells may initially activate a limited number of T cells, which can subsequently secret more TNF and IFN-γ, thereby upregulating the expression of MHC-I and T cell chemoattractant in tumour cells, resulting in activation of more T cells. However, such feed forward cycle seems to be abrogated in the tumour microenvironment due to hypoxia. I showed that the hypoxia-inhibited expressions of MHC-I and T cell chemoattractants were restored by disruption of uORFs in *TNFRSF1A*

and *IFNGR2* in the mouse Yumm1.7 melanoma cells (Figure 5.11). As a result, my data suggest that CD8 T cell dependent anti-tumour immunity was augmented by mutating the uORFs in *TNFRSF1A* and *IFNGR2*, leading to substantial attenuation of tumour growth (Figure 5.12A and 5.12B). In line with this, analysis of the TCGA-SKCM dataset indicates that hypoxia had a negative impact on T cell infiltration and activation in melanoma patients (Figure 5.16). Based on these findings, I propose that during the development of a tumour, hypoxia restricts this feedforward loop by inhibiting TNF and IFN-γ signalling, resulting in impaired CD8 T cell activation and thereby enabling immune evasion (Figure 6.2). I speculate, based on my data, that targeting uORFs in *TNFRSF1A* and *IFNGR2* in human cancer may eradicate hypoxic inhibition of TNF and IFN-γ signalling, thereby enhancing anti-tumour immune responses under hypoxic microenvironment.

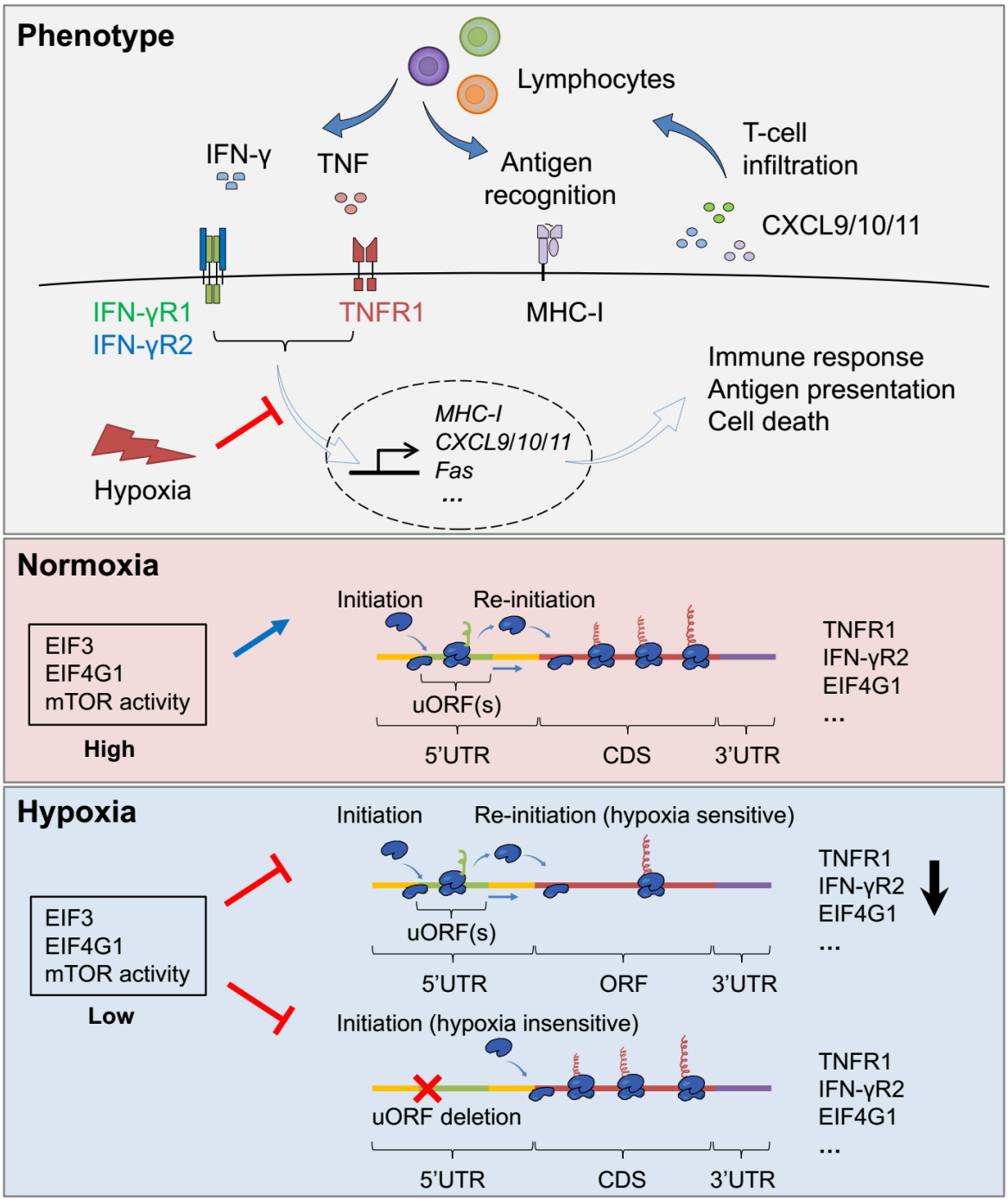


Figure 6.2 Mechanisms of hypoxia regulating immune evasion via uORFs. A proposed model that how hypoxia facilitates cancer immune evasion through downregulating TNF and IFN-γ signalling via uORFs.

6.5 Study limitations

In my study, knockdown of HIF1α had no impact on hypoxia-induced TNFR1 reduction, indicating that HIF1α is not involved in regulation of TNFR1 expression. However, it cannot be completely ruled out that if HIF2α is involved or has a redundant role with HIF1α in regulating the translation of uORF-containing mRNAs. After all, uORF is just a component on mRNA and it inhibits the translation efficiency of the main CDS, thus passively regulating the translational process. It therefore remains unclear if there is an oxygen-sensing mechanism that contributes to the regulation of immune receptors under hypoxia and if so, what this mechanism is.

Another limitation is that the experiments in the tumour mouse model were performed with only one monoclonal Yumm1.7 cell line bearing the uORFs mutations on both *TNFRSF1A* and *IFNGR2*. More clones of double uORFs mutation and of single uORF mutation need to be tested. It is unclear whether a single uORF mutation of *TNFRSF1A* or *IFNGR2* is sufficient to enhance MHC-I-mediated antigen presentation and anti-tumour immunity.

Lastly, epithelial cells were used throughout the study. It is unclear whether hypoxia-mediated inhibition of immune receptor signalling also applies to other cell types. For example, my data indicate that IL-1βR signalling was inhibited by hypoxia in HCT-116 cells (Figure 4.1, 4.2 and 4.3). Whether hypoxia also affects this signalling pathway in T cells is not clear, since IL1 promotes T cell activation and expansion [345, 346]. This may help to understand how hypoxia regulates T cells.

6.6 Conclusion

In this study, I found that hypoxia can inhibit immune signalling induced by multiple pro-inflammatory ligands, including TNF, IL-1β, L18-MDP and IFN-γ. By using the TNFR1 signalling pathway as a model, I identified that hypoxia-mediated inhibition of immune signalling is contributed by translational regulation of immune receptors via uORF(s) present in the 5'UTR. Hypoxia significantly restricts the expression of immune receptors that are encoded by uORF-containing mRNAs. By using a mouse melanoma model, I showed that the presence of uORFs in *TNFRSF1A* and *IFNGR2* restrict the translations of TNFR1 and IFN-γR2. Consequently, their downstream signalling pathways are inhibited, resulting in impairment of antigen presentation induced by TNF and IFN-γ. Therefore, I propose that disruption of uORFs in *TNFRSF1A* and *IFNGR2* may amplify the antigen presentation in tumours, which promotes CD8 T cell-dependent anti-tumour immunity.

7

Appendices

7.1 Supplementary figures

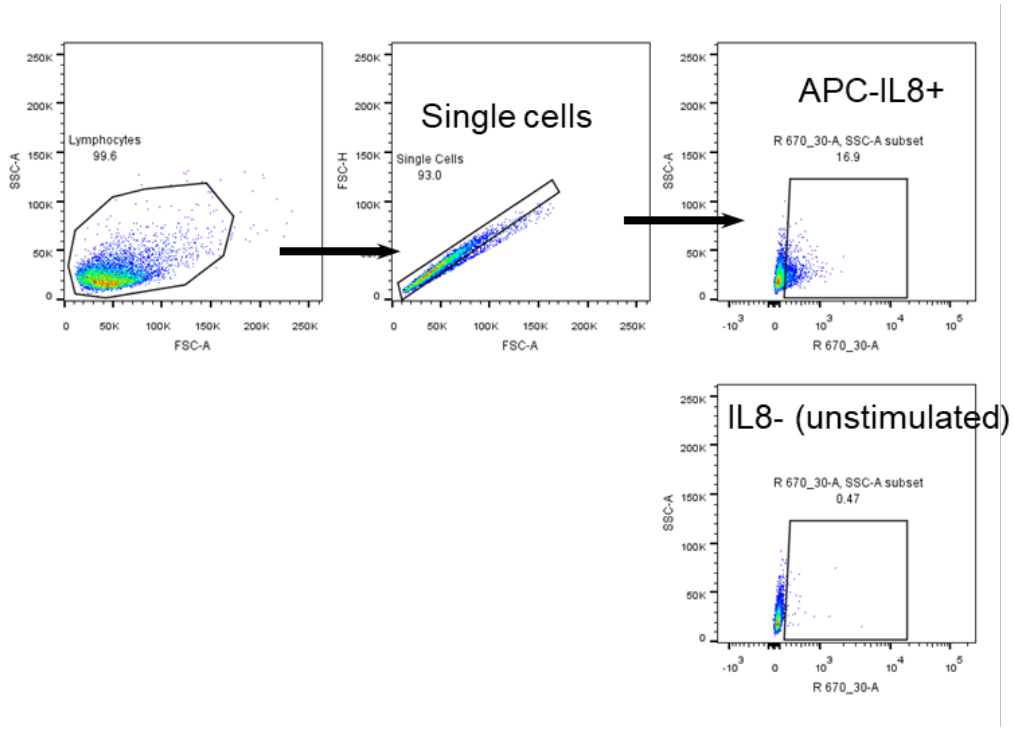


Figure 7.1 Gating strategy of Figure 4.1. Cells were intracellular-stained with APC-anti-human-IL8. Singlets were gated by FSC-H and FSC-A. 10,000 singlets were recorded. Unstimulated cells were used as negative control. Percentage of positivity was used to compare different conditions.

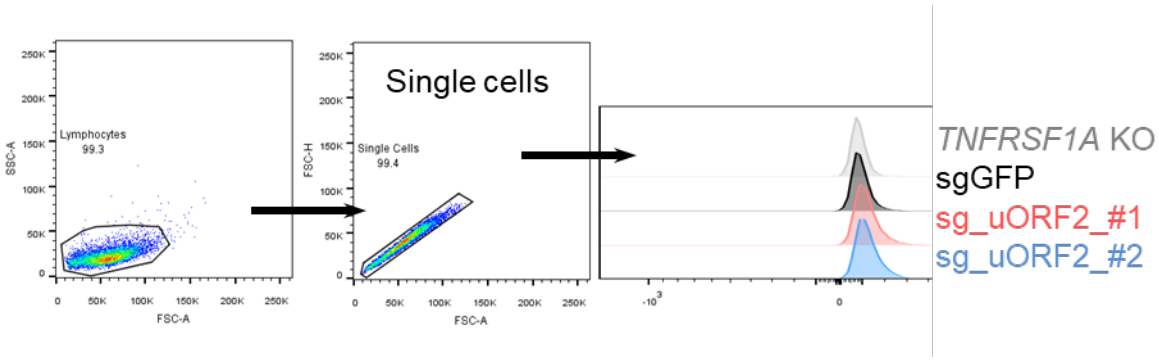


Figure 7.2 Gating strategy of Figure 4.17B. Cells were surface-stained with APC-anti-human-TNFR1. Singlets were gated by FSC-H and FSC-A. 10,000 singlets were recorded. *TNFRSF1A* knockout cells were used as negative control. Median fluorescence intensities were used to compare surface TNFR1 expression levels.

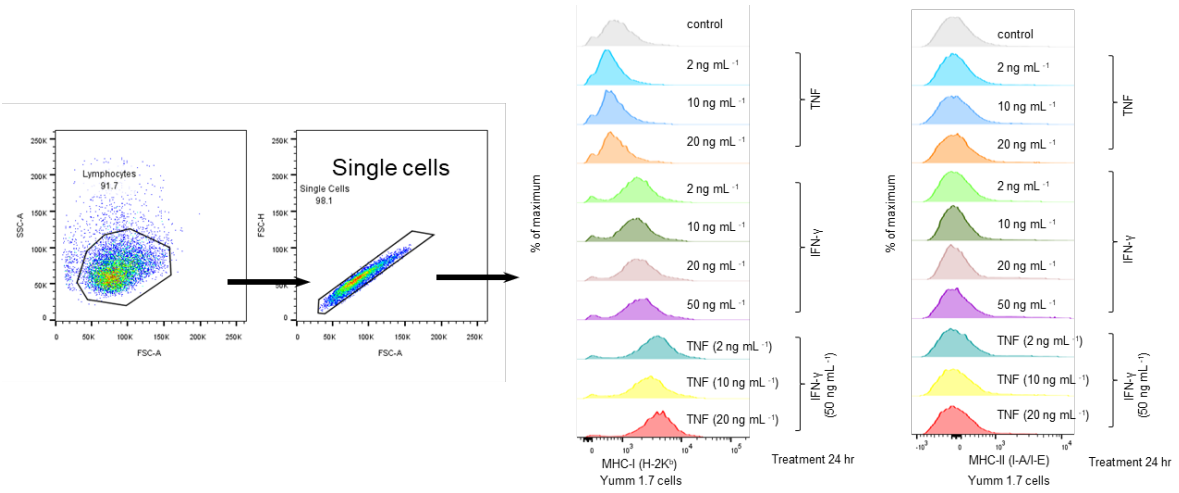


Figure 7.3 Gating strategy of Figure 5.4. Cells were surface-stained with PE-anti-mouse-H-2K^b and APC-anti-mouse-I-A/I-E. Singlets were gated by FSC-H and FSC-A. 10,000 singlets were recorded. Unstimulated cells were used as negative control. Median fluorescence intensities were used to compare surface H-2K^b and I-A/I-E expression levels.

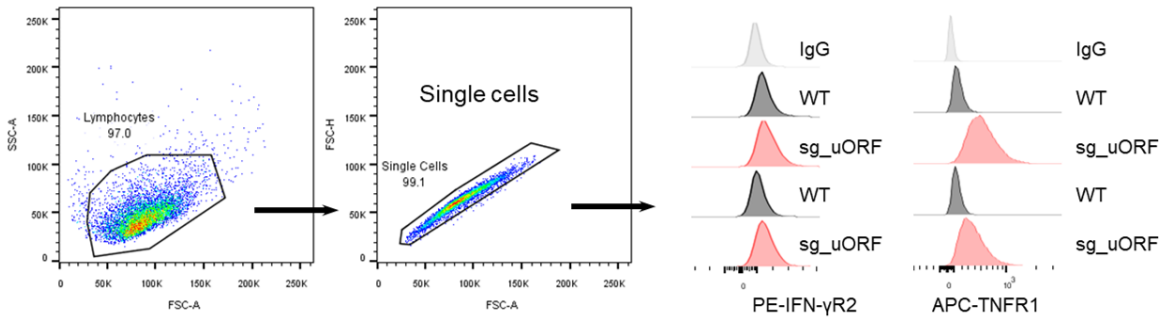


Figure 7.4 Gating strategy of Figure 5.7C. Cells were surface-stained with PE-anti-mouse-IFN-γR2 and APC-anti-mouse-TNFR1. Singlets were gated by FSC-H and FSC-A. 10,000 singlets were recorded. Isotype antibodies were used as negative controls. Median fluorescence intensities were used to compare IFN-γR2 and TNFR1 expression levels.

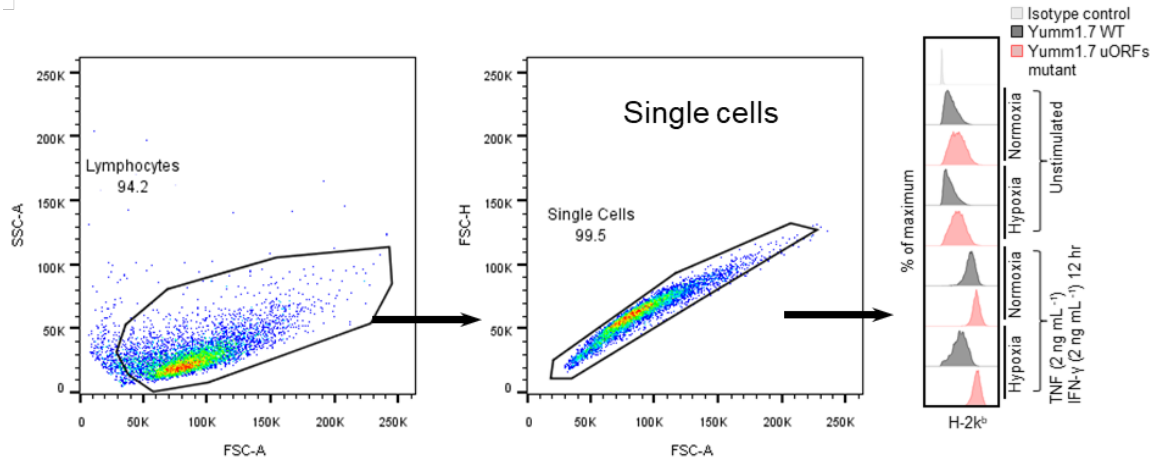


Figure 7.5 Gating strategy of Figure 5.8C. Cells were surface-stained with PE-anti-mouse-H-2K^{b}. Singlets were gated by FSC-H and FSC-A. 10,000 singlets were recorded. Isotype antibody was used as negative controls. Median fluorescence intensities were used to compare H-2K^{b} expression levels.

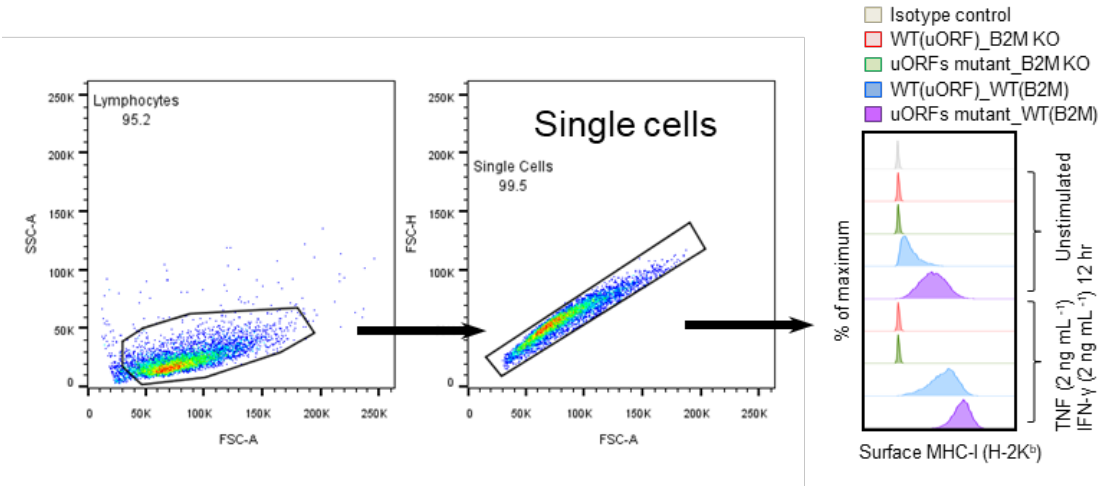


Figure 7.6 Gating strategy of Figure 5.12C. Cells were surface-stained with PE-anti-mouse-H-2K^{b}. Singlets were gated by FSC-H and FSC-A. 10,000 singlets were recorded. Isotype antibody and *B2M* knockout cells were used as negative controls. Median fluorescence intensities were used to compare H-2K^{b} expression levels.

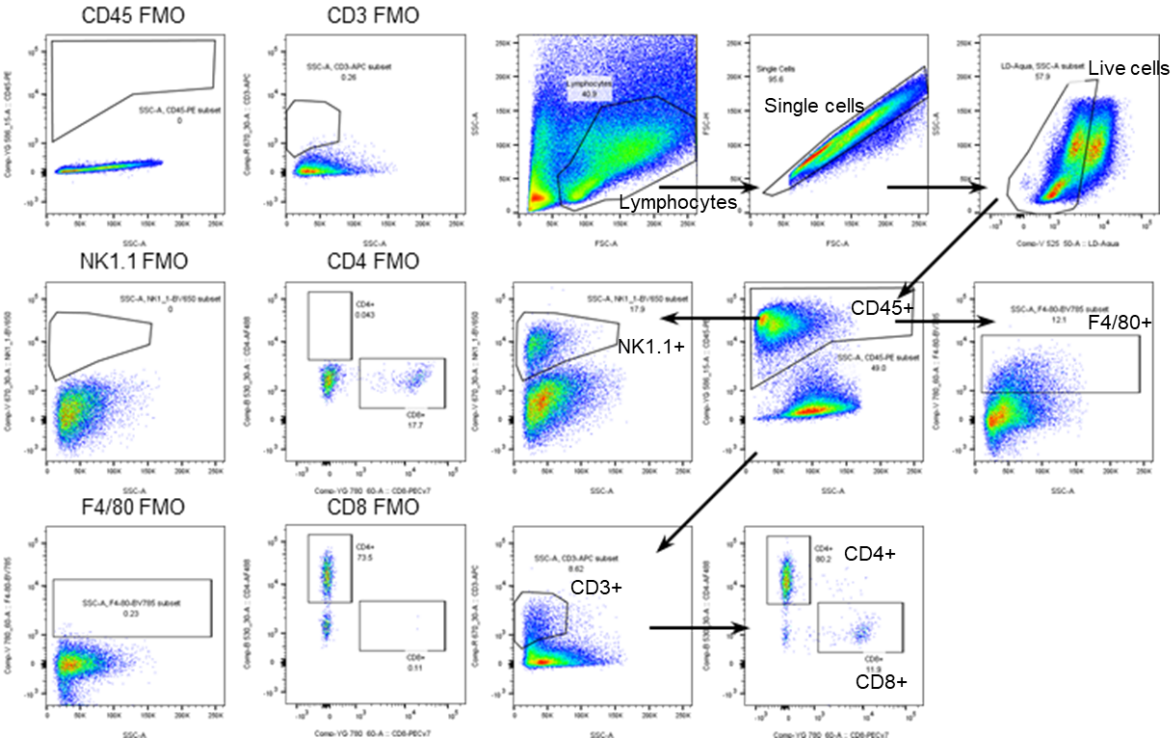


Figure 7.7 Gating strategy of Figure 5.12D-I. Tumour tissues were digested by the mouse tumour dissociation kit from Miltenyibiotec. Lymphocytes were gated by FSC-A and SSC-A. Singlets were gated by FSC-A and FSC-H. Live cells were gated by Fixable Viability Dye eFluor™ 506 negative population. Immune cells were gated by CD45 positive population. Cell surface markers were gated as indicated. Detailed staining information was shown in methods section. Percentage of positivity was used to compare different conditions.

References

1 Chaplin, D.D. (2010) Overview of the immune response. *The Journal of allergy and clinical immunology* 125, S3-23

2 Walsh, D.*, et al.* (2013) Pattern recognition receptors--molecular orchestrators of inflammation in inflammatory bowel disease. *Cytokine & growth factor reviews* 24, 91-104

3 Seong, S.Y. and Matzinger, P. (2004) Hydrophobicity: an ancient damage-associated molecular pattern that initiates innate immune responses. *Nature reviews. Immunology* 4, 469-478

4 Medzhitov, R. and Janeway, C.A., Jr. (1997) Innate immunity: impact on the adaptive immune response. *Current opinion in immunology* 9, 4-9

5 Takeuchi, O. and Akira, S. (2010) Pattern recognition receptors and inflammation. *Cell* 140, 805-820

6 Maelfait, J.*, et al.* (2020) Nucleic Acid Sensors and Programmed Cell Death. *Journal of molecular biology* 432, 552-568

7 Jiang, X. and Chen, Z.J. (2011) The role of ubiquitylation in immune defence and pathogen evasion. *Nature reviews. Immunology* 12, 35-48

8 Caruso, R.*, et al.* (2014) NOD1 and NOD2: signaling, host defense, and inflammatory disease. *Immunity* 41, 898-908

9 Girardin, S.E.*, et al.* (2003) Nod1 detects a unique muropeptide from gram-negative bacterial peptidoglycan. *Science* 300, 1584-1587

10 Kim, M.L.*, et al.* (2010) IKKalpha contributes to canonical NF-kappaB activation downstream of Nod1-mediated peptidoglycan recognition. *PloS one* 5, e15371

11 Allison, C.C.*, et al.* (2009) Helicobacter pylori induces MAPK phosphorylation and AP-1 activation via a NOD1-dependent mechanism. *J Immunol* 183, 8099-8109

12 Hasegawa, M.*, et al.* (2006) Differential release and distribution of Nod1 and Nod2 immunostimulatory molecules among bacterial species and environments. *The Journal of biological chemistry* 281, 29054-29063

13 Opitz, B.*, et al.* (2004) Nucleotide-binding oligomerization domain proteins are innate immune receptors for internalized Streptococcus pneumoniae. *The Journal of biological chemistry* 279, 36426-36432

14 Kobayashi, K.S.*, et al.* (2005) Nod2-dependent regulation of innate and adaptive immunity in the intestinal tract. *Science* 307, 731-734

15 Hisamatsu, T.*, et al.* (2003) CARD15/NOD2 functions as an antibacterial factor in human intestinal epithelial cells. *Gastroenterology* 124, 993-1000

16 Kufer, T.A.*, et al.* (2006) Role for erbin in bacterial activation of Nod2. *Infection and immunity* 74, 3115-3124

17 Ferwerda, G.*, et al.* (2005) NOD2 and toll-like receptors are nonredundant recognition systems of Mycobacterium tuberculosis. *PLoS pathogens* 1, 279-285

18 Kobayashi, K.*, et al.* (2002) RICK/Rip2/CARDIAK mediates signalling for receptors of the innate and adaptive immune systems. *Nature* 416, 194-199

19 Zeissig, Y.*, et al.* (2015) XIAP variants in male Crohn's disease. *Gut* 64, 66-76

20 Damgaard, R.B.*, et al.* (2013) Disease-causing mutations in the XIAP BIR2 domain impair NOD2-dependent immune signalling. *EMBO molecular medicine* 5, 1278-1295

21 Hasegawa, M.*, et al.* (2008) A critical role of RICK/RIP2 polyubiquitination in Nod-induced NF-kappaB activation. *The EMBO journal* 27, 373-383

22 Marinis, J.M.*, et al.* (2011) A novel motif in the Crohn's disease susceptibility protein, NOD2, allows TRAF4 to down-regulate innate immune responses. *The Journal of biological chemistry* 286, 1938-1950

23 Zhang, R.*, et al.* (2014) The E3 ligase RNF34 is a novel negative regulator of the NOD1 pathway.

Cellular physiology and biochemistry : international journal of experimental cellular physiology, biochemistry, and pharmacology 33, 1954-1962
24 Damgaard, R.B.*, et al.* (2012) The ubiquitin ligase XIAP recruits LUBAC for NOD2 signaling in inflammation and innate immunity. *Molecular cell* 46, 746-758
25 Newton, K. and Dixit, V.M. (2012) Signaling in innate immunity and inflammation. *Cold Spring Harbor perspectives in biology* 4
26 Arango Duque, G. and Descoteaux, A. (2014) Macrophage cytokines: involvement in immunity and infectious diseases. *Frontiers in immunology* 5, 491
27 Bruewer, M.*, et al.* (2003) Proinflammatory cytokines disrupt epithelial barrier function by apoptosis-independent mechanisms. *J Immunol* 171, 6164-6172
28 Zhang, J.M. and An, J. (2007) Cytokines, inflammation, and pain. *International anesthesiology clinics* 45, 27-37
29 Waykole, Y.P.*, et al.* (2009) Anticytokine therapy for periodontal diseases: Where are we now? *Journal of Indian Society of Periodontology* 13, 64-68
30 Kany, S.*, et al.* (2019) Cytokines in Inflammatory Disease. *International journal of molecular sciences* 20
31 Heim, A.*, et al.* (2000) Transient induction of cytokine production in human myocardial fibroblasts by coxsackievirus B3. *Circulation research* 86, 753-759
32 Shen, J.*, et al.* (2018) Anti-cancer therapy with TNFalpha and IFNgamma: A comprehensive review. *Cell proliferation* 51, e12441
33 Dinarello, C.A. (2011) Interleukin-1 in the pathogenesis and treatment of inflammatory diseases. *Blood* 117, 3720-3732
34 Pober, J.S. and Sessa, W.C. (2014) Inflammation and the blood microvascular system. *Cold Spring Harbor perspectives in biology* 7, a016345
35 Dinarello, C.A. (1994) The biological properties of interleukin-1. *European cytokine network* 5, 517-531
36 Dinarello, C.A. (2005) Blocking IL-1 in systemic inflammation. *The Journal of experimental medicine* 201, 1355-1359
37 O'Neill, L.A. (2008) The interleukin-1 receptor/Toll-like receptor superfamily: 10 years of progress. *Immunological reviews* 226, 10-18
38 Sims, J.E.*, et al.* (1988) cDNA expression cloning of the IL-1 receptor, a member of the immunoglobulin superfamily. *Science* 241, 585-589
39 Liu, Z.*, et al.* (1992) cDNA cloning of a novel human ubiquitin carrier protein. An antigenic domain specifically recognized by endemic pemphigus foliaceus autoantibodies is encoded in a secondary reading frame of this human epidermal transcript. *The Journal of biological chemistry* 267, 15829-15835
40 Ratner, M. (2008) IL-1 trap go-ahead. *Nature biotechnology* 26, 485
41 Rock, F.L.*, et al.* (1998) A family of human receptors structurally related to Drosophila Toll. *Proceedings of the National Academy of Sciences of the United States of America* 95, 588-593
42 Eisenberg, S.P.*, et al.* (1991) Interleukin 1 receptor antagonist is a member of the interleukin 1 gene family: evolution of a cytokine control mechanism. *Proceedings of the National Academy of Sciences of the United States of America* 88, 5232-5236
43 LaRosa, D.F.*, et al.* (2008) T cell expression of MyD88 is required for resistance to Toxoplasma gondii. *Proceedings of the National Academy of Sciences of the United States of America* 105, 3855-3860
44 Brikos, C.*, et al.* (2007) Mass spectrometric analysis of the endogenous type I interleukin-1 (IL-1) receptor signaling complex formed after IL-1 binding identifies IL-1RAcP, MyD88, and IRAK-4 as the stable components. *Molecular & cellular proteomics : MCP* 6, 1551-1559
45 O'Neill, L.A.*, et al.* (1990) How does interleukin 1 activate cells? Interleukin 1 signal transduction. *Immunology today* 11, 392-394
46 Webster, J.D. and Vucic, D. (2020) The Balance of TNF Mediated Pathways Regulates

Inflammatory Cell Death Signaling in Healthy and Diseased Tissues. *Frontiers in cell and developmental biology* 8, 365
47 Vassalli, P. (1992) The pathophysiology of tumor necrosis factors. *Annual review of immunology* 10, 411-452
48 Moss, M.L.*, et al.* (1997) Cloning of a disintegrin metalloproteinase that processes precursor tumour-necrosis factor-alpha. *Nature* 385, 733-736
49 Grell, M.*, et al.* (1995) The transmembrane form of tumor necrosis factor is the prime activating ligand of the 80 kDa tumor necrosis factor receptor. *Cell* 83, 793-802
50 Reddy, P.*, et al.* (2000) Functional analysis of the domain structure of tumor necrosis factor-alpha converting enzyme. *The Journal of biological chemistry* 275, 14608-14614
51 Wallach, D.*, et al.* (1999) Tumor necrosis factor receptor and Fas signaling mechanisms. *Annual review of immunology* 17, 331-367
52 Sessler, T.*, et al.* (2013) Structural determinants of DISC function: new insights into death receptor-mediated apoptosis signalling. *Pharmacology & therapeutics* 140, 186-199
53 Micheau, O. and Tschopp, J. (2003) Induction of TNF receptor I-mediated apoptosis via two sequential signaling complexes. *Cell* 114, 181-190
54 Bertrand, M.J.*, et al.* (2008) cIAP1 and cIAP2 facilitate cancer cell survival by functioning as E3 ligases that promote RIP1 ubiquitination. *Molecular cell* 30, 689-700
55 Mahoney, D.J.*, et al.* (2008) Both cIAP1 and cIAP2 regulate TNFalpha-mediated NF-kappaB activation. *Proceedings of the National Academy of Sciences of the United States of America* 105, 11778-11783
56 Haas, T.L.*, et al.* (2009) Recruitment of the linear ubiquitin chain assembly complex stabilizes the TNF-R1 signaling complex and is required for TNF-mediated gene induction. *Molecular cell* 36, 831-844
57 Tokunaga, F.*, et al.* (2009) Involvement of linear polyubiquitylation of NEMO in NF-kappaB activation. *Nature cell biology* 11, 123-132
58 Ikeda, F.*, et al.* (2011) SHARPIN forms a linear ubiquitin ligase complex regulating NF-kappaB activity and apoptosis. *Nature* 471, 637-641
59 Shim, J.H.*, et al.* (2005) TAK1, but not TAB1 or TAB2, plays an essential role in multiple signaling pathways in vivo. *Genes & development* 19, 2668-2681
60 Wertz, I.E.*, et al.* (2004) De-ubiquitination and ubiquitin ligase domains of A20 downregulate NF-kappaB signalling. *Nature* 430, 694-699
61 Enesa, K.*, et al.* (2008) NF-kappaB suppression by the deubiquitinating enzyme Cezanne: a novel negative feedback loop in pro-inflammatory signaling. *The Journal of biological chemistry* 283, 7036-7045
62 Kovalenko, A.*, et al.* (2003) The tumour suppressor CYLD negatively regulates NF-kappaB signalling by deubiquitination. *Nature* 424, 801-805
63 Hrdinka, M. and Gyrd-Hansen, M. (2017) The Met1-Linked Ubiquitin Machinery: Emerging Themes of (De)regulation. *Molecular cell* 68, 265-280
64 Elliott, P.R.*, et al.* (2016) SPATA2 Links CYLD to LUBAC, Activates CYLD, and Controls LUBAC Signaling. *Molecular cell* 63, 990-1005
65 Heger, K.*, et al.* (2018) OTULIN limits cell death and inflammation by deubiquitinating LUBAC. *Nature* 559, 120-124
66 Dhuriya, Y.K. and Sharma, D. (2018) Necroptosis: a regulated inflammatory mode of cell death. *Journal of neuroinflammation* 15, 199
67 Van Antwerp, D.J.*, et al.* (1996) Suppression of TNF-alpha-induced apoptosis by NF-kappaB. *Science* 274, 787-789
68 Nirmala, J.G. and Lopus, M. (2020) Cell death mechanisms in eukaryotes. *Cell biology and toxicology* 36, 145-164
69 Vanden Berghe, T.*, et al.* (2014) Regulated necrosis: the expanding network of non-apoptotic cell death pathways. *Nature reviews. Molecular cell biology* 15, 135-147

70 Wang, L.*, et al.* (2008) TNF-alpha induces two distinct caspase-8 activation pathways. *Cell* 133, 693-703
71 Sun, X.*, et al.* (2002) Identification of a novel homotypic interaction motif required for the phosphorylation of receptor-interacting protein (RIP) by RIP3. *The Journal of biological chemistry* 277, 9505-9511
72 He, S.*, et al.* (2009) Receptor interacting protein kinase-3 determines cellular necrotic response to TNF-alpha. *Cell* 137, 1100-1111
73 Wu, X.N.*, et al.* (2014) Distinct roles of RIP1-RIP3 hetero- and RIP3-RIP3 homo-interaction in mediating necroptosis. *Cell death and differentiation* 21, 1709-1720
74 Laurien, L.*, et al.* (2020) Autophosphorylation at serine 166 regulates RIP kinase 1-mediated cell death and inflammation. *Nature communications* 11, 1747
75 Kopitar-Jerala, N. (2017) The Role of Interferons in Inflammation and Inflammasome Activation. *Frontiers in immunology* 8, 873
76 Ikeda, H.*, et al.* (2002) The roles of IFN gamma in protection against tumor development and cancer immunoediting. *Cytokine & growth factor reviews* 13, 95-109
77 Dunn, G.P.*, et al.* (2005) A critical function for type I interferons in cancer immunoediting. *Nature immunology* 6, 722-729
78 Castro, F.*, et al.* (2018) Interferon-Gamma at the Crossroads of Tumor Immune Surveillance or Evasion. *Frontiers in immunology* 9, 847
79 Mitra-Kaushik, S.*, et al.* (2004) Enhanced tumorigenesis in HTLV-1 tax-transgenic mice deficient in interferon-gamma. *Blood* 104, 3305-3311
80 Shankaran, V.*, et al.* (2001) IFNgamma and lymphocytes prevent primary tumour development and shape tumour immunogenicity. *Nature* 410, 1107-1111
81 Yan, N. and Chen, Z.J. (2012) Intrinsic antiviral immunity. *Nature immunology* 13, 214-222
82 Pott, J.*, et al.* (2011) IFN-lambda determines the intestinal epithelial antiviral host defense. *Proceedings of the National Academy of Sciences of the United States of America* 108, 7944-7949
83 McNab, F.*, et al.* (2015) Type I interferons in infectious disease. *Nature reviews. Immunology* 15, 87-103
84 Goldstein, D. and Laszlo, J. (1988) The role of interferon in cancer therapy: a current perspective. *CA: a cancer journal for clinicians* 38, 258-277
85 Hauschild, A.*, et al.* (2008) Practical guidelines for the management of interferon-alpha-2b side effects in patients receiving adjuvant treatment for melanoma: expert opinion. *Cancer* 112, 982-994
86 Ishikawa, T. (2008) Secondary prevention of recurrence by interferon therapy after ablation therapy for hepatocellular carcinoma in chronic hepatitis C patients. *World journal of gastroenterology* 14, 6140-6144
87 Abdolvahab, M.H.*, et al.* (2020) Interferons: role in cancer therapy. *Immunotherapy* 12, 833-855
88 Maeda, S.*, et al.* (2014) Interferon-alpha acts on the S/G2/M phases to induce apoptosis in the G1 phase of an IFNAR2-expressing hepatocellular carcinoma cell line. *The Journal of biological chemistry* 289, 23786-23795
89 Kelker, H.C.*, et al.* (1984) Three molecular weight forms of natural human interferon-gamma revealed by immunoprecipitation with monoclonal antibody. *The Journal of biological chemistry* 259, 4301-4304
90 Wong, L.H.*, et al.* (1998) IFN-gamma priming up-regulates IFN-stimulated gene factor 3 (ISGF3) components, augmenting responsiveness of IFN-resistant melanoma cells to type I IFNs. *J Immunol* 160, 5475-5484
91 Greenlee-Wacker, M.C. and Nauseef, W.M. (2017) IFN-gamma targets macrophage-mediated immune responses toward Staphylococcus aureus. *Journal of leukocyte biology* 101, 751-758
92 Kaplan, D.H.*, et al.* (1998) Demonstration of an interferon gamma-dependent tumor surveillance system in immunocompetent mice. *Proceedings of the National Academy of Sciences of the United States of America* 95, 7556-7561

93 Kasahara, T.*, et al.* (1983) Interleukin 2-mediated immune interferon (IFN-gamma) production by human T cells and T cell subsets. *J Immunol* 130, 1784-1789
94 Mosmann, T.R.*, et al.* (2005) Two types of murine helper T cell clone. I. Definition according to profiles of lymphokine activities and secreted proteins. 1986. *J Immunol* 175, 5-14
95 Corthay, A.*, et al.* (2005) Primary antitumor immune response mediated by CD4+ T cells. *Immunity* 22, 371-383
96 Matsushita, H.*, et al.* (2015) Cytotoxic T lymphocytes block tumor growth both by lytic activity and IFNgamma-dependent cell-cycle arrest. *Cancer immunology research* 3, 26-36
97 Yoshimoto, T.*, et al.* (1998) IL-12 up-regulates IL-18 receptor expression on T cells, Th1 cells, and B cells: synergism with IL-18 for IFN-gamma production. *J Immunol* 161, 3400-3407
98 Flaishon, L.*, et al.* (2000) Autocrine secretion of interferon gamma negatively regulates homing of immature B cells. *The Journal of experimental medicine* 192, 1381-1388
99 Ohteki, T.*, et al.* (1999) Interleukin 12-dependent interferon gamma production by CD8alpha+ lymphoid dendritic cells. *The Journal of experimental medicine* 189, 1981-1986
100 Darwich, L.*, et al.* (2009) Secretion of interferon-gamma by human macrophages demonstrated at the single-cell level after costimulation with interleukin (IL)-12 plus IL-18. *Immunology* 126, 386-393
101 Chan, S.H.*, et al.* (1991) Induction of interferon gamma production by natural killer cell stimulatory factor: characterization of the responder cells and synergy with other inducers. *The Journal of experimental medicine* 173, 869-879
102 Ye, J.*, et al.* (1995) Cellular and molecular mechanisms of IFN-gamma production induced by IL-2 and IL-12 in a human NK cell line. *Journal of leukocyte biology* 58, 225-233
103 Carson, W.E.*, et al.* (1995) Endogenous production of interleukin 15 by activated human monocytes is critical for optimal production of interferon-gamma by natural killer cells in vitro. *The Journal of clinical investigation* 96, 2578-2582
104 Okamura, H.*, et al.* (1995) Cloning of a new cytokine that induces IFN-gamma production by T cells. *Nature* 378, 88-91
105 Takeda, K.*, et al.* (1998) Defective NK cell activity and Th1 response in IL-18-deficient mice. *Immunity* 8, 383-390
106 Bernabei, P.*, et al.* (2001) Interferon-gamma receptor 2 expression as the deciding factor in human T, B, and myeloid cell proliferation or death. *Journal of leukocyte biology* 70, 950-960
107 Bach, E.A.*, et al.* (1995) Ligand-induced autoregulation of IFN-gamma receptor beta chain expression in T helper cell subsets. *Science* 270, 1215-1218
108 Dhatchinamoorthy, K.*, et al.* (2021) Cancer Immune Evasion Through Loss of MHC Class I Antigen Presentation. *Frontiers in immunology* 12, 636568
109 Der, S.D.*, et al.* (1998) Identification of genes differentially regulated by interferon alpha, beta, or gamma using oligonucleotide arrays. *Proceedings of the National Academy of Sciences of the United States of America* 95, 15623-15628
110 Goes, N.*, et al.* (1995) Disturbed MHC regulation in the IFN-gamma knockout mouse. Evidence for three states of MHC expression with distinct roles for IFN-gamma. *J Immunol* 155, 4559-4566
111 Garrido, F.*, et al.* (2016) The urgent need to recover MHC class I in cancers for effective immunotherapy. *Current opinion in immunology* 39, 44-51
112 Chin, Y.E.*, et al.* (1996) Cell growth arrest and induction of cyclin-dependent kinase inhibitor p21 WAF1/CIP1 mediated by STAT1. *Science* 272, 719-722
113 Bromberg, J.F.*, et al.* (1996) Transcriptionally active Stat1 is required for the antiproliferative effects of both interferon alpha and interferon gamma. *Proceedings of the National Academy of Sciences of the United States of America* 93, 7673-7678
114 Fulda, S. and Debatin, K.M. (2002) IFNgamma sensitizes for apoptosis by upregulating caspase-8 expression through the Stat1 pathway. *Oncogene* 21, 2295-2308
115 Chin, Y.E.*, et al.* (1997) Activation of the STAT signaling pathway can cause expression of caspase 1 and apoptosis. *Molecular and cellular biology* 17, 5328-5337

116 Xu, X*., et al.* (1998) IFN-gamma induces cell growth inhibition by Fas-mediated apoptosis: requirement of STAT1 protein for up-regulation of Fas and FasL expression. *Cancer research* 58, 2832-2837
117 Liu, F*., et al.* (2011) TNFalpha cooperates with IFN-gamma to repress Bcl-xL expression to sensitize metastatic colon carcinoma cells to TRAIL-mediated apoptosis. *PloS one* 6, e16241
118 Beatty, G. and Paterson, Y. (2001) IFN-gamma-dependent inhibition of tumor angiogenesis by tumor-infiltrating CD4+ T cells requires tumor responsiveness to IFN-gamma. *J Immunol* 166, 2276-2282
119 Hayakawa, Y*., et al.* (2002) IFN-gamma-mediated inhibition of tumor angiogenesis by natural killer T-cell ligand, alpha-galactosylceramide. *Blood* 100, 1728-1733
120 Kammertoens, T*., et al.* (2017) Tumour ischaemia by interferon-gamma resembles physiological blood vessel regression. *Nature* 545, 98-102
121 Campanella, G.S*., et al.* (2010) CXCL10 can inhibit endothelial cell proliferation independently of CXCR3. *PloS one* 5, e12700
122 Feldman, E.D*., et al.* (2006) Interferon gamma-inducible protein 10 selectively inhibits proliferation and induces apoptosis in endothelial cells. *Annals of surgical oncology* 13, 125-133
123 Groom, J.R. and Luster, A.D. (2011) CXCR3 ligands: redundant, collaborative and antagonistic functions. *Immunology and cell biology* 89, 207-215
124 Melero, I*., et al.* (2014) T-cell and NK-cell infiltration into solid tumors: a key limiting factor for efficacious cancer immunotherapy. *Cancer discovery* 4, 522-526
125 Duluc, D*., et al.* (2009) Interferon-gamma reverses the immunosuppressive and protumoral properties and prevents the generation of human tumor-associated macrophages. *International journal of cancer* 125, 367-373
126 Cardoso, A.P*., et al.* (2015) An interferon-gamma-delivery system based on chitosan/poly(gamma-glutamic acid) polyelectrolyte complexes modulates macrophage-derived stimulation of cancer cell invasion in vitro. *Acta biomaterialia* 23, 157-171
127 Shirayoshi, Y*., et al.* (1988) Interferon-induced transcription of a major histocompatibility class I gene accompanies binding of inducible nuclear factors to the interferon consensus sequence. *Proceedings of the National Academy of Sciences of the United States of America* 85, 5884-5888
128 Gajewski, T.F*., et al.* (2013) Innate and adaptive immune cells in the tumor microenvironment. *Nature immunology* 14, 1014-1022
129 Cornel, A.M*., et al.* (2020) MHC Class I Downregulation in Cancer: Underlying Mechanisms and Potential Targets for Cancer Immunotherapy. *Cancers* 12
130 Trujillo, J.A*., et al.* (2018) T Cell-Inflamed versus Non-T Cell-Inflamed Tumors: A Conceptual Framework for Cancer Immunotherapy Drug Development and Combination Therapy Selection. *Cancer immunology research* 6, 990-1000
131 Pickup, M.W*., et al.* (2014) The extracellular matrix modulates the hallmarks of cancer. *EMBO reports* 15, 1243-1253
132 Sorokin, L. (2010) The impact of the extracellular matrix on inflammation. *Nature reviews. Immunology* 10, 712-723
133 O'Connor, R.S*., et al.* (2012) Substrate rigidity regulates human T cell activation and proliferation. *J Immunol* 189, 1330-1339
134 Houghton, A.M*., et al.* (2006) Elastin fragments drive disease progression in a murine model of emphysema. *The Journal of clinical investigation* 116, 753-759
135 Lardner, A. (2001) The effects of extracellular pH on immune function. *Journal of leukocyte biology* 69, 522-530
136 Hammer, C.H*., et al.* (1983) Activation of the fifth and sixth components of the human complement system: C6-dependent cleavage of C5 in acid and the formation of a bimolecular lytic complex, C5b,6a. *J Immunol* 131, 892-898
137 Reusch, H.P*., et al.* (1993) Na+/H+ exchange in human lymphocytes and platelets in chronic and subacute metabolic acidosis. *The Journal of clinical investigation* 92, 858-865

138 Quednau, B.*, et al.* (1994) Enhanced Na(+)-H+ exchanger activity and NHE-1 mRNA levels in human lymphocytes during metabolic acidosis. *The American journal of physiology* 266, C480-488
139 Palazon, A.*, et al.* (2012) The HIF-1alpha hypoxia response in tumor-infiltrating T lymphocytes induces functional CD137 (4-1BB) for immunotherapy. *Cancer discovery* 2, 608-623
140 Shibahara, I.*, et al.* (2015) OX40 ligand expressed in glioblastoma modulates adaptive immunity depending on the microenvironment: a clue for successful immunotherapy. *Molecular cancer* 14, 41
141 Clambey, E.T.*, et al.* (2012) Hypoxia-inducible factor-1 alpha-dependent induction of FoxP3 drives regulatory T-cell abundance and function during inflammatory hypoxia of the mucosa. *Proceedings of the National Academy of Sciences of the United States of America* 109, E2784-2793
142 Noman, M.Z.*, et al.* (2014) PD-L1 is a novel direct target of HIF-1alpha, and its blockade under hypoxia enhanced MDSC-mediated T cell activation. *The Journal of experimental medicine* 211, 781-790
143 Ma, B.*, et al.* (2019) The SIAH2-NRF1 axis spatially regulates tumor microenvironment remodeling for tumor progression. *Nature communications* 10, 1034
144 Koritzinsky, M.*, et al.* (2013) Two phases of disulfide bond formation have differing requirements for oxygen. *The Journal of cell biology* 203, 615-627
145 Giaccia, A.J.*, et al.* (2004) The biology of hypoxia: the role of oxygen sensing in development, normal function, and disease. *Genes & development* 18, 2183-2194
146 Lane, N. and Martin, W. (2010) The energetics of genome complexity. *Nature* 467, 929-934
147 Semenza, G.L. (2012) Hypoxia-inducible factors in physiology and medicine. *Cell* 148, 399-408
148 Bruick, R.K. and McKnight, S.L. (2001) A conserved family of prolyl-4-hydroxylases that modify HIF. *Science* 294, 1337-1340
149 Loenarz, C.*, et al.* (2011) The hypoxia-inducible transcription factor pathway regulates oxygen sensing in the simplest animal, Trichoplax adhaerens. *EMBO reports* 12, 63-70
150 Epstein, A.C.*, et al.* (2001) C. elegans EGL-9 and mammalian homologs define a family of dioxygenases that regulate HIF by prolyl hydroxylation. *Cell* 107, 43-54
151 Denko, N.C. (2008) Hypoxia, HIF1 and glucose metabolism in the solid tumour. *Nature reviews. Cancer* 8, 705-713
152 Majmundar, A.J.*, et al.* (2010) Hypoxia-inducible factors and the response to hypoxic stress. *Molecular cell* 40, 294-309
153 Schofield, C.J. and Ratcliffe, P.J. (2004) Oxygen sensing by HIF hydroxylases. *Nature reviews. Molecular cell biology* 5, 343-354
154 Hara, S.*, et al.* (2001) Expression and characterization of hypoxia-inducible factor (HIF)-3alpha in human kidney: suppression of HIF-mediated gene expression by HIF-3alpha. *Biochemical and biophysical research communications* 287, 808-813
155 Maynard, M.A.*, et al.* (2005) Human HIF-3alpha4 is a dominant-negative regulator of HIF-1 and is down-regulated in renal cell carcinoma. *FASEB journal : official publication of the Federation of American Societies for Experimental Biology* 19, 1396-1406
156 Tanaka, T.*, et al.* (2009) The human HIF (hypoxia-inducible factor)-3alpha gene is a HIF-1 target gene and may modulate hypoxic gene induction. *The Biochemical journal* 424, 143-151
157 Semenza, G.L.*, et al.* (1996) Hypoxia response elements in the aldolase A, enolase 1, and lactate dehydrogenase A gene promoters contain essential binding sites for hypoxia-inducible factor 1. *The Journal of biological chemistry* 271, 32529-32537
158 Kim, J.W.*, et al.* (2006) HIF-1-mediated expression of pyruvate dehydrogenase kinase: a metabolic switch required for cellular adaptation to hypoxia. *Cell metabolism* 3, 177-185
159 Eubank, T.D.*, et al.* (2011) Opposing roles for HIF-1alpha and HIF-2alpha in the regulation of angiogenesis by mononuclear phagocytes. *Blood* 117, 323-332
160 Yoon, D.*, et al.* (2011) Hypoxia. 5. Hypoxia and hematopoiesis. *American journal of physiology. Cell physiology* 300, C1215-1222
161 Tian, H.*, et al.* (1997) Endothelial PAS domain protein 1 (EPAS1), a transcription factor

selectively expressed in endothelial cells. *Genes & development* 11, 72-82
162 Ema, M.*, et al.* (1997) A novel bHLH-PAS factor with close sequence similarity to hypoxia-inducible factor 1alpha regulates the VEGF expression and is potentially involved in lung and vascular development. *Proceedings of the National Academy of Sciences of the United States of America* 94, 4273-4278
163 Flamme, I.*, et al.* (1997) HRF, a putative basic helix-loop-helix-PAS-domain transcription factor is closely related to hypoxia-inducible factor-1 alpha and developmentally expressed in blood vessels. *Mechanisms of development* 63, 51-60
164 Wiesener, M.S.*, et al.* (2003) Widespread hypoxia-inducible expression of HIF-2alpha in distinct cell populations of different organs. *FASEB journal : official publication of the Federation of American Societies for Experimental Biology* 17, 271-273
165 Bertout, J.A.*, et al.* (2009) HIF2alpha inhibition promotes p53 pathway activity, tumor cell death, and radiation responses. *Proceedings of the National Academy of Sciences of the United States of America* 106, 14391-14396
166 Scortegagna, M.*, et al.* (2003) Multiple organ pathology, metabolic abnormalities and impaired homeostasis of reactive oxygen species in Epas1-/- mice. *Nature genetics* 35, 331-340
167 Koh, M.Y.*, et al.* (2011) The hypoxia-associated factor switches cells from HIF-1alpha- to HIF-2alpha-dependent signaling promoting stem cell characteristics, aggressive tumor growth and invasion. *Cancer research* 71, 4015-4027
168 Holmquist-Mengelbier, L.*, et al.* (2006) Recruitment of HIF-1alpha and HIF-2alpha to common target genes is differentially regulated in neuroblastoma: HIF-2alpha promotes an aggressive phenotype. *Cancer cell* 10, 413-423
169 Zhao, J.*, et al.* (2015) The role of hypoxia-inducible factor-2 in digestive system cancers. *Cell death & disease* 6, e1600
170 Uniacke, J.*, et al.* (2012) An oxygen-regulated switch in the protein synthesis machinery. *Nature* 486, 126-129
171 Zhang, P.*, et al.* (2014) Hypoxia-inducible factor 3 is an oxygen-dependent transcription activator and regulates a distinct transcriptional response to hypoxia. *Cell reports* 6, 1110-1121
172 Heikkila, M.*, et al.* (2011) Roles of the human hypoxia-inducible factor (HIF)-3alpha variants in the hypoxia response. *Cellular and molecular life sciences : CMLS* 68, 3885-3901
173 Drevytska, T.*, et al.* (2012) HIF-3alpha mRNA expression changes in different tissues and their role in adaptation to intermittent hypoxia and physical exercise. *Pathophysiology : the official journal of the International Society for Pathophysiology* 19, 205-214
174 Kaelin, W.G., Jr. and Ratcliffe, P.J. (2008) Oxygen sensing by metazoans: the central role of the HIF hydroxylase pathway. *Molecular cell* 30, 393-402
175 Hon, W.C.*, et al.* (2002) Structural basis for the recognition of hydroxyproline in HIF-1 alpha by pVHL. *Nature* 417, 975-978
176 Jiang, B.H.*, et al.* (1996) Hypoxia-inducible factor 1 levels vary exponentially over a physiologically relevant range of O2 tension. *The American journal of physiology* 271, C1172-1180
177 Yuan, Y.*, et al.* (2003) Cobalt inhibits the interaction between hypoxia-inducible factor-alpha and von Hippel-Lindau protein by direct binding to hypoxia-inducible factor-alpha. *The Journal of biological chemistry* 278, 15911-15916
178 Wang, G.L. and Semenza, G.L. (1993) Desferrioxamine induces erythropoietin gene expression and hypoxia-inducible factor 1 DNA-binding activity: implications for models of hypoxia signal transduction. *Blood* 82, 3610-3615
179 Hanson, E.S.*, et al.* (2003) Oxygen and iron regulation of iron regulatory protein 2. *The Journal of biological chemistry* 278, 40337-40342
180 Grossman, J.I.*, et al.* (1969) Cardiovascular effects of infusion of lidocaine on patients with heart disease. *The American journal of cardiology* 24, 191-197
181 Lando, D.*, et al.* (2002) Asparagine hydroxylation of the HIF transactivation domain a hypoxic switch. *Science* 295, 858-861

182 Muz, B.*, et al.* (2015) The role of hypoxia in cancer progression, angiogenesis, metastasis, and resistance to therapy. *Hypoxia (Auckl)* 3, 83-92
183 Rankin, E.B. and Giaccia, A.J. (2016) Hypoxic control of metastasis. *Science* 352, 175-180
184 Wilson, W.R. and Hay, M.P. (2011) Targeting hypoxia in cancer therapy. *Nature reviews. Cancer* 11, 393-410
185 Rohwer, N. and Cramer, T. (2011) Hypoxia-mediated drug resistance: novel insights on the functional interaction of HIFs and cell death pathways. *Drug resistance updates : reviews and commentaries in antimicrobial and anticancer chemotherapy* 14, 191-201
186 Vaupel, P.*, et al.* (2001) Oxygen status of malignant tumors: pathogenesis of hypoxia and significance for tumor therapy. *Seminars in oncology* 28, 29-35
187 Abraham, J.*, et al.* (2015) The role of P-glycoprotein in drug resistance in multiple myeloma. *Leukemia & lymphoma* 56, 26-33
188 Cosse, J.P. and Michiels, C. (2008) Tumour hypoxia affects the responsiveness of cancer cells to chemotherapy and promotes cancer progression. *Anti-cancer agents in medicinal chemistry* 8, 790-797
189 Taylor, C.T. and Colgan, S.P. (2017) Regulation of immunity and inflammation by hypoxia in immunological niches. *Nature reviews. Immunology* 17, 774-785
190 Cummins, E.P.*, et al.* (2016) The role of HIF in immunity and inflammation. *Molecular aspects of medicine* 47-48, 24-34
191 Campbell, E.L.*, et al.* (2014) Transmigrating neutrophils shape the mucosal microenvironment through localized oxygen depletion to influence resolution of inflammation. *Immunity* 40, 66-77
192 Davis, C.*, et al.* (2003) The role of inflammation in vascular injury and repair. *Journal of thrombosis and haemostasis : JTH* 1, 1699-1709
193 Watts, E.R. and Walmsley, S.R. (2019) Inflammation and Hypoxia: HIF and PHD Isoform Selectivity. *Trends in molecular medicine* 25, 33-46
194 Harris, A.J.*, et al.* (2014) HIF-mediated innate immune responses: cell signaling and therapeutic implications. *Hypoxia (Auckl)* 2, 47-58
195 Lin, N. and Simon, M.C. (2016) Hypoxia-inducible factors: key regulators of myeloid cells during inflammation. *The Journal of clinical investigation* 126, 3661-3671
196 Mills, E. and O'Neill, L.A. (2014) Succinate: a metabolic signal in inflammation. *Trends in cell biology* 24, 313-320
197 Hammami, A.*, et al.* (2015) IRF-5-Mediated Inflammation Limits CD8+ T Cell Expansion by Inducing HIF-1alpha and Impairing Dendritic Cell Functions during Leishmania Infection. *PLoS pathogens* 11, e1004938
198 Wobben, R.*, et al.* (2013) Role of hypoxia inducible factor-1alpha for interferon synthesis in mouse dendritic cells. *Biological chemistry* 394, 495-505
199 Glover, L.E.*, et al.* (2016) Oxygen metabolism and barrier regulation in the intestinal mucosa. *The Journal of clinical investigation* 126, 3680-3688
200 Ward, J.B.*, et al.* (2011) Hydroxylase inhibition attenuates colonic epithelial secretory function and ameliorates experimental diarrhea. *FASEB journal : official publication of the Federation of American Societies for Experimental Biology* 25, 535-543
201 Kelly, C.J.*, et al.* (2013) Fundamental role for HIF-1alpha in constitutive expression of human beta defensin-1. *Mucosal immunology* 6, 1110-1118
202 Cummins, E.P. and Crean, D. (2017) Hypoxia and inflammatory bowel disease. *Microbes and infection* 19, 210-221
203 Ramakrishnan, S.K. and Shah, Y.M. (2016) Role of Intestinal HIF-2alpha in Health and Disease. *Annual review of physiology* 78, 301-325
204 Yamamoto, A.*, et al.* (2019) Systemic silencing of PHD2 causes reversible immune regulatory dysfunction. *The Journal of clinical investigation* 129, 3640-3656
205 Peyssonnaux, C.*, et al.* (2007) Cutting edge: Essential role of hypoxia inducible factor-1alpha in development of lipopolysaccharide-induced sepsis. *J Immunol* 178, 7516-7519

206 Takeda, N.*, et al.* (2010) Differential activation and antagonistic function of HIF-{alpha} isoforms in macrophages are essential for NO homeostasis. *Genes & development* 24, 491-501
207 Peyssonnaux, C.*, et al.* (2005) HIF-1alpha expression regulates the bactericidal capacity of phagocytes. *The Journal of clinical investigation* 115, 1806-1815
208 Nakamura, H.*, et al.* (2005) TCR engagement increases hypoxia-inducible factor-1 alpha protein synthesis via rapamycin-sensitive pathway under hypoxic conditions in human peripheral T cells. *J Immunol* 174, 7592-7599
209 Doedens, A.L.*, et al.* (2013) Hypoxia-inducible factors enhance the effector responses of CD8(+) T cells to persistent antigen. *Nature immunology* 14, 1173-1182
210 Palazon, A.*, et al.* (2017) An HIF-1alpha/VEGF-A Axis in Cytotoxic T Cells Regulates Tumor Progression. *Cancer cell* 32, 669-683 e665
211 Makino, Y.*, et al.* (2003) Hypoxia-inducible factor regulates survival of antigen receptor-driven T cells. *J Immunol* 171, 6534-6540
212 Chan, D.A.*, et al.* (2009) Tumor vasculature is regulated by PHD2-mediated angiogenesis and bone marrow-derived cell recruitment. *Cancer cell* 15, 527-538
213 Li, J.*, et al.* (2015) Prolyl-4-hydroxylase domain protein 2 controls NF-kappaB/p65 transactivation and enhances the catabolic effects of inflammatory cytokines on cells of the nucleus pulposus. *The Journal of biological chemistry* 290, 7195-7207
214 Fitzpatrick, S.F.*, et al.* (2016) Prolyl hydroxylase-1 regulates hepatocyte apoptosis in an NF-kappaB-dependent manner. *Biochemical and biophysical research communications* 474, 579-586
215 Pahl, H.L. (1999) Activators and target genes of Rel/NF-kappaB transcription factors. *Oncogene* 18, 6853-6866
216 Rius, J.*, et al.* (2008) NF-kappaB links innate immunity to the hypoxic response through transcriptional regulation of HIF-1alpha. *Nature* 453, 807-811
217 Walmsley, S.R.*, et al.* (2005) Hypoxia-induced neutrophil survival is mediated by HIF-1alpha-dependent NF-kappaB activity. *The Journal of experimental medicine* 201, 105-115
218 Cummins, E.P.*, et al.* (2006) Prolyl hydroxylase-1 negatively regulates IkappaB kinase-beta, giving insight into hypoxia-induced NFkappaB activity. *Proceedings of the National Academy of Sciences of the United States of America* 103, 18154-18159
219 Rodriguez, J.*, et al.* (2016) Substrate-Trapped Interactors of PHD3 and FIH Cluster in Distinct Signaling Pathways. *Cell reports* 14, 2745-2760
220 Cockman, M.E.*, et al.* (2006) Posttranslational hydroxylation of ankyrin repeats in IkappaB proteins by the hypoxia-inducible factor (HIF) asparaginyl hydroxylase, factor inhibiting HIF (FIH). *Proceedings of the National Academy of Sciences of the United States of America* 103, 14767-14772
221 Fu, J. (2016) Catalytic-independent inhibition of cIAP1-mediated RIP1 ubiquitination by EGLN3. *Cellular signalling* 28, 72-80
222 Oliver, K.M.*, et al.* (2009) Hypoxia activates NF-kappaB-dependent gene expression through the canonical signaling pathway. *Antioxidants & redox signaling* 11, 2057-2064
223 Koong, A.C.*, et al.* (1994) Hypoxia causes the activation of nuclear factor kappa B through the phosphorylation of I kappa B alpha on tyrosine residues. *Cancer research* 54, 1425-1430
224 Shah, P.*, et al.* (2013) Rate-limiting steps in yeast protein translation. *Cell* 153, 1589-1601
225 Gunisova, S.*, et al.* (2018) Please do not recycle! Translation reinitiation in microbes and higher eukaryotes. *FEMS microbiology reviews* 42, 165-192
226 Jackson, R.J.*, et al.* (2010) The mechanism of eukaryotic translation initiation and principles of its regulation. *Nature reviews. Molecular cell biology* 11, 113-127
227 Braunstein, S.*, et al.* (2007) A hypoxia-controlled cap-dependent to cap-independent translation switch in breast cancer. *Molecular cell* 28, 501-512
228 Shatkin, A.J. (1976) Capping of eucaryotic mRNAs. *Cell* 9, 645-653
229 Visa, N.*, et al.* (1996) A nuclear cap-binding complex binds Balbiani ring pre-mRNA cotranscriptionally and accompanies the ribonucleoprotein particle during nuclear export. *The Journal of cell biology* 133, 5-14

230 Bird, J.G., *et al.* (2016) The mechanism of RNA 5' capping with NAD+, NADH and desphospho-CoA. *Nature* 535, 444-447
231 Konarska, M.M., *et al.* (1984) Recognition of cap structure in splicing in vitro of mRNA precursors. *Cell* 38, 731-736
232 Meyer, K.D., *et al.* (2015) 5' UTR m(6)A Promotes Cap-Independent Translation. *Cell* 163, 999-1010
233 Martinez-Salas, E., *et al.* (2017) Insights into Structural and Mechanistic Features of Viral IRES Elements. *Frontiers in microbiology* 8, 2629
234 Kimball, S.R. (1999) Eukaryotic initiation factor eIF2. *The international journal of biochemistry & cell biology* 31, 25-29
235 Vattem, K.M. and Wek, R.C. (2004) Reinitiation involving upstream ORFs regulates ATF4 mRNA translation in mammalian cells. *Proceedings of the National Academy of Sciences of the United States of America* 101, 11269-11274
236 Zhou, D., *et al.* (2008) Phosphorylation of eIF2 directs ATF5 translational control in response to diverse stress conditions. *The Journal of biological chemistry* 283, 7064-7073
237 Ueda, T., *et al.* (2004) Mnk2 and Mnk1 are essential for constitutive and inducible phosphorylation of eukaryotic initiation factor 4E but not for cell growth or development. *Molecular and cellular biology* 24, 6539-6549
238 Calvo, S.E., *et al.* (2009) Upstream open reading frames cause widespread reduction of protein expression and are polymorphic among humans. *Proceedings of the National Academy of Sciences of the United States of America* 106, 7507-7512
239 Young, S.K. and Wek, R.C. (2016) Upstream Open Reading Frames Differentially Regulate Gene-specific Translation in the Integrated Stress Response. *The Journal of biological chemistry* 291, 16927-16935
240 Zhang, H., *et al.* (2021) Determinants of genome-wide distribution and evolution of uORFs in eukaryotes. *Nature communications* 12, 1076
241 Singleton, R.S., *et al.* (2014) OGFOD1 catalyzes prolyl hydroxylation of RPS23 and is involved in translation control and stress granule formation. *Proceedings of the National Academy of Sciences of the United States of America* 111, 4031-4036
242 Feng, T., *et al.* (2014) Optimal translational termination requires C4 lysyl hydroxylation of eRF1. *Molecular cell* 53, 645-654
243 Mekhail, K., *et al.* (2006) Restriction of rRNA synthesis by VHL maintains energy equilibrium under hypoxia. *Cell Cycle* 5, 2401-2413
244 Koritzinsky, M., *et al.* (2007) Phosphorylation of eIF2alpha is required for mRNA translation inhibition and survival during moderate hypoxia. *Radiotherapy and oncology : journal of the European Society for Therapeutic Radiology and Oncology* 83, 353-361
245 Koumenis, C., *et al.* (2002) Regulation of protein synthesis by hypoxia via activation of the endoplasmic reticulum kinase PERK and phosphorylation of the translation initiation factor eIF2alpha. *Molecular and cellular biology* 22, 7405-7416
246 Ameri, K., *et al.* (2004) Anoxic induction of ATF-4 through HIF-1-independent pathways of protein stabilization in human cancer cells. *Blood* 103, 1876-1882
247 Blais, J.D., *et al.* (2004) Activating transcription factor 4 is translationally regulated by hypoxic stress. *Molecular and cellular biology* 24, 7469-7482
248 Lu, P.D., *et al.* (2004) Translation reinitiation at alternative open reading frames regulates gene expression in an integrated stress response. *The Journal of cell biology* 167, 27-33
249 Starck, S.R., *et al.* (2016) Translation from the 5' untranslated region shapes the integrated stress response. *Science* 351, aad3867
250 Andreev, D.E., *et al.* (2015) Translation of 5' leaders is pervasive in genes resistant to eIF2 repression. *eLife* 4, e03971
251 Sidrauski, C., *et al.* (2015) The small molecule ISRIB reverses the effects of eIF2alpha phosphorylation on translation and stress granule assembly. *eLife* 4

252 Liu, L.*, et al.* (2006) Hypoxia-induced energy stress regulates mRNA translation and cell growth. *Molecular cell* 21, 521-531
253 Brugarolas, J.*, et al.* (2004) Regulation of mTOR function in response to hypoxia by REDD1 and the TSC1/TSC2 tumor suppressor complex. *Genes & development* 18, 2893-2904
254 Reiling, J.H. and Hafen, E. (2004) The hypoxia-induced paralogs Scylla and Charybdis inhibit growth by down-regulating S6K activity upstream of TSC in Drosophila. *Genes & development* 18, 2879-2892
255 Sofer, A.*, et al.* (2005) Regulation of mTOR and cell growth in response to energy stress by REDD1. *Molecular and cellular biology* 25, 5834-5845
256 Li, Y.*, et al.* (2007) Bnip3 mediates the hypoxia-induced inhibition on mammalian target of rapamycin by interacting with Rheb. *The Journal of biological chemistry* 282, 35803-35813
257 Bernardi, R.*, et al.* (2006) PML inhibits HIF-1alpha translation and neoangiogenesis through repression of mTOR. *Nature* 442, 779-785
258 Ge, W.*, et al.* (2012) Oxygenase-catalyzed ribosome hydroxylation occurs in prokaryotes and humans. *Nature chemical biology* 8, 960-962
259 Loenarz, C.*, et al.* (2014) Hydroxylation of the eukaryotic ribosomal decoding center affects translational accuracy. *Proceedings of the National Academy of Sciences of the United States of America* 111, 4019-4024
260 Metge, B.J.*, et al.* (2021) Hypoxia re-programs 2'-O-Me modifications on ribosomal RNA. *iScience* 24, 102010
261 Anderson, L.L.*, et al.* (2009) Survival from hypoxia in C. elegans by inactivation of aminoacyl-tRNA synthetases. *Science* 323, 630-633
262 Chionh, Y.H.*, et al.* (2016) tRNA-mediated codon-biased translation in mycobacterial hypoxic persistence. *Nature communications* 7, 13302
263 Elkordy, A.*, et al.* (2018) Stress-induced tRNA cleavage and tiRNA generation in rat neuronal PC12 cells. *Journal of neurochemistry* 146, 560-569
264 Zheng, D.*, et al.* (2020) Interaction between microbiota and immunity in health and disease. *Cell research* 30, 492-506
265 Moor, A.E.*, et al.* (2018) Spatial Reconstruction of Single Enterocytes Uncovers Broad Zonation along the Intestinal Villus Axis. *Cell* 175, 1156-1167 e1115
266 Zheng, L.*, et al.* (2015) Physiologic hypoxia and oxygen homeostasis in the healthy intestine. A Review in the Theme: Cellular Responses to Hypoxia. *American journal of physiology. Cell physiology* 309, C350-360
267 Abou Khouzam, R.*, et al.* (2020) Tumor Hypoxia Regulates Immune Escape/Invasion: Influence on Angiogenesis and Potential Impact of Hypoxic Biomarkers on Cancer Therapies. *Frontiers in immunology* 11, 613114
268 Ho, J.J.D.*, et al.* (2020) A network of RNA-binding proteins controls translation efficiency to activate anaerobic metabolism. *Nature communications* 11, 2677
269 Sese, M.*, et al.* (2017) Hypoxia-mediated translational activation of ITGB3 in breast cancer cells enhances TGF-beta signaling and malignant features in vitro and in vivo. *Oncotarget* 8, 114856-114876
270 Buffa, F.M.*, et al.* (2010) Large meta-analysis of multiple cancers reveals a common, compact and highly prognostic hypoxia metagene. *British journal of cancer* 102, 428-435
271 Leone, P.*, et al.* (2013) MHC class I antigen processing and presenting machinery: organization, function, and defects in tumor cells. *Journal of the National Cancer Institute* 105, 1172-1187
272 Wang, S.*, et al.* (2019) Antigen presentation and tumor immunogenicity in cancer immunotherapy response prediction. *eLife* 8
273 Li, Y.*, et al.* (2019) The SMART App: an interactive web application for comprehensive DNA methylation analysis and visualization. *Epigenetics & chromatin* 12, 71
274 Singhal, R. and Shah, Y.M. (2020) Oxygen battle in the gut: Hypoxia and hypoxia-inducible factors in metabolic and inflammatory responses in the intestine. *The Journal of biological*

chemistry 295, 10493-10505
275 Hrdinka, M*., et al.* (2016) CYLD Limits Lys63- and Met1-Linked Ubiquitin at Receptor Complexes to Regulate Innate Immune Signaling. *Cell reports* 14, 2846-2858
276 Li, Y*., et al.* (2012) IL-1beta promotes stemness and invasiveness of colon cancer cells through Zeb1 activation. *Molecular cancer* 11, 87
277 Demers, M.J*., et al.* (2009) Intestinal epithelial cancer cell anoikis resistance: EGFR-mediated sustained activation of Src overrides Fak-dependent signaling to MEK/Erk and/or PI3-K/Akt-1. *Journal of cellular biochemistry* 107, 639-654
278 Fiil, B.K*., et al.* (2013) OTULIN restricts Met1-linked ubiquitination to control innate immune signaling. *Molecular cell* 50, 818-830
279 Schneider-Brachert, W*., et al.* (2004) Compartmentalization of TNF receptor 1 signaling: internalized TNF receptosomes as death signaling vesicles. *Immunity* 21, 415-428
280 Fallahi-Sichani, M*., et al.* (2011) Multiscale computational modeling reveals a critical role for TNF-alpha receptor 1 dynamics in tuberculosis granuloma formation. *J Immunol* 186, 3472-3483
281 Yang, W.S*., et al.* (2015) 1,25-dihydroxyvitamin D3 causes ADAM10-dependent ectodomain shedding of tumor necrosis factor receptor 1 in vascular smooth muscle cells. *Molecular pharmacology* 87, 533-542
282 Rzymski, T*., et al.* (2012) The unfolded protein response controls induction and activation of ADAM17/TACE by severe hypoxia and ER stress. *Oncogene* 31, 3621-3634
283 Edwards, D.R*., et al.* (2008) The ADAM metalloproteinases. *Molecular aspects of medicine* 29, 258-289
284 Arribas, J*., et al.* (1996) Diverse cell surface protein ectodomains are shed by a system sensitive to metalloprotease inhibitors. *The Journal of biological chemistry* 271, 11376-11382
285 Dreschers, S*., et al.* (2017) Reduced internalization of TNF-a/TNFR1 down-regulates caspase dependent phagocytosis induced cell death (PICD) in neonatal monocytes. *PloS one* 12, e0182415
286 Fijalkowska, D*., et al.* (2017) eIF1 modulates the recognition of suboptimal translation initiation sites and steers gene expression via uORFs. *Nucleic acids research* 45, 7997-8013
287 Ji, Z*., et al.* (2015) Many lncRNAs, 5'UTRs, and pseudogenes are translated and some are likely to express functional proteins. *eLife* 4, e08890
288 Crappe, J*., et al.* (2015) PROTEOFORMER: deep proteome coverage through ribosome profiling and MS integration. *Nucleic acids research* 43, e29
289 Gao, X*., et al.* (2015) Quantitative profiling of initiating ribosomes in vivo. *Nature methods* 12, 147-153
290 Zhang, P*., et al.* (2017) Genome-wide identification and differential analysis of translational initiation. *Nature communications* 8, 1749
291 Chen, J*., et al.* (2020) Pervasive functional translation of noncanonical human open reading frames. *Science* 367, 1140-1146
292 Gawron, D*., et al.* (2016) Positional proteomics reveals differences in N-terminal proteoform stability. *Molecular systems biology* 12, 858
293 Raj, A*., et al.* (2016) Thousands of novel translated open reading frames in humans inferred by ribosome footprint profiling. *eLife* 5
294 Lee, S*., et al.* (2012) Global mapping of translation initiation sites in mammalian cells at single-nucleotide resolution. *Proceedings of the National Academy of Sciences of the United States of America* 109, E2424-2432
295 Ingolia, N.T*., et al.* (2011) Ribosome profiling of mouse embryonic stem cells reveals the complexity and dynamics of mammalian proteomes. *Cell* 147, 789-802
296 Luukkonen, B.G*., et al.* (1995) Efficiency of reinitiation of translation on human immunodeficiency virus type 1 mRNAs is determined by the length of the upstream open reading frame and by intercistronic distance. *Journal of virology* 69, 4086-4094
297 Wagner, S*., et al.* (2014) Functional and biochemical characterization of human eukaryotic translation initiation factor 3 in living cells. *Molecular and cellular biology* 34, 3041-3052

298 Ho, J.J.D*., et al.* (2016) Systemic Reprogramming of Translation Efficiencies on Oxygen Stimulus. *Cell reports* 14, 1293-1300
299 Koritzinsky, M*., et al.* (2006) Gene expression during acute and prolonged hypoxia is regulated by distinct mechanisms of translational control. *The EMBO journal* 25, 1114-1125
300 Shenton, D*., et al.* (2006) Global translational responses to oxidative stress impact upon multiple levels of protein synthesis. *The Journal of biological chemistry* 281, 29011-29021
301 Gao, J*., et al.* (2016) Loss of IFN-gamma Pathway Genes in Tumor Cells as a Mechanism of Resistance to Anti-CTLA-4 Therapy. *Cell* 167, 397-404 e399
302 Kearney, C.J*., et al.* (2018) Tumor immune evasion arises through loss of TNF sensitivity. *Science immunology* 3
303 Zhang, B*., et al.* (2008) IFN-gamma- and TNF-dependent bystander eradication of antigen-loss variants in established mouse cancers. *The Journal of clinical investigation* 118, 1398-1404
304 Bonaventura, P*., et al.* (2019) Cold Tumors: A Therapeutic Challenge for Immunotherapy. *Frontiers in immunology* 10, 168
305 Neefjes, J*., et al.* (2011) Towards a systems understanding of MHC class I and MHC class II antigen presentation. *Nature reviews. Immunology* 11, 823-836
306 Serrano, A*., et al.* (2001) Rexpression of HLA class I antigens and restoration of antigen-specific CTL response in melanoma cells following 5-aza-2'-deoxycytidine treatment. *International journal of cancer* 94, 243-251
307 Nie, Y*., et al.* (2001) DNA hypermethylation is a mechanism for loss of expression of the HLA class I genes in human esophageal squamous cell carcinomas. *Carcinogenesis* 22, 1615-1623
308 Ye, Q*., et al.* (2010) Hypermethylation of HLA class I gene is associated with HLA class I down-regulation in human gastric cancer. *Tissue antigens* 75, 30-39
309 Luo, N*., et al.* (2018) DNA methyltransferase inhibition upregulates MHC-I to potentiate cytotoxic T lymphocyte responses in breast cancer. *Nature communications* 9, 248
310 Tirosh, I*., et al.* (2016) Dissecting the multicellular ecosystem of metastatic melanoma by single-cell RNA-seq. *Science* 352, 189-196
311 Meeth, K*., et al.* (2016) The YUMM lines: a series of congenic mouse melanoma cell lines with defined genetic alterations. *Pigment cell & melanoma research* 29, 590-597
312 Tokunaga, R*., et al.* (2018) CXCL9, CXCL10, CXCL11/CXCR3 axis for immune activation - A target for novel cancer therapy. *Cancer treatment reviews* 63, 40-47
313 Zhang, Y*., et al.* (2020) Cytokine and Chemokine Signals of T-Cell Exclusion in Tumors. *Frontiers in immunology* 11, 594609
314 Dangaj, D*., et al.* (2019) Cooperation between Constitutive and Inducible Chemokines Enables T Cell Engraftment and Immune Attack in Solid Tumors. *Cancer cell* 35, 885-900 e810
315 Oo, Y.H*., et al.* (2010) The role of chemokines in the recruitment of lymphocytes to the liver. *Dig Dis* 28, 31-44
316 Chen, L. and Flies, D.B. (2013) Molecular mechanisms of T cell co-stimulation and co-inhibition. *Nature reviews. Immunology* 13, 227-242
317 Verma, N.K*., et al.* (2016) LFA-1/ICAM-1 Ligation in Human T Cells Promotes Th1 Polarization through a GSK3beta Signaling-Dependent Notch Pathway. *J Immunol* 197, 108-118
318 Deeths, M.J. and Mescher, M.F. (1999) ICAM-1 and B7-1 provide similar but distinct costimulation for CD8+ T cells, while CD4+ T cells are poorly costimulated by ICAM-1. *European journal of immunology* 29, 45-53
319 Meissner, T.B*., et al.* (2010) NLR family member NLRC5 is a transcriptional regulator of MHC class I genes. *Proceedings of the National Academy of Sciences of the United States of America* 107, 13794-13799
320 Sreejit, G*., et al.* (2014) The ESAT-6 protein of Mycobacterium tuberculosis interacts with beta-2-microglobulin (beta2M) affecting antigen presentation function of macrophage. *PLoS pathogens* 10, e1004446
321 Paul, S. and Lal, G. (2017) The Molecular Mechanism of Natural Killer Cells Function and Its

Importance in Cancer Immunotherapy. *Frontiers in immunology* 8, 1124
322 Noy, R. and Pollard, J.W. (2014) Tumor-associated macrophages: from mechanisms to therapy. *Immunity* 41, 49-61
323 Dudley, M.E.*, et al.* (2002) Cancer regression and autoimmunity in patients after clonal repopulation with antitumor lymphocytes. *Science* 298, 850-854
324 Harel, M.*, et al.* (2019) Proteomics of Melanoma Response to Immunotherapy Reveals Mitochondrial Dependence. *Cell* 179, 236-250 e218
325 Arthur, J.S. and Ley, S.C. (2013) Mitogen-activated protein kinases in innate immunity. *Nature reviews. Immunology* 13, 679-692
326 Lee, D.S.M.*, et al.* (2021) Disrupting upstream translation in mRNAs is associated with human disease. *Nature communications* 12, 1515
327 Thalhammer, A.*, et al.* (2011) Human AlkB homologue 5 is a nuclear 2-oxoglutarate dependent oxygenase and a direct target of hypoxia-inducible factor 1alpha (HIF-1alpha). *PloS one* 6, e16210
328 Masson, N.*, et al.* (2019) Conserved N-terminal cysteine dioxygenases transduce responses to hypoxia in animals and plants. *Science* 365, 65-69
329 Islam, M.S.*, et al.* (2018) 2-Oxoglutarate-Dependent Oxygenases. *Annual review of biochemistry* 87, 585-620
330 Iacono, M.*, et al.* (2005) uAUG and uORFs in human and rodent 5'untranslated mRNAs. *Gene* 349, 97-105
331 Nelde, A.*, et al.* (2022) Upstream open reading frames regulate translation of cancer-associated transcripts and encode HLA-presented immunogenic tumor antigens. *Cellular and molecular life sciences : CMLS* 79, 171
332 Huang, N.*, et al.* (2021) An Upstream Open Reading Frame in Phosphatase and Tensin Homolog Encodes a Circuit Breaker of Lactate Metabolism. *Cell metabolism* 33, 128-144 e129
333 Ogryzko, N.V.*, et al.* (2019) Hif-1alpha-Induced Expression of Il-1beta Protects against Mycobacterial Infection in Zebrafish. *J Immunol* 202, 494-502
334 Jeong, H.J.*, et al.* (2005) Hypoxia-induced IL-6 production is associated with activation of MAP kinase, HIF-1, and NF-kappaB on HEI-OC1 cells. *Hearing research* 207, 59-67
335 Cane, G.*, et al.* (2010) HIF-1alpha mediates the induction of IL-8 and VEGF expression on infection with Afa/Dr diffusely adhering E. coli and promotes EMT-like behaviour. *Cellular microbiology* 12, 640-653
336 Sartori-Cintra, A.R.*, et al.* (2012) Regulation of hypoxia-inducible factor-1alpha (HIF-1alpha) expression by interleukin-1beta (IL-1 beta), insulin-like growth factors I (IGF-I) and II (IGF-II) in human osteoarthritic chondrocytes. *Clinics (Sao Paulo)* 67, 35-40
337 Yoshida, T.*, et al.* (2013) Transcriptional upregulation of HIF-1alpha by NF-kappaB/p65 and its associations with beta-catenin/p300 complexes in endometrial carcinoma cells. *Laboratory investigation; a journal of technical methods and pathology* 93, 1184-1193
338 Singhal, R.*, et al.* (2021) HIF-2alpha activation potentiates oxidative cell death in colorectal cancers by increasing cellular iron. *The Journal of clinical investigation* 131
339 Qi, Y.*, et al.* (2015) PTEN induces apoptosis and cavitation via HIF-2-dependent Bnip3 upregulation during epithelial lumen formation. *Cell death and differentiation* 22, 875-884
340 Kubli, D.A.*, et al.* (2007) Bnip3 mediates mitochondrial dysfunction and cell death through Bax and Bak. *The Biochemical journal* 405, 407-415
341 Taylor, C.T.*, et al.* (2016) Hypoxia-dependent regulation of inflammatory pathways in immune cells. *The Journal of clinical investigation* 126, 3716-3724
342 Burr, S.*, et al.* (2018) Oxygen gradients can determine epigenetic asymmetry and cellular differentiation via differential regulation of Tet activity in embryonic stem cells. *Nucleic acids research* 46, 1210-1226
343 Thienpont, B.*, et al.* (2016) Tumour hypoxia causes DNA hypermethylation by reducing TET activity. *Nature* 537, 63-68
344 Hockel, M. and Vaupel, P. (2001) Tumor hypoxia: definitions and current clinical, biologic, and

molecular aspects. *Journal of the National Cancer Institute* 93, 266-276
345 Jain, A.*, et al.* (2018) T cell-intrinsic IL-1R signaling licenses effector cytokine production by memory CD4 T cells. *Nature communications* 9, 3185
346 Ben-Sasson, S.Z.*, et al.* (2011) IL-1 acts on T cells to enhance the magnitude of in vivo immune responses. *Cytokine* 56, 122-125